

Master thesis : Implementation of heterosynaptic plasticity in biological neuron models and application in the context of allodynia

Auteur : Sautois, Nora

Promoteur(s) : Drion, Guillaume

Faculté : Faculté des Sciences appliquées

Diplôme : Master en ingénieur civil biomédical, à finalité spécialisée

Année académique : 2021-2022

URI/URL : <http://hdl.handle.net/2268.2/14394>

Avertissement à l'attention des usagers :

Tous les documents placés en accès ouvert sur le site le site MatheO sont protégés par le droit d'auteur. Conformément aux principes énoncés par la "Budapest Open Access Initiative"(BOAI, 2002), l'utilisateur du site peut lire, télécharger, copier, transmettre, imprimer, chercher ou faire un lien vers le texte intégral de ces documents, les disséquer pour les indexer, s'en servir de données pour un logiciel, ou s'en servir à toute autre fin légale (ou prévue par la réglementation relative au droit d'auteur). Toute utilisation du document à des fins commerciales est strictement interdite.

Par ailleurs, l'utilisateur s'engage à respecter les droits moraux de l'auteur, principalement le droit à l'intégrité de l'oeuvre et le droit de paternité et ce dans toute utilisation que l'utilisateur entreprend. Ainsi, à titre d'exemple, lorsqu'il reproduira un document par extrait ou dans son intégralité, l'utilisateur citera de manière complète les sources telles que mentionnées ci-dessus. Toute utilisation non explicitement autorisée ci-avant (telle que par exemple, la modification du document ou son résumé) nécessite l'autorisation préalable et expresse des auteurs ou de leurs ayants droit.



Implementation of heterosynaptic plasticity in biological neuron models and application in the context of allodynia.

*Master thesis realised with the aim of obtaining the degree of Master in
Biomedical Engineering*

Nora Sautois

Promoters:

Guillaume Drion

Pierre Sacré

Jury members:

Guillaume Drion

Pierre Sacré

Christophe Philips

Alban Latremolière

UNIVERSITY OF LIÈGE
FACULTY OF APPLIED SCIENCES
ACADEMIC YEAR 2021 - 2022

Implementation of heterosynaptic plasticity in biological neuron models and application in the context of allodynia

Nora Sautois

Supervisors: G. Drion and P. Sacré

Master in Biomedical Engineering, University of Liège

Academic year 2021-2022

Abstract

Synaptic plasticity, defined as the modification of synaptic strength, plays a very important role in many mechanisms such as memory or learning. There are several types of synaptic plasticity, the best known and most studied being homosynaptic plasticity where a synapse strength is modified by its own activity. However, this type of plasticity cannot explain all phenomena and other types of plasticity are needed. Heterosynaptic plasticity is defined as changes in the synaptic strength induced by the activity of adjacent synapses. Until now, only scarce data, either experimental or computational, have been generated to study heterosynaptic plasticity. Yet, this type of plasticity is necessary, especially to study pain-related phenomena.

Pain may be triggered by various causes. Moreover, following an injury, one can notice an increase in sensitivity to touch on and around the wound. Thus, a caress, no matter how gentle, will cause a sensation of pain. This phenomenon is known as allodynia. Studies have shown that central sensitization, an increase in the excitation of synapses in the spinal cord, has a role to play in the induction of allodynia. Both homosynaptic and heterosynaptic plasticities are involved.

The aim of this thesis is to establish a new model of heterosynaptic plasticity with the subsidiary goal of modeling allodynia. To do so, we started with two homosynaptic plasticity models (calcium-based and pair-based spike-timing dependent plasticity (STDP)) to which we added a heterosynaptic dimension by modeling two presynaptic neurons and one postsynaptic neuron. In the calcium-based model, this has been done through the integration of a new parameter α , intervening when presynaptic neurons spike, which could represent the distance between two presynaptic neurons or the amount of calcium diffusing (or being released) through the postsynaptic neuron. In the pair-based model, this has been done through the integration of two new parameters α , governing the potentiation, and A_{het} governing the depression of synaptic weights. Both parameters intervene when the presynaptic neurons spike. We studied the dependency between α and A_{het} which shows that when they are independent of each other, a phenomenon of pruning, the mechanism by which some neuronal connections are eliminated after some time, can be inferred with the right set of parameters. Our new calcium-based heterosynaptic models were evaluated in the same experimental conditions previously reported by Chistiakova et al. and we were able to reproduce a Mexican hat pattern where the induction of homosynaptic long-term potentiation (LTP) provokes weaker LTP at the closest neighbor synapses, long-term depression (LTD) at further neighbor synapses and no modification at the furthest neighbor synapses. Finally, we were able to customize our new models to reproduce a mechanism of heterosynaptic central sensitization causing allodynia. However, our models have shown a certain fragility that may be related to suboptimal physiological modeling.

In conclusion, our new models introduce for the first time two new parameters namely α and A_{het} which, in our view, could contribute to better model heterosynaptic plasticity. However, further work will be needed to flesh out our models in the future.

Acknowledgements

First of all, I would like to warmly thank my promotor Guillaume Drion and Pierre Sacré for their supervision, their wise guidance and their availability in the construction of this thesis. Then obviously I would like to express my sincere gratitude to the PhD students, Kathleen Jacquerie and Caroline Minne, who supported me with their extraordinary enthusiasm and their kindness. I am very grateful for their involvement, their wise advice and their sharp sense of details and aesthetic. I also would like to thank Anaëlle Deworm for her sound advice and her time.

I am also very thankful for having shared during this semester the good company of Nora Beng-halem, Pauline Garcia and Juliette Ponnet who were a great support during this adventure.

I must express my very profound gratitude to my parents for the proofreading, the support and the love during these five years. I am also very grateful to my sisters, my little nieces and Léon for the moral support at all times but also to Lucas for his optimism, his communicative motivation and his unconditional support. Finally, I would like to thank my friends who, from near or far, have been rays of sunshine.

Liège, June 9th, 2022

Nora Sautois

Contents

1	Introduction	1
1.1	Motivation: finding a new way to model heterosynaptic plasticity	1
1.2	Structure	2
I	Background	5
2	What is pain?	7
2.1	Types of pain	7
2.2	Pain neural circuit	8
2.2.1	Dorsal horn neurons (DHNs)	10
2.3	Central sensitization	11
2.3.1	What is central sensitization?	11
2.3.2	Other plasticity phenomena participating in central sensitization	13
2.4	Summary	15
3	Synaptic plasticity from a biological point of view	17
3.1	Neuronal communication	17
3.2	Homosynaptic plasticity	18
3.2.1	Short-term plasticity	18
3.2.2	Long-term plasticity	19
3.2.3	Spike-Timing Dependent Plasticity	22
3.2.4	Homosynaptic plasticity drawbacks	24
3.3	Homeostatic plasticity	24
3.4	Heterosynaptic plasticity	24
3.4.1	Homosynaptic plasticity versus heterosynaptic plasticity	24
3.4.2	Characteristics	25
3.5	The case of <i>Aplysia Californica</i>	26
3.5.1	Habituation	27
3.5.2	Sensitization	28
3.6	Summary	30
4	Homosynaptic plasticity from a modeling point of view	31
4.1	Homosynaptic plasticity with calcium rules	31
4.2	Homosynaptic plasticity with STDP rules	33
4.3	Summary	36

5	Heterosynaptic plasticity from a modeling point of view	37
5.1	Runaway phenomenon prevention	37
5.1.1	Computational Model	37
5.1.2	Results	39
5.2	Heterosynaptic excitatory-inhibitory balance	40
5.2.1	Effect of pairing presynaptic and postsynaptic activity	40
5.2.2	Introduction of heterosynaptic rules in calcium-based homosynaptic models . .	43
5.3	Other models	46
5.4	Summary	46
II	Computational study	47
6	Laying of the foundations	49
6.1	Choice of neurons	49
6.2	Spike train with a Poisson process	50
6.3	Protocols	51
6.3.1	First two protocols: Homosynaptic protocols	51
6.3.2	Third protocol	52
6.3.3	Fourth protocol	52
6.3.4	Fifth protocol	53
6.3.5	Sixth protocol	53
7	Integration of heterosynaptic rules in the different models	55
7.1	Modelisation of postsynaptic membrane	55
7.2	Heterosynaptic plasticity with calcium rules	55
7.2.1	Description of the model	56
7.2.2	Methodology	57
7.2.3	Results	57
7.3	Heterosynaptic plasticity with STDP rules	61
7.3.1	Description of the model	61
7.3.2	Methodology	63
7.3.3	Results	64
8	Heterosynaptic models: Discussion and application	73
8.1	Calcium discussion	73
8.1.1	Distance interpretation	73
8.1.2	Calcium release	73
8.1.3	Conditioning	75
8.1.4	Questionable results	75
8.1.5	Discussion of protocol 6	75
8.2	Pair-based STDP discussion	76
8.2.1	Dependency between α and A_{het}	76
8.2.2	Conditioning	77
8.2.3	Pruning	77
8.2.4	Prevention of saturation	77
8.2.5	Questionable results	77
8.2.6	Discussion of the protocol 6	78

8.3	Summary	79
9	Toy model: implementation of heterosynaptic rules in the context of allodynia	81
9.1	Adaptation of the models	81
9.1.1	Choice of the neurons	82
9.1.2	New Poisson train	82
9.1.3	Tuning of parameters α , A_{het} and C_{pre2}	82
9.1.4	Tuning of current intensity	83
9.1.5	Tuning of the weight evolution	83
9.2	Methodology	84
9.2.1	Calcium-based model	84
9.2.2	Pair-based model	84
9.3	Results	85
9.3.1	Calcium-based model	85
9.3.2	Pair-based model	85
9.3.3	Fragility of the model	85
9.4	Discussion	86
9.5	Summary	88
III	Conclusion and perspectives	89
10	Conclusion and perspectives	91
10.1	Thesis summary	91
10.2	Perspectives	92
	Bibliography	96
IV	Appendix	97
A	Computational details	A1
A.1	Pyramidal neuron model [Chen et al., 2013]	A1
B	Hodgkin and Huxley model	A3
C	Additional results from the Toy model	A5

Chapter 1

Introduction

1.1 Motivation: finding a new way to model heterosynaptic plasticity

Synaptic plasticity is the phenomenon governing the modification of neuronal connection strength. This phenomenon governs all the interactions between the neurons and thus, is the basis of many mechanisms such as memory or learning. Although several types of plasticity have been described, this thesis will introduce two of them, homosynaptic plasticity and heterosynaptic plasticity. While the homosynaptic plasticity has been largely studied and modeled, heterosynaptic plasticity, because of a lack of understanding that still surrounds it, is a subject deserving to be further developed.

On the other hand, pain is a sensation well known for most people. It can be caused by a fall, tissue damage or even nothing particular. Complex mechanisms are involved in pain and some of them could be caused by heterosynaptic plasticity.

The aim of this thesis is to construct two new heterosynaptic plasticity models. For this, we will start from established homosynaptic plasticity models on which we will graft heterosynaptic plasticity laws. These laws will be constructed based on the reported experimental observations that define heterosynaptic plasticity such as calcium propagation. The goal of our new models is to represent the interactions between two presynaptic neurons and one postsynaptic neuron, all three excitatory. After the analysis of the results obtained with these new models, we will customize them in order to illustrate a concrete case related to the context of pain: the central sensitization causing the phenomenon of allodynia.

In the context of this study, the following questions will be answered:

- *What is pain? In particular, what is central sensitization and allodynia?* (CHAPTER 2)
- *What is synaptic plasticity, in particular homosynaptic plasticity and heterosynaptic plasticity?* (CHAPTER 3)
- *How can we model homosynaptic plasticity and heterosynaptic plasticity?* (CHAPTER 4 AND 5)
- *How to adapt existing homosynaptic models into heterosynaptic models?* (CHAPTER 6, 7 AND 8)
- *How to model central sensitization in the context of allodynia?* (CHAPTER 9)

1.2 Structure

To answer those questions, this thesis is divided into three main parts:

Part I first explains what is pain and how it happens. A description of the neural circuits and of the mechanisms happening in the spinal cord such as central sensitization will be presented in CHAPTER 2. Then, CHAPTER 3 will investigate the different types of plasticity from a biological point of view. This chapter describes the biological mechanisms happening during the communication between two neurons. Homosynaptic, homeostatic and heterosynaptic plasticity will be introduced. Chapters 4 and 5 focus on the modeling of those types of plasticity. Thus CHAPTER 4 discusses the homosynaptic plasticity models useful in the next part of the thesis while CHAPTER 5 reviews known existing heterosynaptic models.

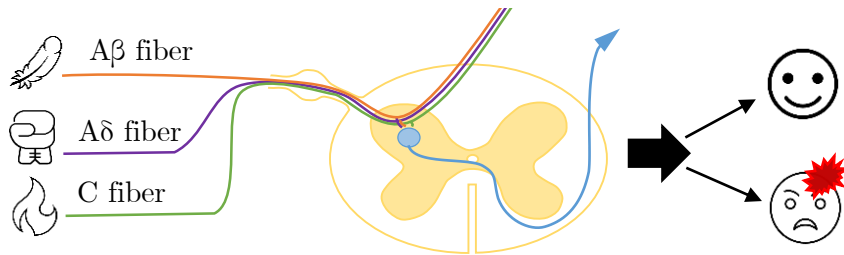
Part II consists in a computational study and thus in the presentation of our new models. At first, we lay the foundations with a description of the used protocols in CHAPTER 6. Then, our new heterosynaptic models are introduced and the obtained results presented in CHAPTER 7. Those results are then discussed and interpreted in CHAPTER 8. Finally, an adaptation of our new models will be performed in order to illustrate the phenomenon of allodynia in CHAPTER 9.

Part III draws the conclusion of this thesis. The limitations observed during our work linked to the models are enumerated and a list of future perspectives to improve the new models is drawn.

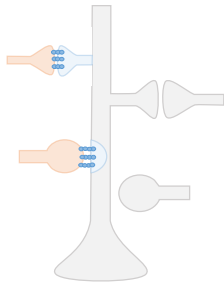
SUMMARY: STRUCTURE

PART I: Background

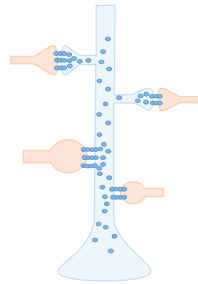
1. What is pain?
2. What is homosynaptic plasticity?
3. What is heterosynaptic plasticity?
4. Homosynaptic models
5. Heterosynaptic models



Homosynaptic plasticity



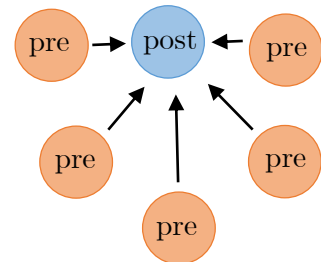
Heterosynaptic plasticity



Homosynaptic models



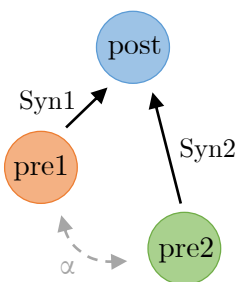
Heterosynaptic models



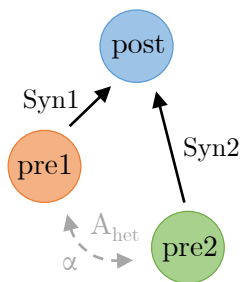
PART II: Computational study

1. Integration of heterosynaptic rules in existing homosynaptic models
2. Customization of our models to illustrate Allodynia

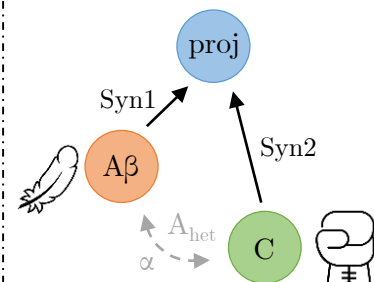
Adapted calcium-based model



Adapted pair-based model



Modelling of allodynia



Part I

Background

Chapter 2

What is pain?

Almost everyone has experienced pain at some point in their lives. This pain may have been caused by exposure to high heat, a sharp blade, or even a piece of furniture that was too hard. But what is pain and what happens when we feel it?

First of all, pain is defined by the International Association for the Study of Pain (IASP) as *"an unpleasant sensory and emotional experience associated with, or resembling that associated with, actual or potential tissue damage."* [IASP, 2020] In addition, pain is considered a personal experience. It is influenced by many factors that may be social, psychological or biological. Therefore, when a person says she/he is in pain, her/his feelings cannot be denied and must be respected. It is important to differentiate between nociception and pain. Indeed, where nociception depends on the activity of sensory neurons, pain, because of its psychological and individual dimension, cannot be reduced to the activity or not of nociceptors.

2.1 Types of pain

Three types of pain are recognized. First one is the **nociceptive pain** which is the pain we feel when touching something too hot, cold, or sharp. It is a high-threshold pain only activated in the presence of intense noxious stimuli. This type of pain has an immediate protective role. It cries out to us to immediately move away from the source of our pain so as not to be hurt further. It is then a protective system (see Figure 2.1(A)). People who cannot feel pain are in a dangerous situation because they cannot protect themselves from the hurtful things around them. They could get a third degree burn without realising it and be hurt very badly. This type of pain is therefore necessary.

Second type is the **inflammatory pain**. It is the pain we feel after being injured. When we are injured, a simple caress on or around a wound hurts us. That pain assists in the healing of the injured body part by discouraging physical contact or movement. This pain has a protective and adaptive role since it prevents an injury from getting worse by discouraging contact with it. This type of pain is created by the nociceptive system when it detects inflammation factors that are produced by the immune system after tissues have been injured. The nociceptive system therefore supports the immune system (see Figure 2.1(B)). Despite its protective role, this pain can be uncomfortable, sometimes very intense and requires temporary medication, for example after surgery.

Finally the third type of pain is called the **pathological pain** which is not protective but mal-

adaptive resulting from abnormal functioning of the nervous system. That pain can be of two types: **neuropathic pain** and **dysfunctional pain**. Neuropathic pain appears when the nervous system is damaged. A part of our brain then believes that we are injured although we are not and we feel pain. On the other hand, dysfunctionnal pain appears even when the nervous system is not injured. This can be observed in conditions such as fibromyalgia, irritable bowel syndrome, tension type headache, temporomandibular joint disease or interstitial cystitis (see Figure 2.1(C)). Those types of pain are more difficult to understand than the nociceptive or the inflammatory pain because there is no real cause to the pain the patient feels. However, they exist and are real for the patient. It is therefore important to understand these types of pain correctly in order to find a suitable treatment for these patients [Woolf, 2010].

2.2 Pain neural circuit

Now that we know the different types of pain, we can look at what happens in our body when the sensation of pain is experienced. First of all, when we feel pain, it is the somato-sensory system that is involved. This system can be divided into two sub-systems which have different functions and different paths.

- First the mechano-sensory system detects mechanical stimuli (light touch, vibration, pressure, skin tension). The touch receptors are called mechanoreceptors and their axons are the $A\alpha$ and $A\beta$ fibers.
- Second the nociceptive system detects pain and temperature. The role of the nociceptive system is to alert the brain about danger. This system is composed of receptors called nociceptors and thermoceptors. As their names suggest, they are used to detect noxious stimuli and temperatures. Nociceptors can be categorized by the properties of their associated axons. A distinction is made between $A\delta$ fibers and C fibers:
 - $A\delta$ fibers are myelinated and wide, which makes them fast channels for transmitting information (about 20 m/s).
 - C fibers are non-myelinated and rather narrow, which makes them rather slow channels for transmitting information (less than 2m/s). Those fibers have their cell bodies in segmental dorsal root ganglia and enter the dorsal horn of the spinal cord. Then, after the fibers branch, they travel a short distance on both sides of the spinal cord in the zone of Lissauer and finally synapse on cells in the outer part of the dorsal horn in the substantia gelatinosa [Purves, 2004]. This path can be seen on Figure 2.2.

The difference in the speed of information is expressed by two categories of pain sensation. When we stub our toe against a piece of furniture, we feel the pain in two phases. The first sensation of pain is sharp and sudden and is conducted by the $A\delta$ fibers. The second sensation of pain arrives rather like a wave. It is longer and less intense and is driven by the C fibers [Purves, 2004]. This is observable on Figure 2.3(A). When $A\delta$ fibers are inactivated, only the weak and long sensation of pain is perceived (Figure 2.3(B)). On the other hand, when the C fibers are inactivated, only the sharp and sudden sensation of pain is experimented (Figure 2.3(C)).

As said before, the mechanosensitive system and the nociceptor system have different pathways. There are three main differences. First, where the touch pathway ends with specialized structures in

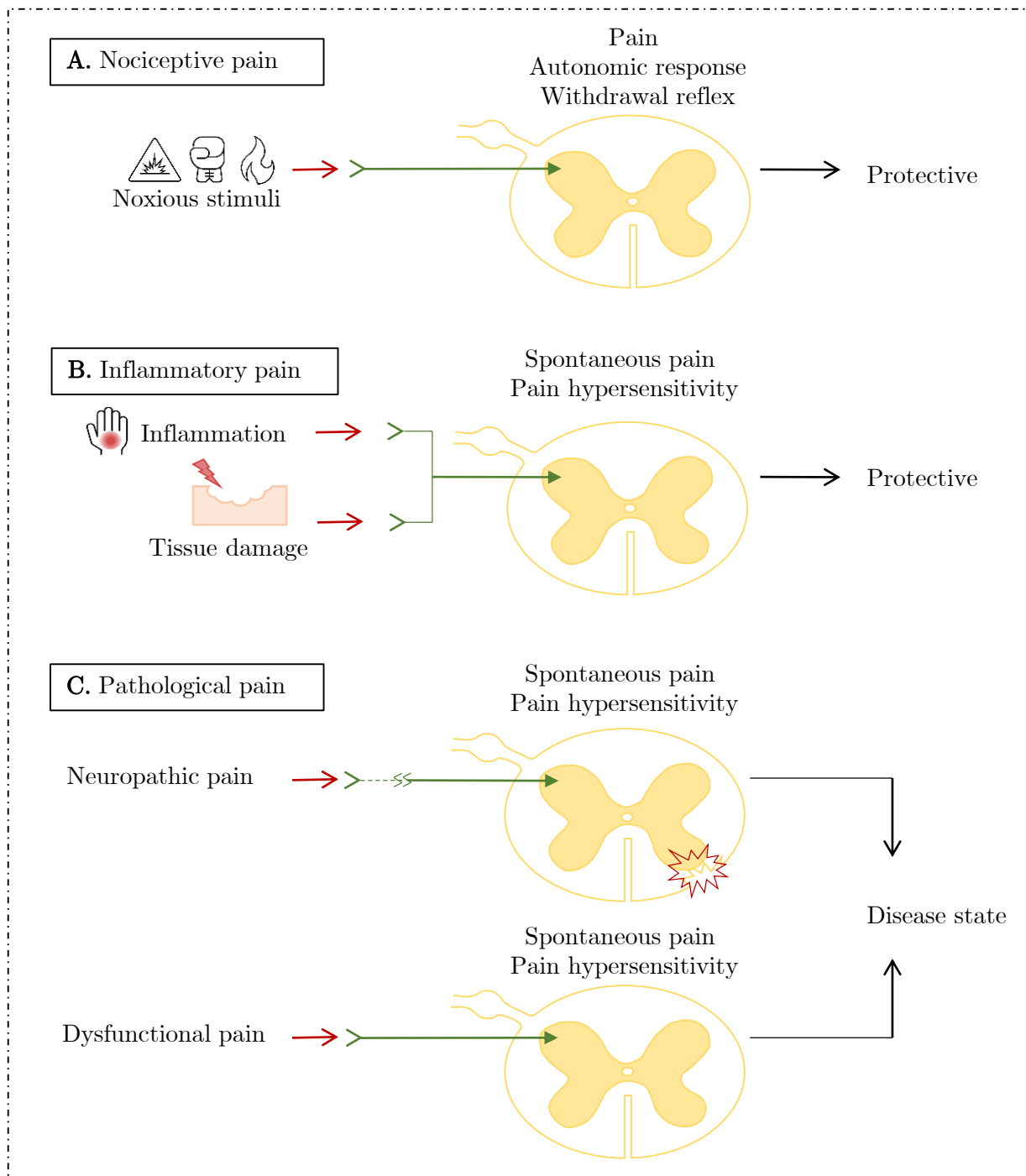


Figure 2.1 – *Three types of pain.* (A) Nociceptive pain has a protective function. It is the response to a noxious stimuli. (B) Inflammatory pain has a protective function. It is the response of the nociceptive system to a tissue damage or to an inflammation. (C) Pathological pain is maladaptive. It can be divided into neuropathic pain where the nervous system is damaged and in dysfunctionnal pain where no damage are known. It is a disease state. *Adapted from [Woolf, 2010]*

the skin, the pain pathway ends with free endings in the skin. Secondly, the $A\beta$ fibers of the touch pathway are fast and myelinated unlike the $A\delta$ and C fibers which are only weakly myelinated or not at all and therefore slower. Finally, where $A\beta$ axons end in the deep dorsal horn, as explained before $A\delta$ and C fibers end in the substantia gelatinosa.

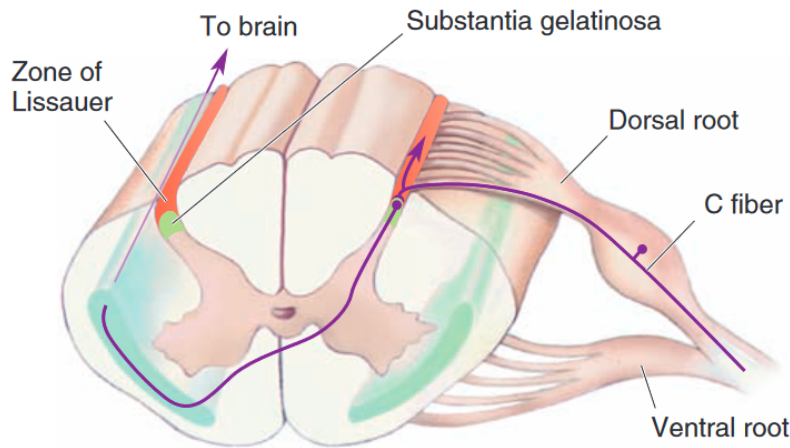


Figure 2.2 – *Path of C fibers in the spinal cord.* C fibers enter the dorsal horn of the spinal cord via the dorsal root ganglia. Then they branch, travel a short distance on both sides of the spinal cord in the zone of Lissauer and synapse on cells in the outer part of the dorsal horn in the substantia gelatinosa. From [Bear et al., 2007]

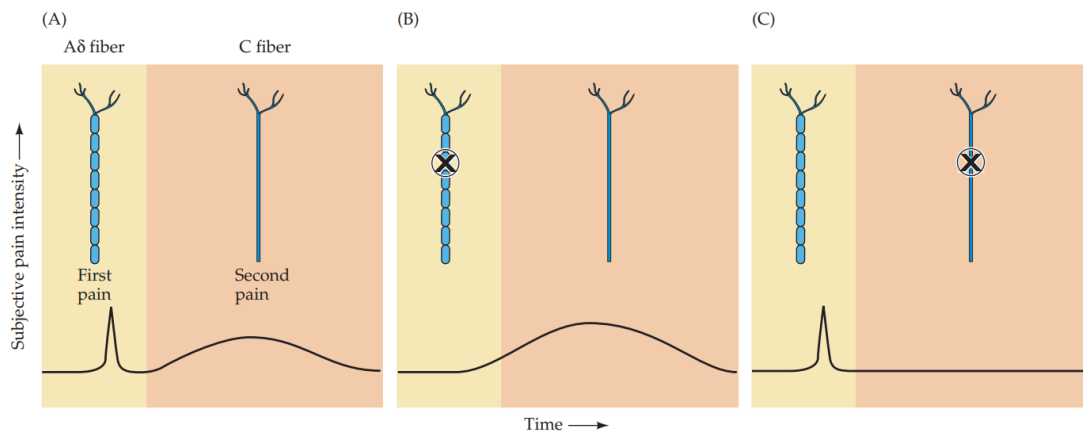


Figure 2.3 – *Fast versus slow pain.* (A) First pain which is sharp and fast is conducted by A δ fibers which are thicker and myelinated. Second pain which is smoother but longer is conducted by C fibers which are thinner and non myelinated. (B) The inhibition of A δ fibers shows the apparition of the second pain only. (C) The inhibition of C fibers shows the apparition of the first pain only. From [Purves, 2004]

2.2.1 Dorsal horn neurons (DHNs)

The neurons of the dorsal horn constitute the first relay of nociceptive information. They are the first site of processing of nociceptive signals such as action potential which are then transmitted to the supra-spinal centers. However, they do not communicate only with nociceptors, since they also receive signals from mechanoreceptors such as A β fibers. The role of dorsal horn neurons is to integrate and modulate the inputs received from nociceptors [De Worm, 2021, Bear et al., 2007]. Thus, a dorsal horn projection neuron receives signals from several mechanoreceptor and nociceptor fibers. Under normal circumstances, this projection neuron only reacts to nociceptive stimuli. This signal is then sent through the spinothalamic pathway. However, it can happen in case of allodynia for example that the projection neuron also reacts to mechanoreceptor stimuli, which results in pain. This phenomenon

is described in more detail in section 2.3.

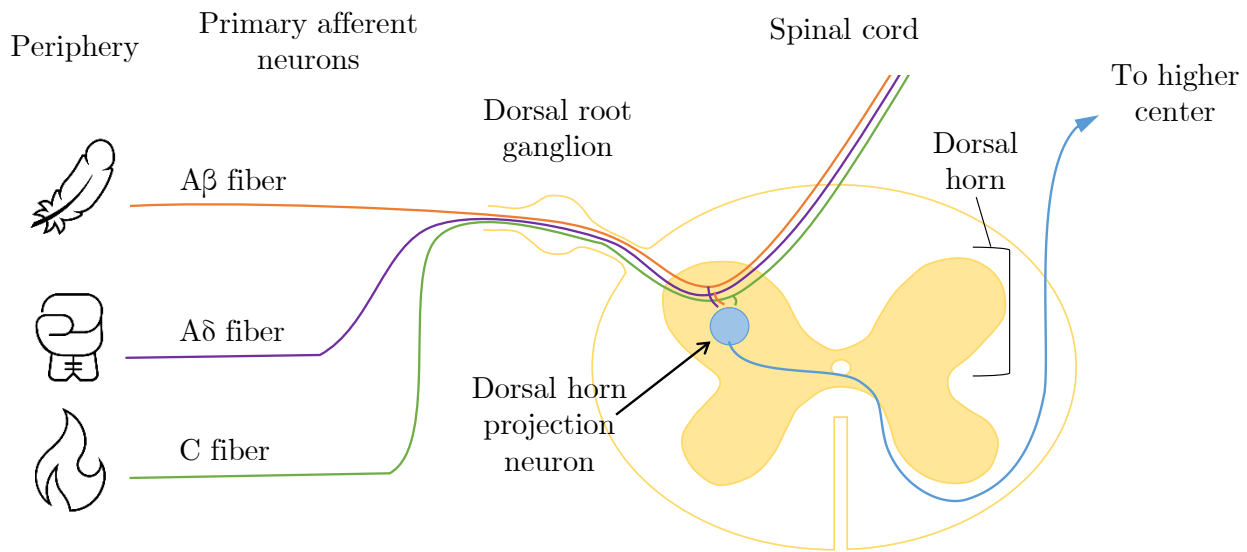


Figure 2.4 – *Representation of the dorsal horn of the spinal cord.* Primary afferent neurons enter the dorsal horn of the spinal cord via the dorsal root ganglion. The fibers meet there some projection neuron of the dorsal horn with which they communicate. Dorsal horn projection neuron send the information to higher center while the fibers continue their path to the spinal cord. *Adapted from [Chr, 2017]*

2.3 Central sensitization

The dorsal horn being an important relay in the pain pathway, it undergoes numerous plasticity mechanisms in order to best regulate pain responses. The most important mechanism is central sensitization which "represents an enhancement in the function of neurons and circuits in nociceptive pathways caused by increases in membrane excitability and synaptic efficacy as well as to reduced inhibition and is a manifestation of the remarkable plasticity of the somatosensory nervous system in response to activity, inflammation, and neural injury" [Latremoliere and Woolf, 2009]. Heterosynaptic plasticity is seen as an important plasticity phenomenon in the spinal cord because it can be initiated by low frequency nociceptive inputs [Tsagareli, 2013].

2.3.1 What is central sensitization?

Central sensitization is characterized by an enhancement of excitability in somatosensory neurons in the dorsal horn of the spinal cord after an intense nociceptive stimulus or nerve injury. This is a good illustration of the plasticity of the somatosensory system in response to inflammation or nerve injury. Central sensitization results in increased sensitivity to pain, particularly dynamic tactile allodynia and secondary or pressure hyperalgesia. It is characterized by a reduction in the pain threshold (allodynia), prolonged effects and intensification of response to noxious stimuli (hyperalgesia) and finally a propagation of the painful area that allows stimuli on uninjured tissues to trigger a painful response (secondary hyperalgesia). In other words neurons of the dorsal horn of the spinal cord subjected to

central sensitization show specific properties such as the development or increase of spontaneous activity, a decrease in the threshold of activation by peripheral stimuli, an increase in the response to supra-threshold stimuli and a widening of their reception field. These properties may be fully or only partially expressed. Central sensitization is involved in inflammatory and neuropathic pain. Thus, it is found in diseases such as migraine or irritable bowel syndrome. An important plasticity phenomenon in central sensitization is the heterosynaptic facilitation. In this type of plasticity, by sensitizing the whole neuron, a group of stimulated synapses can increase or even produce activity in another group of non-activated neighboring synapses. This type of phenomenon never occurs in cortical Long Term Potentiation (LTP, see section 3.2). Central sensitization represents a state where an input to nociceptive fibers (conditioning input) induces an enhancement of the response to noxious or non-noxious, unstimulated fibers (test input) (see Figure 2.5(b)). The conditioning input triggers the C nociceptive fibers while the test input will involve the $A\delta$ and $A\beta$ fibers at medium and low threshold for the appearance of punctate mechanical hyperalgesia and dynamic mechanical allodynia respectively. The central sensitization stems from a homosynaptic dimension to potentiate the C fibers and make them conditioned fibers as well as a heterosynaptic dimension to facilitate the unconditioned fibers. The discovery of central sensitization permitted to admit that the induction of pain wasn't always due to a noxious stimuli [Ji et al., 2003, Latremoliere and Woolf, 2009, Woolf, 2011, Tsagareli, 2013, Klein et al., 2008].

Distinct from central sensitization is the peripheral sensitization, which is an increase in the sensitivity and excitability of nociceptor terminals and which is thus restricted to the site of inflammation. Peripheral sensitization allows weak stimuli to cause pain via the $A\delta$ and C fibers while central sensitization allows low threshold $A\beta$ fibers to produce pain as a result of a change in sensory management in the spinal cord [Tsagareli, 2013]. After a wound, the peripheral terminals of the nociceptors affected by the wound may become more sensitive to the heat stimulus especially by decreasing their threshold. This phenomenon is confined to the wounded area only, making primary hyperalgesia [Woolf, 2011].

As said earlier, central sensitization and peripheral sensitization play an important role in the establishment of two mechanisms observable during an injury: allodynia and hyperalgesia.

- **Allodynia** is defined by the fact that a normally non-painful stimulus causes pain in an injured individual. This painful reaction is evoked by $A\beta$ fibers, from the touch pathway, which normally don't activate pain. There is thus a crosstalk between the paths of the pain fibers and the touch fibers [Sandkühler, 2009, Bear et al., 2007].
- **Hyperalgesia** has a somewhat broader definition, defining the induction of higher than normal pain in response to a painful or non-painful stimulus after injury. Thus, there is an increased pain response to a normally painful stimulus. An injury generally results in two types of hyperalgesia:
 - *Primary hyperalgesia* is targeted to the precise location of the injury. This can be called homotopic hyperalgesia. It is characterized by hypersensitivity to heat and mechanical stimuli.
 - *Secondary hyperalgesia* is a hypersensitivity targeting the non-injured skin around the wound. We can then speak of heterotopic hyperalgesia. It is characterized by hypersensitivity to mechanical stimuli. This second type depends on the central sensitization of spinal excitatory nociceptive neurons.

Primary hyperalgesia is caused by homosynaptic plasticity and peripheral sensitization while secondary hyperalgesia and allodynia are caused by heterosynaptic facilitation only [Woolf, 2011]. However although the exact mechanism of primary and secondary hyperalgesia is not yet fully

understood, Klein and his colleagues found a high correlation between the phenomena observed homotopically and heterotopically, which leads them to believe that heterosynaptic plasticity also has a role to play in primary hyperalgesia [Klein et al., 2008].

2.3.2 Other plasticity phenomena participating in central sensitization

Central sensitization is a general name for hyper-excitability in the dorsal horn. However, there is not only one type of central sensitization. Other mechanisms which can be early onset or late onset have been identified. Here, we'll only focus on the early onset phenomena. Two early onset homosynaptic phenomena have been identified playing a role in the synaptic facilitation in the dorsal horn and thus in the central sensitization: wind up and dorsal horn LTP.

Wind-up

The first phenomenon is the wind up. When *C* fibers are stimulated with noxious stimuli of similar intensity at low frequency, a progressive increase in response is observed throughout the stimulation. Wind up is a phenomenon of homosynaptic plasticity occurring in the dorsal horn of the spinal cord. In the context of pain, this could be illustrated when a heat or pain stimulus is applied several times in a row without changing intensity with the pain felt in response to these stimuli increasing over time. This phenomenon is observed during the stimulation and lasts few tens of seconds afterwards until the membrane returns to its initial potential. This is different from the activity-dependent central sensitization which is translated by a brief, low frequency burst of action potential applied into the central nervous system (CNS) increasing the synaptic efficacy in nociceptive neurons in the dorsal horn. Unlike wind up this phenomenon has been observed lasting for tens of minutes after the end of the stimulation. Central sensitization only needs low level of active nociceptor or not at all to maintain its effect [Woolf, 2011, Li et al., 1999, Mendell, 2022, Woolf, 1996, Thompson et al., 1993].

Dorsal horn LTP

The second mechanism is dorsal horn LTP. As in the hippocampus, a phenomenon of LTP can be observed in the dorsal horn. There is a facilitation of post-synaptic potentials in the dorsal horn in response to a brief train of nociceptive inputs repeated at high frequency. The exact duration of this phenomenon is not known [Ji et al., 2003, Woolf, 2011, Latremoliere and Woolf, 2009].

Figure 2.5, adapted from [Ji et al., 2003] shows the three early onset types of central sensitization. These authors consider the activity-dependent central sensitization as being the heterosynaptic phenomenon governing the general central sensitization. This type of central sensitization is the phenomenon described in subsection 2.3.1 when a strong noxious input activating *C* fibers has the impact of conditioning the $A\beta$ fibers which can now elicit a response [Ji et al., 2003].

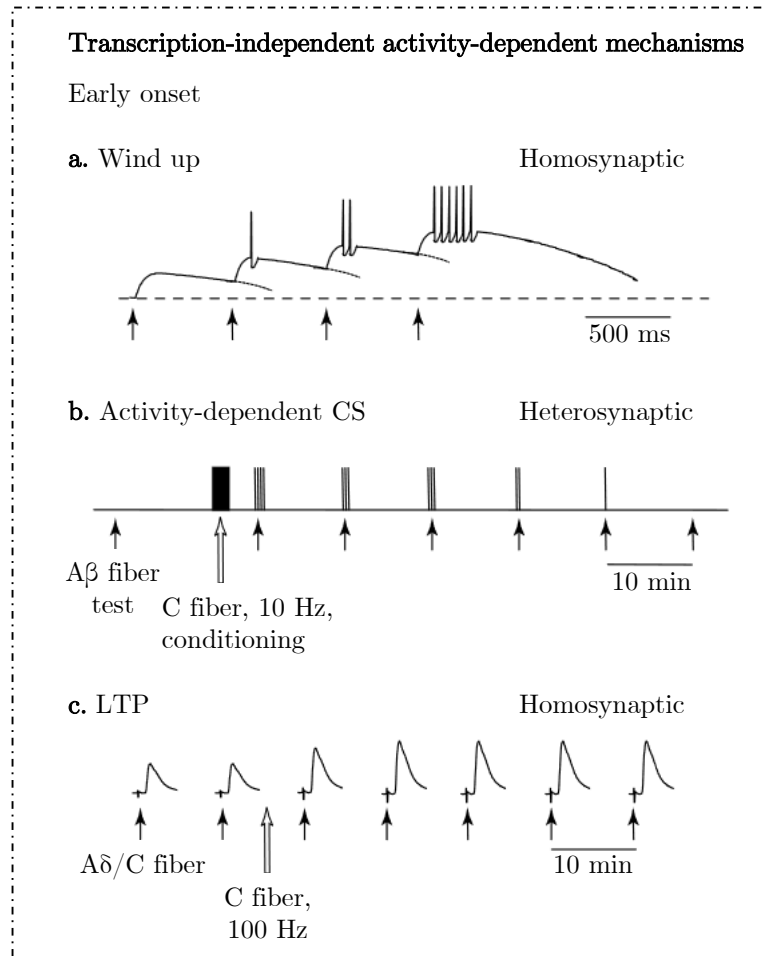


Figure 2.5 – *Three early onset mechanisms of central sensitization.* (a) Wind up is a homosynaptic facilitation phenomenon. Application of the same slightly noxious stimulus repetitively will trigger an enhancement of the reaction of the neuron. Thus the pain experienced will be higher while the intensity of the input stimulus stays constant. It can last for hundreds of milliseconds after the stimulation. (b) Activity-dependent central sensitization is a heterosynaptic facilitation phenomenon. Application of a strong noxious stimulus at 10 Hz will have the impact of conditioning non-noxious fibers through noxious fibers. Thus the activation of *C* fibers will trigger the activation of *A β* fibers which couldn't elicit any response before. It can last for tens of minutes after the stimulation. (c) LTP is a homosynaptic facilitation phenomenon. The application of a strong noxious stimulus at 100 Hz has the impact of facilitating the *A δ /C* fibers for several minutes after the stimulation. *Adapted from* [Ji et al., 2003]

2.4 Summary

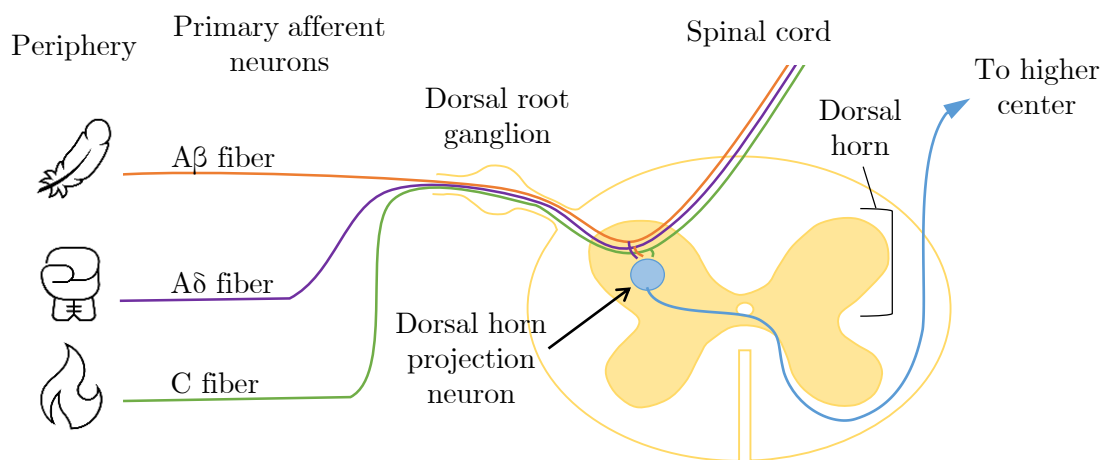
SUMMARY: PAIN

3 types of pain:

- Nociceptive pain
→ Protective
- Inflammatory pain
→ Protective
- Pathological pain
→ Maladaptive

Somatosensory system:

- Mechano-sensory system :
 - Detects touch
 - A α and A β fibers
- Nociceptive system :
 - Detects pain and temperature
 - A δ and C fibers



Central sensitization (CS): Enhancement of excitability in somatosensory neurons in the dorsal horn

- *Wind up*
→ Short term plasticity
- *Activity-dependent CS*
→ Long term plasticity
- *Dorsal horn LTP*
→ Long term plasticity

Situation	Wound	Stimuli	Consequence	Area
Control				
Allodynia:				
Hyperalgesia:				
- Primary				
- Secondary				

Chapter 3

Synaptic plasticity from a biological point of view

3.1 Neuronal communication

Synapses (and synaptic connections) allow communication between different neurons. Synapses connect two neurons: a presynaptic neuron and a postsynaptic neuron. This communication is done by chemical means using neurotransmitters and different ions. The classical communication scheme is as follows (see Figure 3.1):

- First, an action potential reaches the presynaptic neuron, which opens the voltage-dependent ion channels.
- Through these ion channels, an influx of calcium can enter the cell and bind to presynaptic proteins.
- These activated proteins allow the fusion with the neuron membrane of presynaptic vesicles containing neurotransmitters.
- These neurotransmitters are then released into the intersynaptic space and can bind to postsynaptic receptors sensitive to these specific neurotransmitters.
- This binding then induces a postsynaptic cascade that will result in what is called an EPSP (or IPSP) which stands for Excitatory Post Synaptic Potential (or Inhibitory Post Synaptic Potential) [Meriney and Fanselow, 2019].

Synaptic connections are not static means of communication. They are constantly undergoing remodeling. This remodeling is called synaptic plasticity. This means that a synaptic connection uses its own experience to strengthen or weaken itself. Thus the impact of a presynaptic neuron on a postsynaptic neuron is not always the same. There are several types of synaptic plasticity. In this chapter, we will focus on homosynaptic plasticity by describing short-term synaptic plasticity and long-term plasticity [Heidelberger et al., 2014]. Then, we will introduce homeostatic plasticity as well as heterosynaptic plasticity and its particularities. Finally, we will analyze the case of *Aplysia Californica* to illustrate a homosynaptic phenomenon and a heterosynaptic phenomenon.

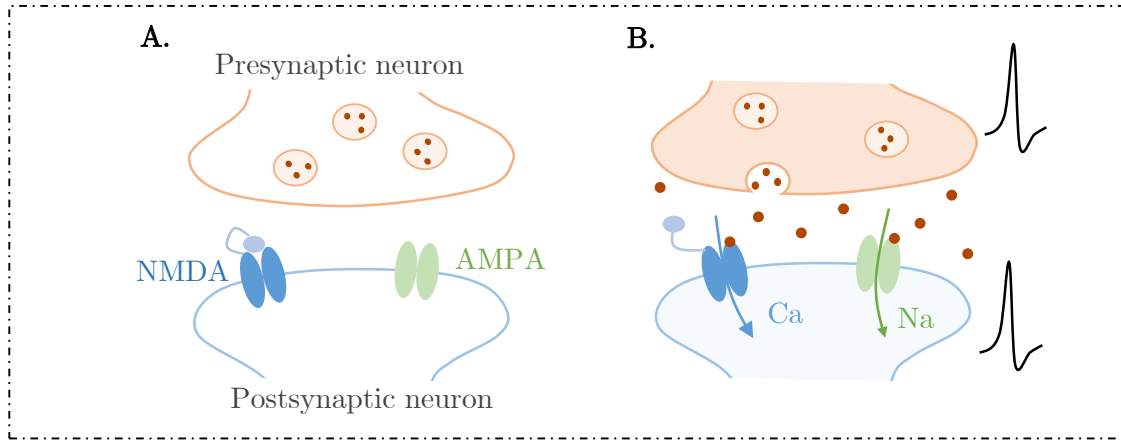


Figure 3.1 – *Synaptic plasticity* (A) Presynaptic and postsynaptic neurons are both inactive. (B) Presynaptic neuron receives an action potential which triggers a cascade leading to the release of neurotransmitters in the intersynaptic space. These neurotransmitters bind to postsynaptic membrane receptors which trigger a postsynaptic cascade leading to the emission of an EPSP or an action potential. *Adapted from [Jacquerie et al., 2022a]*

3.2 Homosynaptic plasticity

3.2.1 Short-term plasticity

Short-term synaptic plasticity is plasticity whose effects last from seconds to minutes. This type of plasticity can cause an increase or a decrease in synaptic transmissions. As explained above, synaptic communication occurs via an action potential at the presynaptic level causing an EPSP (or IPSP) at the postsynaptic level. When two presynaptic action potentials occur within a short period of time (a few milliseconds), the postsynaptic neuron responds to the first action potential in the usual way but the response to the second action potential is different. The second EPSP (or IPSP) may be either larger (referred to as **facilitation**) or smaller (referred to as **depression**). This is called synaptic plasticity. More precisely, paired-pulse plasticity (because of the two action potentials in a short period of time) [Heidelberg et al., 2014].

This facilitation or depression occurs because of the short time interval between the two action potentials. In fact, when the second action potential appears, the events caused by the first action potential are not completed yet. In particular, the calcium ions binding to proteins and the fusion and docking of vesicles. These two events have different effects on the synaptic connection:

- In the case of calcium ions, when the second action potential occurs, the calcium ions related to the first action potential had no time to detach from the proteins to which they were bound. In this case, the flow of calcium ions induced by the second action potential increases the calcium ions load. This results in an increase in the release of neurotransmitters and thus an **increase** in the postsynaptic response.
- Concerning the vesicles, when the second action potential occurs, the vesicles that fused in response to the first action potential are no longer there and it takes some time to renew these vesicles. This is called the vesicle depletion. If the second action potential arrives too quickly, fewer vesicles are available and then less neurotransmitters released, which leads to reduced synaptic communication and a **decrease** in the post-synaptic response [Meriney and Fanselow, 2019].

These two events having opposite effects and appearing at the same time, the final effect on the synaptic connection is determined by the number of calcium ions remaining and the number of vesicles available. In particular, it will depend on the synaptic strength. Indeed, if the synapse is weak, few vesicles will be mobilized during the first action potential. Thus, more vesicles will be available during the second action potential and the synapse will be facilitated. On the other hand, if the synapse is stronger, a lot of calcium will enter the presynaptic neuron during the first action potential, which will cause the fusion of many vesicles and therefore the release of many neurotransmitters. During the second action potential, few vesicles will then be available and the synapse will undergo depression [Meriney and Fanselow, 2019, Minne, 2021]. Then a strong synapse will tend to be depressed while a weak synapse will tend to be facilitated. This can be seen in Figure 3.2.

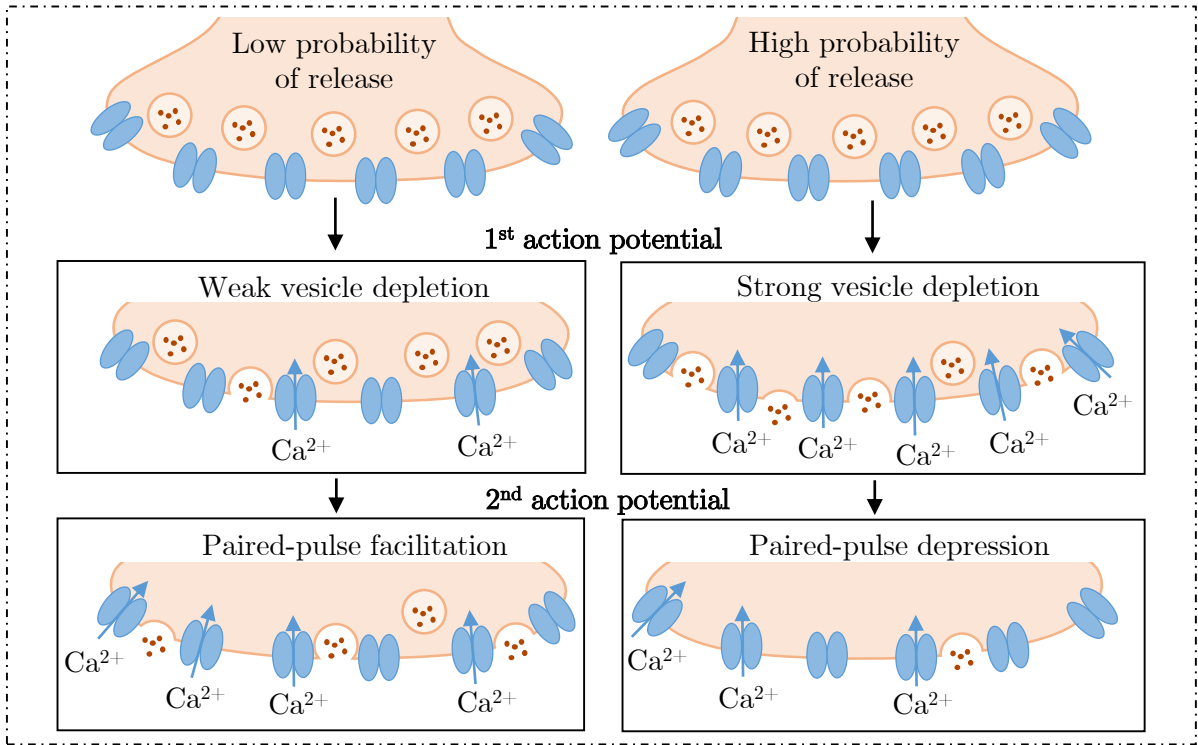


Figure 3.2 – *Mechanisms of short-term plasticity*. A synapse with a low probability of release will release only few vesicles after the 1st action potential. When a second action potential is induced, lots of vesicles are ready to be released. This synapse undergoes facilitation. A synapse with a high probability of release will release lots of vesicles after the 1st action potential. When the second action potential arises, only a few vesicles are ready to be released. This synapse undergoes depression. Adapted from [Meriney and Fanselow, 2019]

3.2.2 Long-term plasticity

Long-term plasticity can last for minutes, hours, weeks or even years [Purves, 2004]. The most studied mechanism is long term potentiation (LTP). It consists of a persistent increase in synaptic strength measured by the amplitude of the EPSP in the post-synaptic neuron [Leprince, 2019]. This potentiation is induced by a train of high frequency stimulations. It has been particularly well studied experimentally in hippocampal synapses since the 1960s by Bliss and Lomo [Bliss and Lomo, 1973]. More particularly, it has been studied at the level of the synaptic connection between Schaffer collaterals (CA3), playing the pre-synaptic role, and the dendrites of pyramidal cells (CA1), playing the

post-synaptic role. In this experimental protocol, it was observed that when the Scaffer collaterals were stimulated at a rate of 2-3 stimuli per minute, EPSPs of constant amplitudes were expressed by the pyramidal cells. On the other hand, when a high frequency stimulation train is applied, an increase in the amplitude of the EPSPs is observed over the long term. This is called long-term potentiation (LTP) [Purves, 2004].

Synaptic plasticity has been described by Donald Hebb in 1949 with the sentence *"When an axon of cell A is near enough to excite a cell B and repeatedly or persistently takes part in firing it, some growth process or metabolic change takes place in one or both cells such that A's efficiency, as one of the cells firing B, is increased"* or *"neurons that fire together wire together"* [Hebb, 1949]. This means that the induction of LTP at a synapse requires the simultaneous activity of the presynaptic and postsynaptic neuron. However, LTP alone cannot be physiologically possible. Indeed, if only LTP was possible, synapses would quickly reach a maximum weight and a general saturation phenomenon would be observed. Therefore another phenomenon called long-term depression (LTD) comes into play to counteract LTP. LTD is the opposite phenomenon of LTP. It consists of a persistent decrease in synaptic strength measured by the amplitude of the EPSP in the post-synaptic neuron. It can be induced by a train of low frequency stimulation (1 Hz) during a period of 10-15 minutes [Purves, 2004].

Properties

LTP and LTD compensate each other. This makes explicit the **bidirectional** property of long-term plasticity. Moreover, long-term plasticity also called Hebbian plasticity is defined by three properties: cooperativity, associativity and input specificity.

- **Cooperativity** expresses the fact that the probability of inducing LTP increases with the number of stimulated afferents. Several axons stimulated at the same time thus cooperate to induce LTP.
- **Associativity** expresses the fact that a weak stimulus is able to induce LTP when a strong stimulation is applied to an afference innervating the same target at the same time. There is therefore an association between the different synapses. Those two first properties define the heterosynaptic plasticity.
- Finally, **input specificity** indicates that when stimulation of one synapse induces LTP, this LTP is not induced in other inactive synapses. This means that LTP is only induced at active synapses [Purves, 2004] [Kandel, 2013]. This is called homosynaptic plasticity.

How does it work?

LTP can be explained by several phenomena. These phenomena can be applied at the presynaptic and postsynaptic level. There are therefore postsynaptic plasticity, presynaptic plasticity and structural plasticity, involving both pre- and postsynaptic phenomena.

Post-synaptic plasticity

From a molecular point of view, the main players in the induction of postsynaptic LTP are the N-methyl-d-aspartic acid receptor (NMDAr) and the α -amino-3-hydroxy-5-methyl-4-isoxazolepropionic acid receptor (AMPA) located on the postsynaptic membrane. These receptors are both receptive to glutamate but have some very important differences.

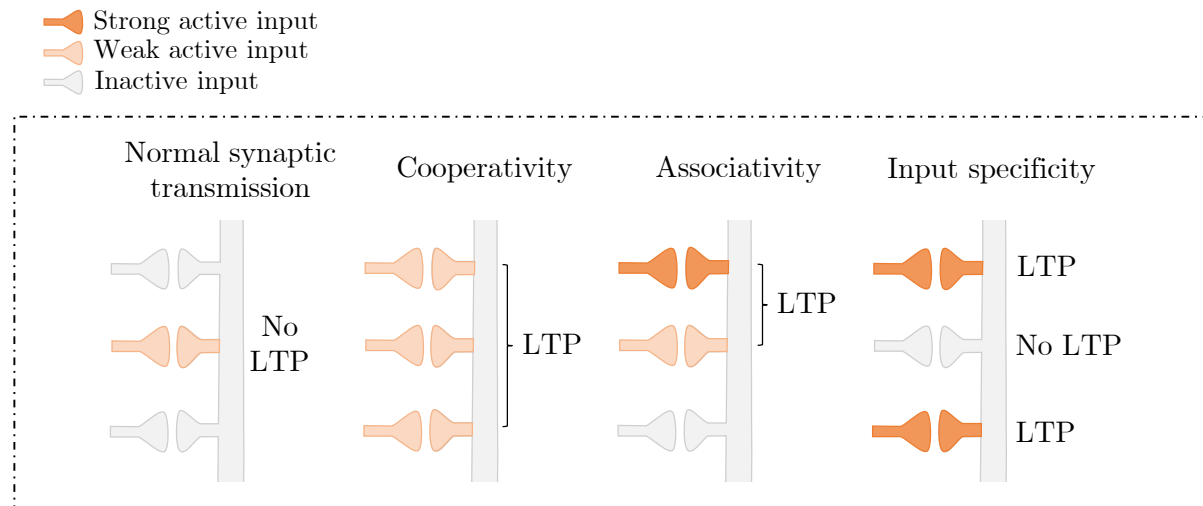


Figure 3.3 – *Hebbian-type plasticity properties*. Long term plasticity is defined by three main properties: cooperativity, associativity and input specificity. *Adapted from [Kandel, 2013]*

- NMDAr have the particularity of being permeable to Ca^{2+} ions when activated by glutamate. At rest, this receptor is blocked by a Mg^{2+} ion acting as a plug. This plug is ejectable when the membrane is depolarized which will permit a Ca^{2+} influx in the cell. It is then said that NMDAr are voltage-dependent.
- AMPAr are only slightly permeable to Ca^{2+} . Moreover, they do not have Mg^{2+} caps and are voltage independent. When they are activated by glutamate, these receptors will let through ions that will have a depolarizing effect on the cell. It is this depolarization that will allow the activation of NMDAr [Purves, 2004].

Then the binding of glutamate induces the activation of AMPAr and the depolarization of the cell. This depolarization linked with the glutamate activate the NMDAr which can let Ca^{2+} entering the cell and triggering the LTP by acting on different proteins (such as CaMKII and PKC) and triggering a cascade of events. Ca^{2+} can also have the effect of maintaining LTP by modifying gene expression and promoting new proteins synthesis [Nicoll, 2017].

Now that LTP is induced, the question is to know how it is expressed. LTP is expressed by a change in the sensitivity of the postsynaptic membrane to glutamate. This is achieved by the insertion of novel AMPAr on the postsynaptic membrane. These new receptors will allow an increase of the reactivity to glutamate and thus a more important LTP. As for the maintenance of LTD, on the other hand, there is a decrease in AMPAr which are sucked up by endocytosis by the post-synaptic membrane.

Pre-synaptic plasticity

In addition to postsynaptic plasticity, there is also presynaptic plasticity. This plasticity is also carried out thanks to the action of calcium which will allow the increase or the decrease of the number of neurotransmitter released by the presynaptic neuron.

Structural plasticity

During LTP establishment, an increase in the number and stability of dendritic spines is observed. Indeed, the volume of dendritic spines may increase with synaptic strengthening or decrease with

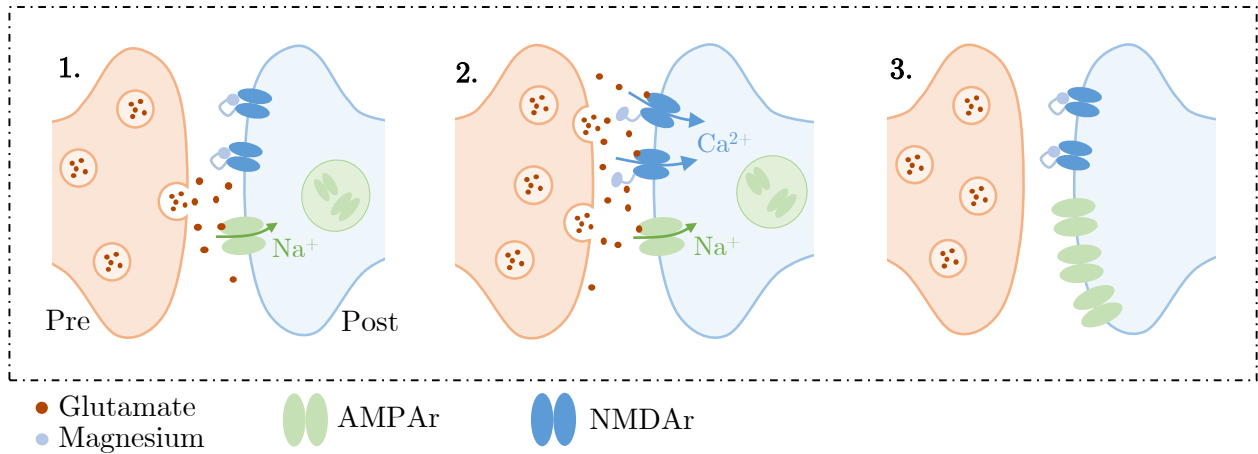


Figure 3.4 – *Post synaptic LTP*. Liberation of neurotransmitters by presynaptic neuron activate AMPAR which depolarize the post synaptic membrane which in turns unlock the NMDAR by removing its Mg^{2+} cap. Neurotransmitter in addition with the depolarization activate the NMDAR through which Ca^{2+} can enter the cell. By a molecular cascade, this triggers the liberation of new AMPAR in the postsynaptic membrane. *Adapted from [Minne, 2021]*

synaptic weakening. When their volume is increased, these spines have a greater number of AMPAR and are said to be more stable. They participate in high synaptic connection. On the other hand, when they are smaller, the spines are more mobile and less stable. They participate in a weaker synaptic connection. This change in volume is again caused by a calcium cascade. Indeed, it is known that the Ca^{2+} entering through NMDA receptors activates CaMKII which has an effect on the actin cytoskeleton and thus participates in the enlargement or not of spines [Nicoll, 2017]. In addition to the increase or decrease in the volume of dendritic spines, we can also observe an increase in the number of spines or a pruning of spines that are no longer needed [Leprince, 2019].

3.2.3 Spike-Timing Dependent Plasticity

Spike-Timing Dependent Plasticity (STDP) is a type of homosynaptic plasticity in which the strength of a synapse is modified as a function of the time delay between the activity of the presynaptic and the postsynaptic neurons constituting the synapse. This was first shown by Bi and Poo in the hippocampus [Bi and Poo, 1998]. They discovered that when the presynaptic neuron spikes within a few milliseconds before the postsynaptic neuron, the synapse formed by those two neurons will be potentiated. Inversely, when the presynaptic neuron spikes within few milliseconds after the postsynaptic neuron, their synapse will be depressed. The shorter the interval between the two spikes, the higher the potentiation or the depression experienced by the synapse will be [Fröhlich, 2016]. Other papers showed later that different results could be obtained for different parts of the brain [Abbott and Nelson, 2000].

Experimental protocol

This phenomenon can be observed through the induction of a pairing protocol in which both presynaptic and postsynaptic neurons are stimulated by the injection of a short current pulse one after the other with a short negative or positive time delay between them. The strength of the synapse is then measured and can be plotted as a function of the time delay between the spikes of the presynaptic and the postsynaptic neurons. This plot is what is called the time window of the synapse

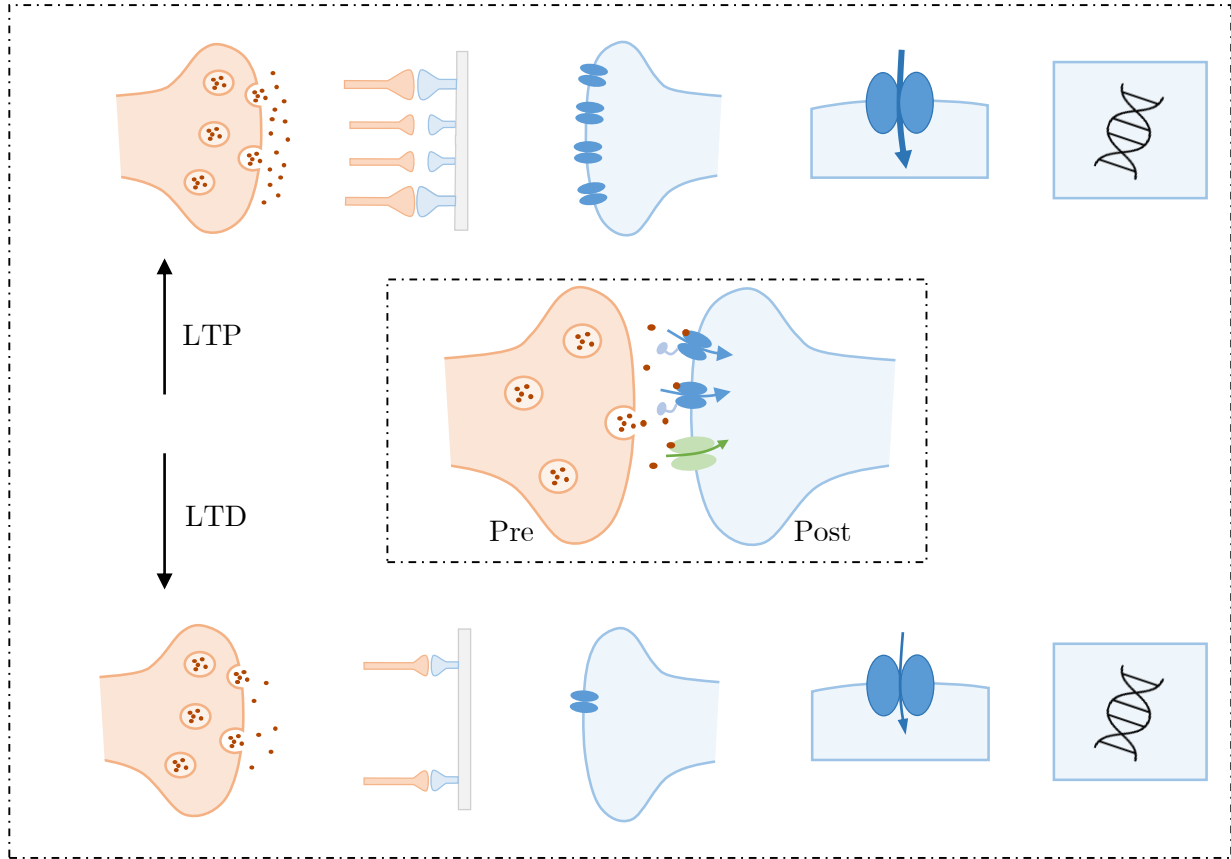


Figure 3.5 – *Summary of the different types of induction of LTP/LTD.* Different types of long term plasticity through presynaptic modifications (orange) and postsynaptic modifications (blue). Those modification can induce LTP or LTD. *Adapted from [Minne, 2021]*

[Sjöström and Gerstner, 2010].

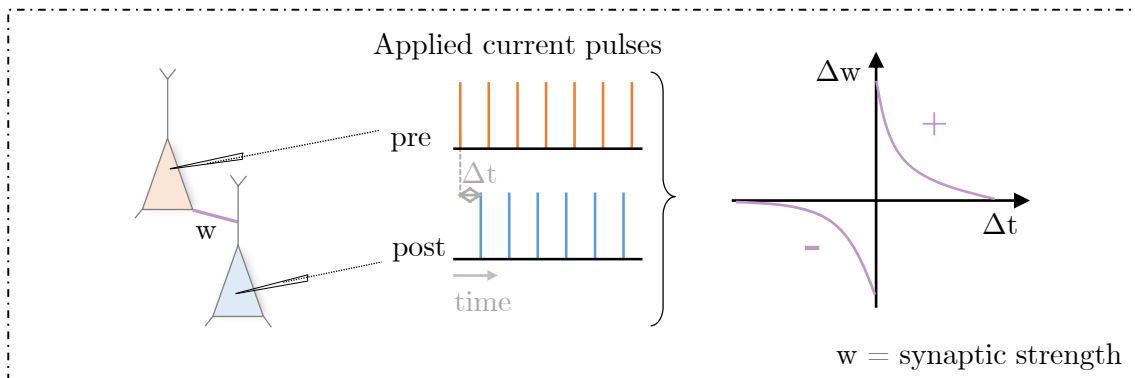


Figure 3.6 – *STDP experimental protocol.* Presynaptic and postsynaptic neurons are stimulated through the injection of short current pulses. The modification of their synaptic strength can then be measured and plotted as a function of the time delay between the time of pre and post applied current pulses. *Adapted from [Jacquerie et al., 2022a]*

3.2.4 Homosynaptic plasticity drawbacks

If STDP can be a good way to explain interaction between neurons and the evolution of the synaptic strength, it happens sometimes that it is not enough. For example, at high frequencies, LTP is favored regardless of the spike timing between the neurons. This lead to two undesirable phenomena: a runaway dynamics and a lack of synaptic competition. Indeed, when a presynaptic and a postsynaptic neuron fire in a correlated manner at a high frequency, this leads to the LTP of their synapse. This increase in the strength of the synapse favor the possibility that those two neurons will spike again in the future in a correlated manner, which would lead to a higher potentiation of their synapse. Thus their synaptic weight will tend to increase continuously until it reaches its maximum value. As a consequence, the firing rate of the postsynaptic neuron would slowly increase, having the impact of being correlated with other presynaptic neurons, uncorrelated until then. Finally, this would lead to a generalization of this synaptic saturation to all the presynaptic neurons. This is what is called "runaway potentiation" [Watt, 2010]. Since all the presynaptic neurons will have the same maximal strength, this lead to another phenomenon: the lack of competition between synapses [Meriney and Fanselow, 2019, Chistiakova et al., 2015, Bannon et al., 2015, Chen et al., 2013]. To avoid these phenomena, other type of plasticity need to be found to support homosynaptic plasticity. In the following sections, we will introduce homeostatic plasticity as well as heterosynaptic plasticity.

3.3 Homeostatic plasticity

A solution to prevent runaway dynamics is **homeostatic plasticity** or synaptic scaling. This form of plasticity has the particularity to scale synaptic weights by increasing or decreasing the strength of all the synaptic inputs of a neuron as a function of activity [Turrigiano et al., 1998]. Thus, the synaptic weight scales up after a long period of inhibition and scales down after a long period of excitation. This implies that synaptic scaling is bidirectional, as homosynaptic plasticity. This scaling appears by taking the form of higher currents to respond to spontaneous and/or evoked vesicle release [Watt, 2010] which has the effect of maintaining a synaptic weight balance. This phenomenon is considered as global, it takes into account all the mechanisms governing synaptic weights. This has the particularity to prevent the runaway mechanisms, to stabilize the synaptic strengths during Hebbian modification and to enhance the synaptic competition [Turrigiano et al., 1998]. However, this form of plasticity presents two major problems which are a very long time scale (of the order of several hours at least) as well as a prolonged (in)activity necessary for the synapses to undergo scaling [Watt, 2010, Bannon et al., 2015].

3.4 Heterosynaptic plasticity

This section introduces heterosynaptic plasticity. In particular, a comparison between homosynaptic and heterosynaptic plasticity is shown and finally, experimental observations of heterosynaptic plasticity phenomena are presented.

3.4.1 Homosynaptic plasticity versus heterosynaptic plasticity

What is the difference between homosynaptic and heterosynaptic plasticity? In Figure 3.7, several synaptic connections are drawn. In particular, we can see a large neuron, the postsynaptic neuron, which is connected to several other neurons, the presynaptic neurons. Now if we focus on the homosynaptic modifications in the middle, we can see that the post-synaptic neuron has interactions with two presynaptic neurons (in orange). Those synapses are active while the two others are inactive since we can see there is no exchange. Thus, the two orange presynaptic neurons are both interacting with the

same postsynaptic neuron. However, those two interactions have no impact on each other and have no impact on the inactive connections either. Then we can see that the homosynaptic rule considers each connection separately. This illustrates the input specificity property explained in subsection 3.2.2.

Now if we focus on the heterosynaptic plasticity on the right, we have the same connections but, this time, we can observe that the interaction between the orange presynaptic neurons and the postsynaptic neuron have an impact on each other. Indeed, if we consider the blue dots as calcium, the calcium exchanged at a synapse propagates into the postsynaptic neuron and impacts other neighbor synapses. Moreover, the presynaptic neurons previously inactive (in grey) interact now with the postsynaptic neuron because of the propagation of the calcium caused by the activity in neighbor synapses. Thus an inactive synapse can become active being influenced by the activity of other synapses. Indeed, heterosynaptic plasticity considers all the connections in a set.

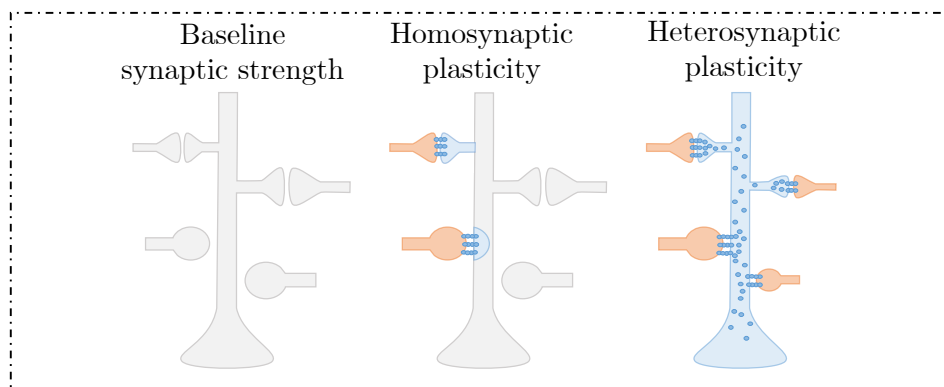


Figure 3.7 – *Comparison between homosynaptic plasticity and heterosynaptic plasticity.* In homosynaptic plasticity, the communication between a presynaptic neuron and a postsynaptic neuron is local. Thus, all synapses are independent from each other. Inactive synapses stay inactive, no matter the activity of other neighboring synapses. In heterosynaptic plasticity, there is a diffusion of the substances. Thus, presynaptic neurons connected to a same postsynaptic neuron have an impact on each other. Moreover, inactive synapses can become activated because of the activity of other synapses connected to the same postsynaptic neuron. *Adapted from [Field et al., 2020]*

3.4.2 Characteristics

Definition

Heterosynaptic plasticity is defined as changes in the synaptic strength induced by activity of adjacent synapses [Meriney and Fanselow, 2019]. It is therefore no longer necessary for the synapse to be active to be modified [Bannon et al., 2015].

Experimental evidences

Experimentally, heterosynaptic plasticity has been discovered in hippocampal cells shortly after the discovery of LTP. Researchers were able to observe that the induction of LTP in apical dendrites provoked the appearance of LTD in basal dendrites, previously inactive. Conversely, the induction of LTP in basal dendrites caused the appearance of LTD in apical dendrites, which were then inactive [Lynch et al., 1977]. These findings went against the theory of input specificity. Indeed, this showed that inactive neighbors of an active synapse can undergo LTP due to the activity of the active synapse [Bannon et al., 2015]. Since then, other experimental results showed that LTD could also induce LTP

at inactive synapses. Moreover, heterosynaptic plasticity does not only induce change in opposite direction. It has been observed that LTP (resp. LTD) could provoke the apparition of lower LTP (resp. LTD) at inactive synapses [Chater and Goda, 2021, Jenks et al., 2021].

Properties

Heterosynaptic plasticity can be classified in three observed types [Jenks et al., 2021]:

- **Compensation:** The type of plasticity discovered by Lynch et al. is a type of compensation mechanism since the depression induced at the inactive synapse could have an homeostatic role to compensate the potentiation of the stimulated synapse [Lynch et al., 1977]. However, it is different from homeostatic plasticity since the depression occurs because of the induction of the LTP. Moreover, it occurs specifically at an inactive synapse and finally, this occurs on a similar timescale as homosynaptic potentiation. By having a compensatory role, heterosynaptic plasticity can counter the runaway mechanism and increase the synaptic competition [Chen et al., 2013, Chistiakova et al., 2014, Bannon et al., 2015].
- **Facilitation:** Heterosynaptic plasticity doesn't act only on inactive synapses. Indeed, it has been shown that induction of LTP by three high frequency stimulus trains could induce longer LTP than the application of a single train [Jenks et al., 2021].
- **Cooperation:** When a synapse receives a stimulus which is not strong enough to induce LTP, a cooperation with other synapses receiving a similar subthreshold stimulus can induce LTP at those synapses. This principle is one of the properties of long term plasticity described in subsection 3.2.2.

In additions of those phenomena, what has been observed is that *distance between the synapses plays a big role in the effects of heterosynaptic plasticity*. Several experimental results were able to put a pattern of influence on the neighboring synapses of the active synapse. What is called a "Mexican hat" profile could indeed be observed around the active synapse. Thus, induction of LTP at one synapse causes lower LTP at its close neighbors, LTD at its farther neighbors and no change at all at the farthest synapses. Similarly, induction of LTD at a synapse causes weaker LTD at its near neighbors, LTP at its farther neighbors, and no change at all at the farthest synapses [Chistiakova et al., 2014, Meriney and Fanselow, 2019, Chater and Goda, 2021]. Thus, this suggests that a diffusion factor or an electrical conductance could mediate heterosynaptic plasticity [Jenks et al., 2021].

3.5 The case of *Aplysia Californica*

Aplysia (or sea slug) is a sea mollusk that has the particularity to have a rather simple nervous system. Indeed, the latter is composed of a few tens of thousands of neurons up to one millimeter in diameter which makes it easy to record and observe. Several very interesting phenomena of synaptic plasticity are observable. In particular habituation (an homosynaptic plasticity phenomenon) and sensitization (an heterosynaptic plasticity phenomenon) have been observed by Kandel and his colleagues [Carew and Kandel, 1973].

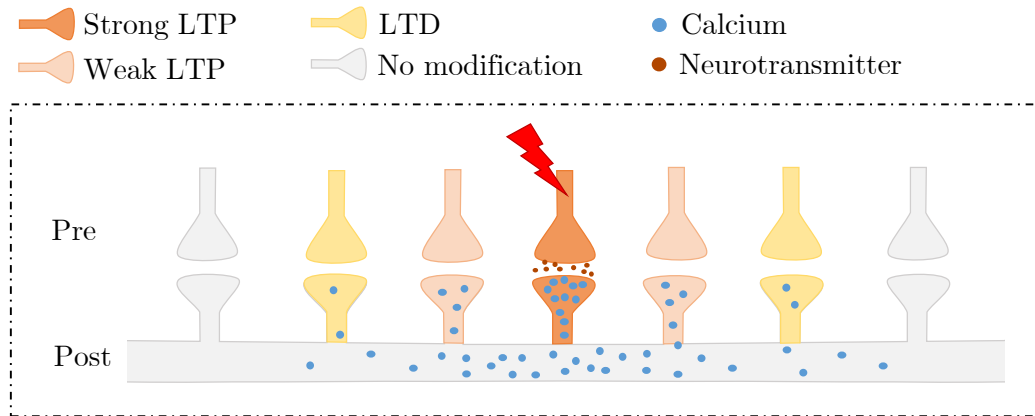


Figure 3.8 – *Mexican hat pattern*. The induction of LTP at an active synapse causes weak LTP at the closest neighbor synapses, LTD at further neighbor synapses and no modification at the furthest neighbor synapses. This pattern can be explained by the diffusion of calcium in the postsynaptic neuron.

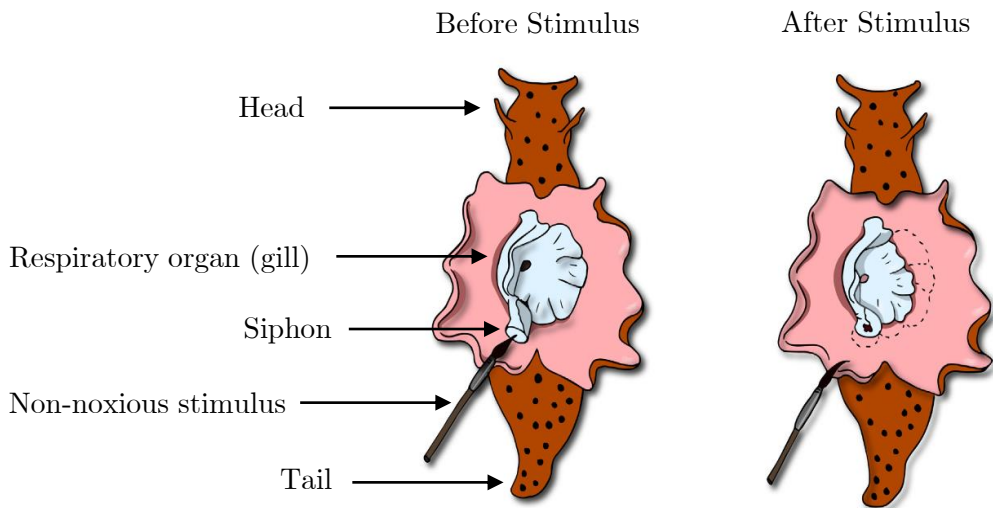


Figure 3.9 – *Description of Aplysia Californica*. *Aplysia* is composed of a head, a tail, a siphon and a respiratory organ. The application of a non-noxious stimulus on the siphon induces a refractory movement of the gill. *Adapted from* [Meriney and Fanselow, 2019]

3.5.1 Habituation

The first interesting phenomenon is **habituation**. This phenomenon shows that if a stimulus is applied repeatedly at low frequency (one per second), the response to that stimulus becomes weaker and weaker [Groves and Thompson, 1970, Kandel, 2013, Purves, 2004]. This phenomenon is also observed in several species including humans with, for example, the rubbing of our clothes on our skin which makes us no longer react after putting them on. But how is this phenomenon observed in *Aplysia*? We can take into account four parts in *Aplysia*: the head, the tail, the siphon and the gill (see Figure 3.9). When a tactile stimulus is applied to the mollusk siphon, a retraction reflex is observed at the gill (see Figure 3.9 on the right). Now if this stimulus is applied repeatedly over a short period of time, we notice that the gill reflex decreases over time. Thus, the retraction movement is less and less strong. This phenomenon is homosynaptic. A sensory presynaptic neuron connected to the siphon acts on a motor post-neuron connected to the gill (visible on Figure 3.10). With each stimulus, the same action

potential is observed at the level of the sensory neuron but the EPSP at the level of the motor neuron progressively decreases and thus causes a less marked retraction. We can differentiate short term habituation whose effects last from second to several hours after the stimulation and long term habituation whose duration of the effects can go up to several weeks [Kandel, 2013, Carew and Kandel, 1973].

3.5.2 Sensitization

The second type of plasticity phenomenon that can be observed in *Aplysia* is **sensitization**. This phenomenon can be observed when a noxious stimulus is applied to the tail of the mollusk and a tactile stimulus on the siphon (the same was applied in the habituation process). This will have the effect of canceling the habituation observed until then and provoke **a strong reaction of the gill in response to the noxious stimulus and to the next non noxious stimuli**. This time this phenomenon involves **heterosynaptic plasticity**. Indeed, the sensory neuron connected to the tail of the mollusk makes its entry via a facilitating neuron. This facilitating neuron acts on the sensory neuron of the siphon, which will have for effect an increase of the exchanges between the sensory neuron of the siphon and the motor neuron of the gill (Figure 3.10).

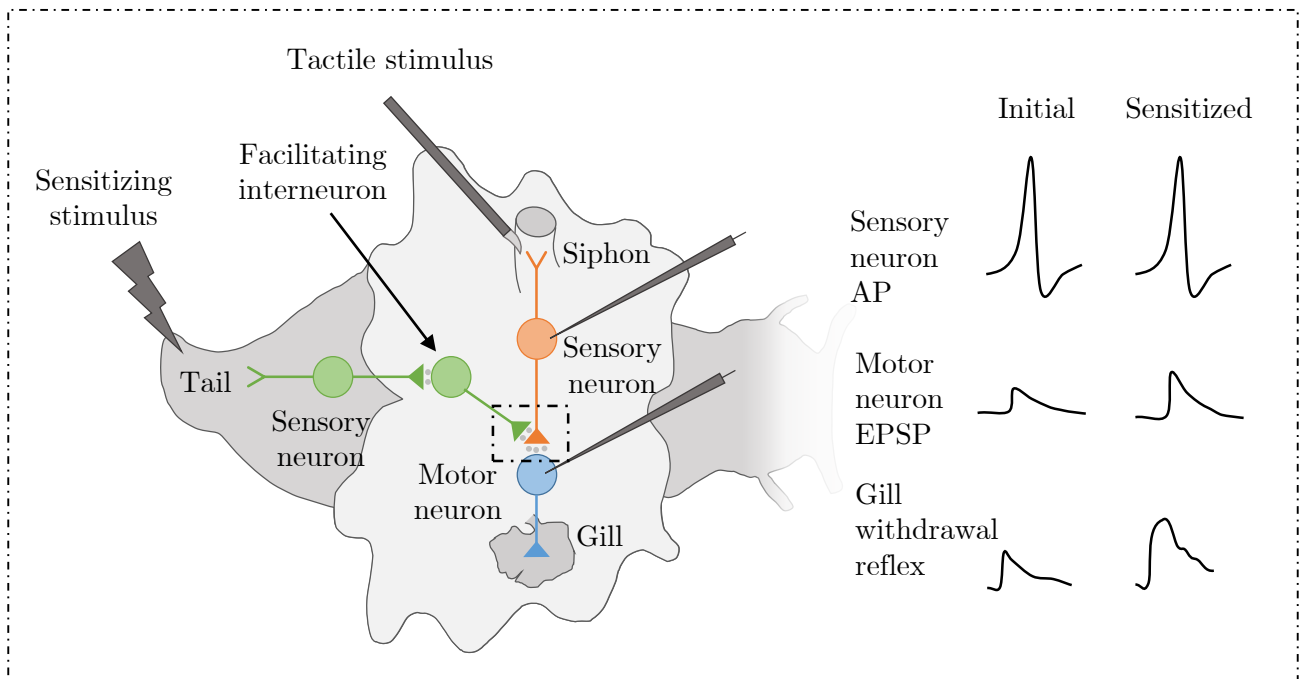


Figure 3.10 – *Neuronal pathway for the induction of habituation and sensitization in Aplysia* In the case of habituation, a tactile stimulus on the siphon activates its sensory neuron connected to the motor neuron of the gill. This is a homosynaptic plasticity phenomenon. In the case of sensitization, a noxious stimulus is applied to the tail which has the effect of activating its sensory neuron. This neuron is connected to the sensory neuron of the siphon via a facilitating interneuron. This connection has the effect to enhance the communication between the sensory neuron of the siphon and the motor neuron of the gill. Thus, the action potential emitted by the sensory neuron of the siphon will induce a larger EPSP from the motor neuron and thus a bigger gill withdrawal reflex. This is an heterosynaptic plasticity phenomenon. *Adapted from* [Kandel, 2013]

This can be explained by a biological process involving neuromodulators (in Figure 3.11):

1. When the tail is stimulated, the facilitatory neuron releases serotonin which binds to G-protein receptors on the surface of the sensory siphon neuron.

2. Activation of these receptors causes the production of cAMP.
3. cAMP binds to protein kinase A (PKA) subunits, resulting in the release of PKA which can then phosphorylate several proteins.
4. In particular, K^+ channels are phosphorylated by PKA. This increases the likelihood that the channels will be closed and thus prolongs the presynaptic action potential.
5. More Ca^{2+} can then enter the neuron.
6. Finally, this influx of calcium increases the number of transmitters released by the sensory presynaptic neuron towards the motor postsynaptic neuron of the gill [Meriney and Fanselow, 2019, Kandel, 2013, Heidelberger et al., 2014].

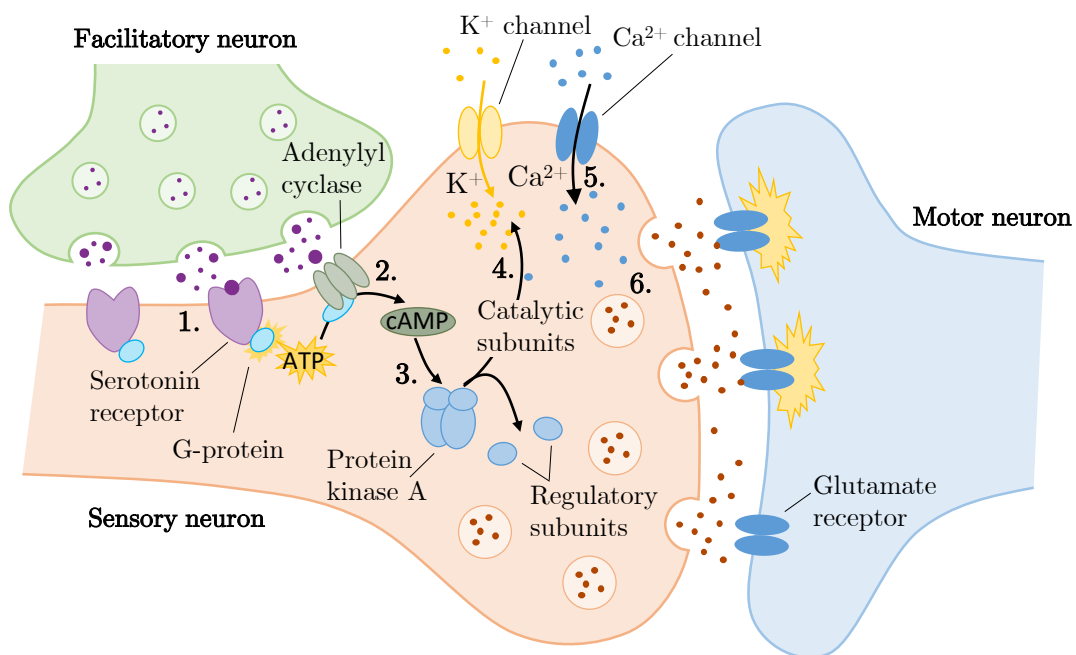
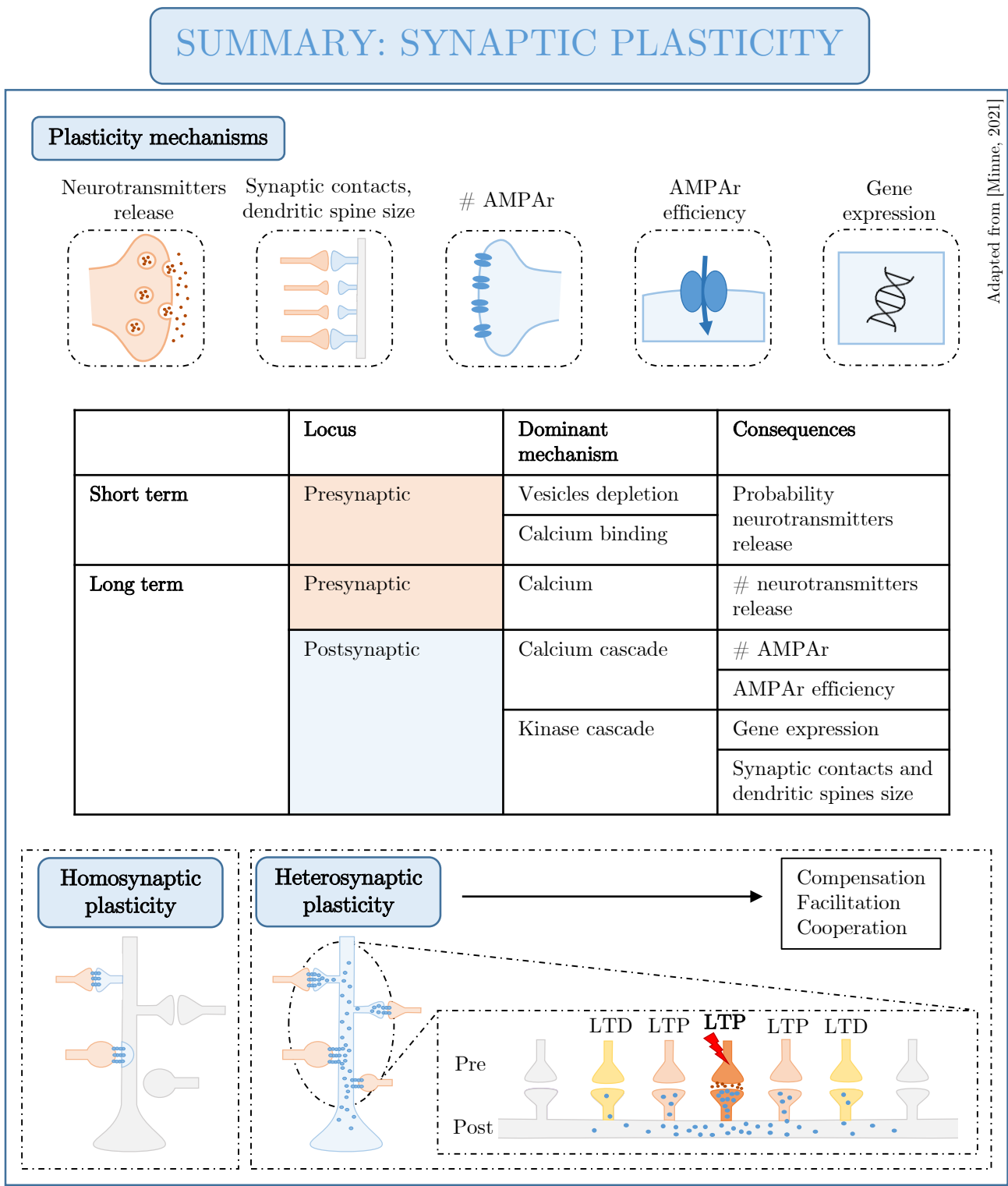


Figure 3.11 – *Molecular cascade happening during the induction of sensitization in Aplysia*. Facilitating neuron releases serotonin which activates G-protein receptor, causing the production of cAMP by adenylyl cyclase. cAMP, by binding to PKA subunits, induces the release of PKA catalytic subunits which can phosphorylate K^+ channels. This has the effect of prolonging the action potential which allows more Ca^{2+} to enter the cell, resulting in the release of more neurotransmitters. *Adapted from* [Purves, 2004]

Sensitization observed in *Aplysia Californica* is a **neuromodulatory** type of heterosynaptic plasticity. Here, we consider an homosynaptic interaction between one presynaptic neuron (the sensory neuron of the siphon) and one postsynaptic neuron (the motor neuron of the gill) on which the heterosynaptic phenomenon intervenes by the action of a second presynaptic neuron (the sensory neuron of the tail) on the first presynaptic neuron. This action, as explained in details before, is performed through the intervention of neuromodulators (here serotonin) which induces a molecular cascade in the first presynaptic neuron. Thus, the neurotransmitters release of the first presynaptic neuron will be increased through the action of the second presynaptic neuron. This is different from the heterosynaptic plasticity we will focus on in this thesis. In the following, we will consider two presynaptic neurons both connected to the same postsynaptic neuron. Heterosynaptic plasticity will be expressed

through the propagation of calcium into the postsynaptic neuron. Figure 3.7 illustrates this type of heterosynaptic plasticity.

3.6 Summary



Chapter 4

Homosynaptic plasticity from a modeling point of view

There are several ways to model homosynaptic plasticity. In particular, two main categories of models exist:

- **Biological models** which will focus on biological phenomena such as the amount of calcium in neurons.
- **Phenomenological models** which will focus on more phenomenological events such as the timing between the spikes of the presynaptic and the postsynaptic neurons.

In this thesis, we have chosen to focus on two homosynaptic models, one of each category. For the biological model, we have chosen a calcium-based model of a synapse in which potentiation and depression are activated above calcium thresholds established by Graupner et al. [Graupner et al., 2016] as implemented in [Jacquerie et al., 2022b]. For the phenomenological model, we have chosen a pair-based model fitted on experimental results obtained with the spike-timing dependent plasticity (STDP) protocol [Morrison et al., 2008]. Those models represent the homosynaptic activity of neurons. Here, we will consider one presynaptic neuron and one postsynaptic neuron. A summary of those models can be seen on Figure 4.1.

4.1 Homosynaptic plasticity with calcium rules

The implementation of the calcium rules is done according to the [Graupner et al., 2016] model implemented in [Jacquerie et al., 2022b]. Those rules model a synapse in which potentiation and depression are activated above calcium thresholds. Thus they take into account the amount of calcium in the neurons constituting the synapse to modify the strength of this synapse. Here, the strength of a synapse is called the weight. To represent the amount of calcium in each neuron and its evolution over time, calcium traces are introduced. This model provides three calcium traces: a trace for the presynaptic neuron, a trace for the post synaptic neuron and finally, a trace for the synapse between the two neurons will be obtained, adding up all the calcium traces of the concerned neurons.

To vary the level of calcium in the different neurons, the following calcium rules are used:

$$\tau_{Ca} \frac{dC^{pre}}{dt} = -C^{pre} + C_{max}^{pre} \delta(t - t^{pre} - D) , \quad (4.1)$$

$$\tau_{Ca} \frac{dC^{post}}{dt} = -C^{post} + C_{max}^{post} \delta(t - t^{post}) , \quad (4.2)$$

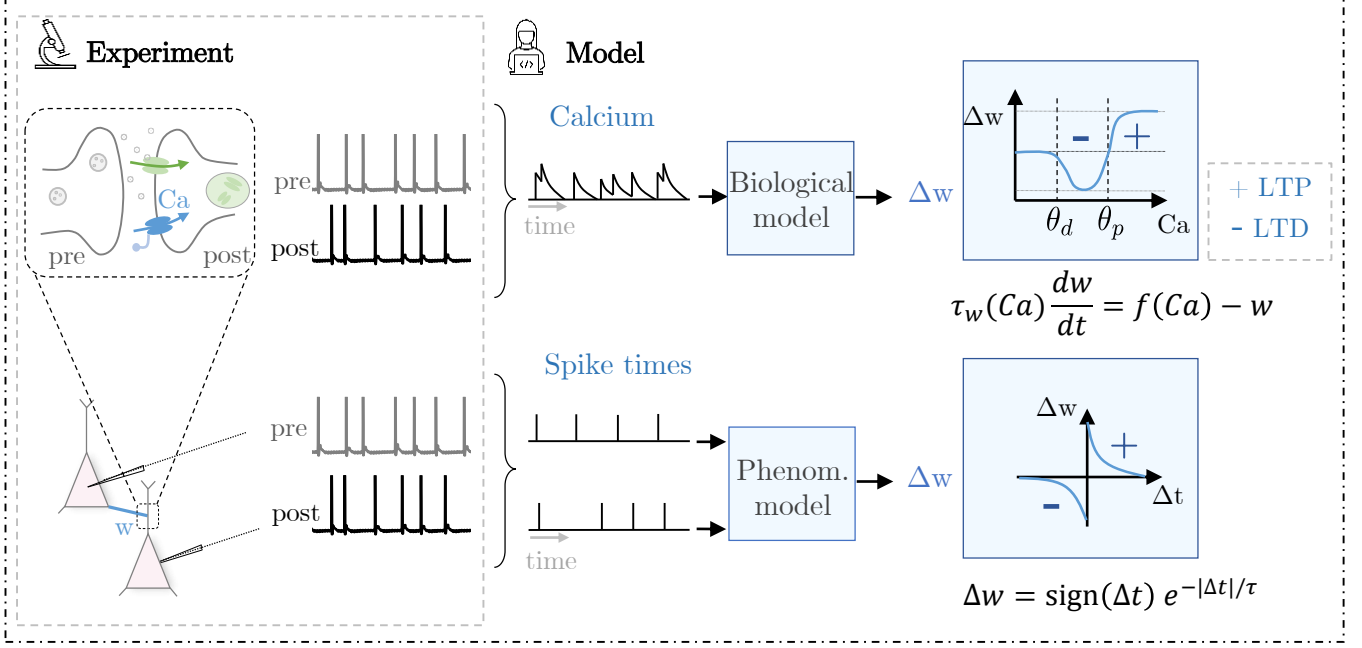


Figure 4.1 – *Two categories of synaptic plasticity model.* Biological models are based on biological mechanisms such as the amount of calcium in a neuron. This calcium-based model uses calcium thresholds to determine the evolution of the synaptic weight. Phenomenological model are based on observation. The pair-based STDP model uses the spike times of presynaptic and postsynaptic neurons to govern the change of the synaptic weight. This model is fitted on experimental results. *Adapted from [Jacquerie et al., 2022a]*

where τ_{Ca} is the rate constant by which a calcium trace decreases, C^{pre} is the calcium concentration of the presynaptic neuron, C_{max}^{pre} is the maximum calcium concentration of the presynaptic neuron, C^{post} is the calcium concentration of the postsynaptic neuron, C_{max}^{post} is the maximum calcium concentration of the postsynaptic neuron, t^{pre} and t^{post} are the spike timings of presynaptic and postsynaptic neuron respectively and $D = 9.53709$ ms is a time delay between the presynaptic spike and its impact on the postsynaptic neuron. It explains the slow time rise of the NMDAr-mediated calcium influx.

These equations express the fact that the calcium level in a cell decreases over time governed by a constant τ_{Ca} . However, as soon as the neuron spikes, the calcium level is set to its maximum value again.

The calcium concentration that drives the change of weight of the synaptic connection is obtained by summing the calcium levels of each neuron constituting this synaptic connection. Thus we have

$$C^{tot} = C^{pre} + C^{post} . \quad (4.3)$$

The weight of a synaptic connection w evolves according to the calcium concentration of the synaptic connection. In particular, two thresholds are introduced: θ_p , the potentiation threshold and θ_d , the depression threshold. If the amount of calcium in the synapse is above θ_p , the synapse will be potentiated. Thus its weight w will evolve following the equation:

$$\tau_w^p \frac{dw}{dt} = \Omega^p - w , \quad \text{if } C^{tot} > \theta_p. \quad (4.4)$$

If the amount of calcium is between θ_d and θ_p , the synapse will be depressed and its weight w will evolve following the equation:

$$\tau_w^d \frac{dw}{dt} = \Omega^d - w, \quad \text{if } \theta_d < C^{tot} < \theta_p. \quad (4.5)$$

Finally, if the amount of calcium is below θ_d , the weight of the synapse will remain stable. In other words, nothing happens and we have

$$\frac{dw}{dt} = 0, \quad \text{if } C^{tot} < \theta_d. \quad (4.6)$$

We simulated the model using a train of four spikes for each neuron for 100 ms. The presynaptic train is generated in such a way that the presynaptic neuron spikes 10 ms before the postsynaptic neuron. The final traces obtained with this implementation can be seen in Figure 4.2.

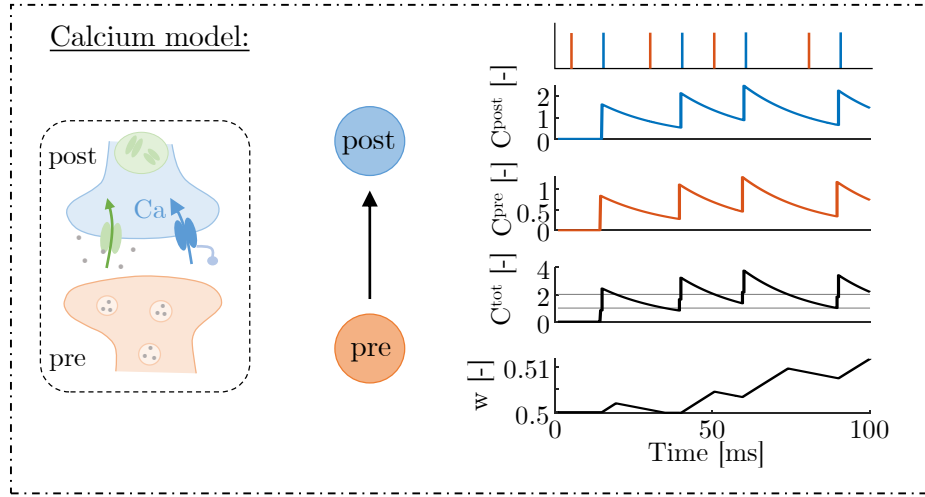


Figure 4.2 – *Simulation of the Graupner's calcium-based model for one synapse formed by one presynaptic neuron and one postsynaptic neuron.* Spike times of each neuron are represented on the top-right (pre in orange, post in blue). The weight of the synapse evolves as a function of the total amount of calcium in each neuron constituting the synapse.

4.2 Homosynaptic plasticity with STDP rules

The phenomenological model chosen in this thesis is a so-called pair-based Spike Timing-Dependent Plasticity (pair-based STDP) model. As its name indicates, this model is based on the timing between the spikes of the presynaptic neuron and the spikes of the postsynaptic neuron. This model has the particularity to be based on experimental data [Bi and Poo, 1998]. Thus, based on the data obtained via an STDP experimental protocol on specific areas of the brain (see subsection 3.2.3), the researchers fitted the experimental data by precisely tuning the parameters of the following equations [Bi and Poo, 2001, van Rossum et al., 2000].

$$\Delta w(\Delta t) = \begin{cases} A_+ e^{-\Delta t/\tau_+}, & \text{for } \Delta t \geq 0 \\ -A_- e^{\Delta t/\tau_-}, & \text{for } \Delta t \leq 0 \end{cases} \quad (4.7)$$

where A_+ and A_- are the constants governing the potentiation or the depression. A_+ is the maximum

amount of potentiation while A_- is the maximum of depression. Δt is the delay between the postsynaptic and the presynaptic spikes. $\Delta t > 0$ means that we are in a pre-post configuration and $\Delta t < 0$ means that we are in a post-pre configuration. Thus STDP rules are designed in such a way that if the presynaptic spike occurs before the postsynaptic spike ($\Delta t > 0$) within the proper time window, the weight of the synapse is increased while if the presynaptic spike occurs after the postsynaptic spike ($\Delta t < 0$) within the proper time window, the weight of the synapse is depressed.

To know the timing of each spikes of the pre and the postsynaptic neurons, we introduce one internal trace for each neuron. Those traces decrease exponentially and are incremented by 1 each time the concerned neuron spikes. Those traces could be seen as the amount of neurotransmitters in the synapse or the amount of calcium in the post synaptic neuron as in a biological model. However, in this model, only the timing of the spikes is necessary. Thus there is no direct need for a biological interpretation. The functions x represent the internal trace of the presynaptic neuron or a low-pass filtered version of the presynaptic spike train and y represents the internal trace of the postsynaptic neuron [Morrison et al., 2008]. The evolution of those functions follows the rules:

$$\tau_+ \frac{dx}{dt} = -x + \delta(t - t^{pre}), \quad (4.8)$$

$$\tau_- \frac{dy}{dt} = -y + \delta(t - t^{post}), \quad (4.9)$$

where τ_+ and τ_- are the time constants governing the decrease of x and y respectively, dx and dy are the changes of the traces x and y over time, and t^{pre} and t^{post} are the spike timing of the presynaptic and postsynaptic neurons respectively.

Thanks to those traces, we can know when the neuron has spiked by looking at the value of the corresponding trace function. This way of retaining internal traces is called the *all to all* method. This means that we consider all previous spikes in the trace of the neuron. Thus, each time a neuron spikes, its trace is **increased by 1**. This method is different from the *nearest-neighbor* method which only considers the single previous spike of the neuron. Thus, each time a neuron spikes, its trace is **set to 1** and can never go beyond [Minne, 2021].

Each time a neuron spikes, the weight will tend to a new value. To know the new weight value w_{new} , two pieces of information are needed. The first is to know if we are in a pre-post or post-pre configuration in order to know if a potentiation or a depression will be applied. Once this information is known, it is necessary to look at the value of the x -function (if we are in a pre-post configuration) or the y -function (if we are in a post-pre configuration). Then, for a pre-post configuration, we have

$$w_{new} = (1 - w) * A_+ * x + w, \quad (4.10)$$

while for a post-pre configuration we have

$$w_{new} = -w * A_- * y + w. \quad (4.11)$$

Finally, if no neuron spikes, w_{new} keeps its previous value:

$$w_{new} = w_{new}. \quad (4.12)$$

Here, we use what we call soft bounds, in contrast with hard bounds. Soft bounds, thanks to a

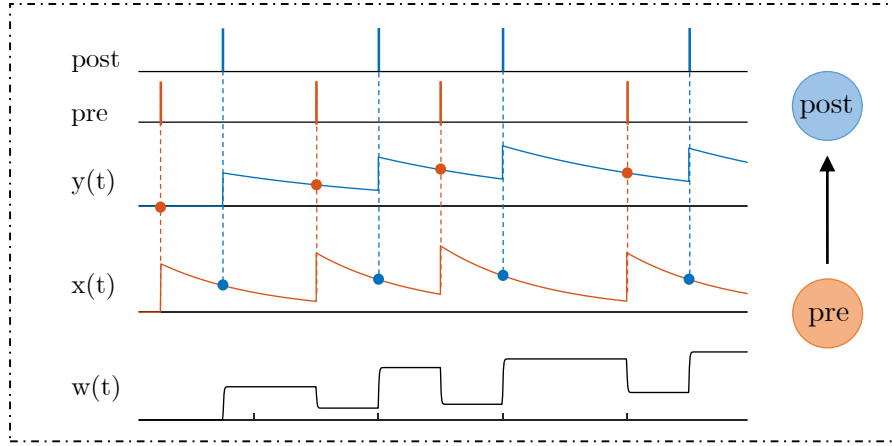


Figure 4.3 – *Evolution of traces over time.* The spikings of the presynaptic and the postsynaptic neurons leave two traces x (in orange) and y (in blue) which decrease exponentially over time and are increased by one at each spike. The weight of the synapse w evolves at each spike. When the presynaptic neuron spikes at a time t , w decreases as a function of the value of the postsynaptic trace y at the same time t . When the postsynaptic neuron spikes at a time t , the synaptic weight w increases as a function of the value of the presynaptic trace x at the same time t . *Adapted from [Morrison et al., 2008]*

multiplication by the terms $1 - w$ and w allow to keep the weight of the synapses between 0 and 1. Thus, the evolution of the weight of a synapse depends on its current weight. On the other hand, the hard bounds let the weight evolve until it reaches the maximum or minimum limit. Thus, in this case, the evolution of the weight of a synapse does not depend on its current weight but is stopped as soon as the limits are reached.

Establishing maximum and minimum weight limits is important in order to be as faithful as possible to biological rules. Indeed, a minimum limit of 0 is necessary so that the weight of a synapse is never negative which would not make sense. Similarly, a maximum limit allows to express that the resources of the neurons are not infinite. When a neuron spikes, it requires the mobilization of calcium for example. Thus, the weight of a synapse cannot continuously increase without a limit, here equal to 1.

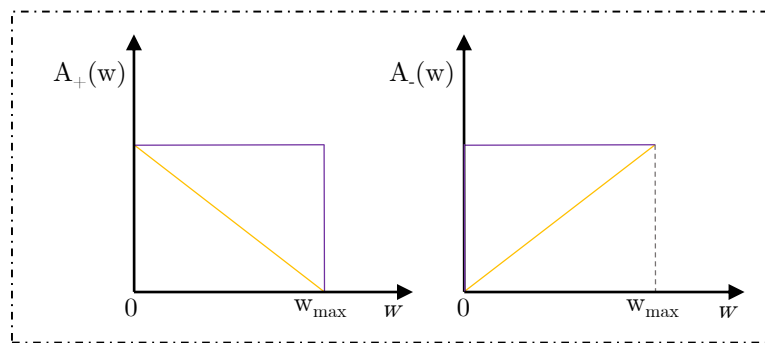


Figure 4.4 – *Soft bounds and hard bounds.* Illustration of soft bounds (yellow) and hard bounds (purple). The potentiation (resp. depression) parameter A_+ (resp. A_-) decreases (resp. increases) with the value of w in order to stay between the minimum and the maximal bounds. *Adapted from [Sjöström and Gerstner, 2010, Minne, 2021]*

Finally, the weight of a synaptic connection evolves as

$$\tau_w \frac{dw}{dt} = (w_{new} - w) \quad (4.13)$$

where τ_w is the time constant governing the convergence of w towards w_{new} , dw is the change of the weight of the synaptic connection, w is the weight of the synaptic connection, and w_{new} is the value to which w converges. τ_w is not really necessary since it only slightly softens the weight change curve. Thus, it is also possible to consider that the weight change is immediate by directly considering

$$w = w_{new} . \quad (4.14)$$

4.3 Summary

In this section, we described two homosynaptic plasticity models that will be our basis for establishing our two new heterosynaptic models. The first model is the calcium-based model illustrating a synapse in which potentiation and depression are activated above calcium thresholds established by [Graupner et al., 2016] and implemented in [Jacquerie et al., 2022b]. This model is based on the amount of calcium C^{tot} in the neurons composing a synapse. They also introduce two threshold θ_d and θ_p . Based on this information, the synaptic weight can be:

- increased if $C^{tot} > \theta_p$,
- decreased if $\theta_d < C^{tot} < \theta_p$,
- unchanged if $C^{tot} < \theta_d$.

The second model is the pair-based model fitted on experimental data obtained with an STDP protocol described in [Morrison et al., 2008]. This model is based on the timing Δt between the spikes of the presynaptic neuron and the spikes of the postsynaptic neuron. Based on this time delay, the synaptic weight can be:

- increased if $\Delta t > 0$,
- decreased if $\Delta t < 0$.

The intensity of the modification experienced by the synaptic weight is governed by internal traces (one for each neuron) which are incremented by 1 each time the neuron in question spikes and decrease exponentially otherwise.

Chapter 5

Heterosynaptic plasticity from a modeling point of view

Modeling heterosynaptic plasticity is not yet very common. Thus, for the moment, few models have been established. In this review, three models illustrating heterosynaptic plasticity rules are presented. The first model, established by Chen and colleagues [Chen et al., 2013], uses a combination of a pair-based and a calcium-based models. The primary goal of this model is to avoid the runaway phenomenon often observed when using homosynaptic STDP models. The second model, established by Field and colleagues [Field et al., 2020], focuses on the cortical excitatory-inhibitory balance which can be controlled by heterosynaptic plasticity. This model focuses on the pairing between presynaptic and postsynaptic inputs. Third, Hiratani and Fukai have established a model of the excitatory-inhibitory balance of a dendrite using spike-timing dependent heterosynaptic plasticity [Hiratani and Fukai, 2017]. Finally, we introduce two heterosynaptic models whose goal is to maintain stability by combining homosynaptic plasticity with other types of plasticity, including heterosynaptic plasticity. First model is established by Chen and Xie [Chen and Xie, 2021]. Second model is established by Zenke et al. [Zenke et al., 2015].

5.1 Runaway phenomenon prevention

Chen et al. developed a model combining homosynaptic pair-based rules and heterosynaptic rules with properties based on the experimental data obtained previously to prevent the runaway mechanism [Chen et al., 2013] [Bannon et al., 2015] [Chistiakova et al., 2015]. Chen and colleagues, with their model, decided to tackle the runaway problem related to STDP rules and other conventional Hebbian plasticity. Indeed, with these types of rules, when a synapse is potentiated, it will have a higher probability of spiking and therefore of being further potentiated in the future. On the other hand, when a synapse is depressed, its probability of spiking will be lower and it will tend to be more and more depressed. This leads to the runaway phenomenon where the synapses have all reached their maximum potentiation or depression value described in subsection 3.2.4. This phenomenon can be circumvented by modulating the rules of synaptic plasticity that dictate the potentiation and depression that synapses undergo.

5.1.1 Computational Model

The computational model is made up of several parts. First part is the model of pyramidal neuron. The authors chose to use an established reduced model of a cortical pyramidal cell which consists of two electrically coupled compartments, dendritic and axosomatic.

For the synaptic currents modeling, one hundred synapses with AMPA-type channels were located at the dendritic compartment. The synaptic current at each synapse was simulated by a first-order activation kinetics.

About the input spike trains: The model neuron received 100 synaptic inputs from 100 presynaptic neurons. Each synaptic input is in the form of spike train with Poisson distributed interspike intervals.

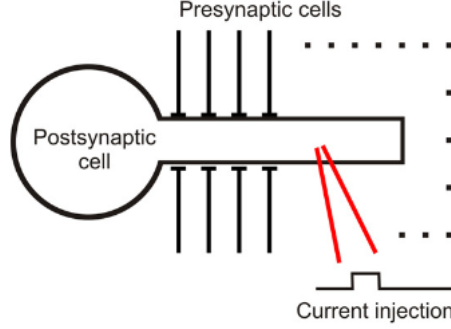


Figure 5.1 – *Illustration of the model neuron* Neuron receives 100 synaptic inputs as current pulses injected in the dendrites. *From [Chen et al., 2013]*

Pair-based STDP model is designed as already described in section 4.2.

Heterosynaptic plasticity is implemented based on their *in vitro* experiments. First, a calcium threshold is set to $0.4\mu\text{M}$ to express the fact that heterosynaptic plasticity was induced in the presence of a rise of intracellular $[\text{Ca}^{2+}]$ in the postsynaptic neuron. Since no experimental data provided an estimation of the threshold of calcium rise, they choose to set this threshold to $0.4\mu\text{M}$ in the standard model but tested other values ranging between 0.2 and $0.8\mu\text{M}$. During the *in vitro* experiments, it has been noticed that "synapses with initially low release probability have a tendency to be potentiated while synapses with initially high release probability tended to be depressed or did not change after intracellular tetanization. Furthermore, the probability of change was higher for the strong or weak synapses but lower for synapses of intermediate strength". Thus when a spike arrives, the algorithm checks if the $[\text{Ca}^{2+}]$ at the postsynaptic level is above the threshold. If so, a probability P is computed such as

$$P = 3000 \times (W_{syn} - W_{max}/2)^2 + 0.1, \quad \text{if } [\text{Ca}^{2+}] > \text{threshold} \quad (5.1)$$

where P is the probability of the synaptic change resulting from heterosynaptic plasticity and the magnitude of synaptic weight change. $P = 0.1$ for synapses with intermediate strength and $P = 0.775$ for synapses with maximal/minimal strength. This probability is then compared to a random variable X generated from a uniform distribution from 0 to 1. If $P > X$, the synaptic weight W_{syn} is changed by dW_{syn} which evolves as

$$dW_{syn} = ([1/(1 + \exp([W_{syn} - (0.5 \times w_{max})]) \times 100)]) - 0.5] + \sigma \times 0.02) \times 0.0001, \quad \text{if } P > X \quad (5.2)$$

where W_{syn} is the current synaptic strength, and $W_{max} = 0.03 \text{ mS/cm}^2$ is the maximal synaptic strength. dW_{syn} indicates the change of synaptic strength and σ is a random variables drawn from Gaussian distribution with mean equaling to zero and SD equal to 3. Thus, plastic changes can only take place when a postsynaptic action potential is generated.

5.1.2 Results

In a first time, Chen studied the effect of intracellular tetanization, consisting of three trains (one per minute) of 10 bursts (1 Hz), each burst containing five pulses (5ms, 100 Hz, 0.4-1.1 nA), on synaptic transmission to layer 2/3 pyramidal neurons in slices of visual and auditory cortex of rats. Since there is no presynaptic stimulation, plastic changes resulting from intracellular tetanization can be considered equivalent to heterosynaptic changes. The results demonstrated experimentally in the paper are consistent with those demonstrated during their previous *in vitro* experiments. Thus when the synaptic plasticity is induced by intracellular postsynaptic tetanization:

- It is induced by an intracellular increase in calcium concentration.
- Heterosynaptic changes can occur at synapses not active during tetanization.
- The direction and amount of synaptic weight change depends on the initial conditions of the synapses: weaker synapses have a greater tendency to be potentiated while stronger synapses have a greater tendency to be depressed.
- The probability of synaptic weight change is higher for strong or weak synapses than for so-called intermediate synapses.

While applying the model, postsynaptic action potentials were first evoked at 1 Hz but frequency weren't high enough to allow the $[Ca^{2+}]$ to be higher than the threshold. This was possible with a frequency of 50 Hz. This allowed the observation of heterosynaptic rules and the confirmation of previous observations.

Computationally, the paper compared STDP rules and STDP rules + heterosynaptic rules. When the model was simulated with STDP rules only (with symmetrical potentiation and depression window) a runaway phenomenon of potentiation and an increase of the firing rate (initially at 1 Hz) were observed. Thus after 100 seconds, all the synapses were at maximum weight (see Figure 5.2(B,C)). On the other hand, when the model was stimulated with STDP rules + heterosynaptic rules, runaway phenomenon and increase of the firing rate were prevented. Thus after 100 seconds, synaptic weights were distributed approximately evenly ((see Figure 5.2(D,E)). Same results could be observed with depression by setting the depression window wider than the potentiation window in the STDP rules. Thus, after 150 seconds, synaptic weights followed a runaway dynamic toward zero and a decreasing of the firing rate (put at 1 Hz for the first 50s, then 2 Hz for the next 50s and 3 Hz for the last 50s) (see Figure 5.2(F,G)). Once again, the add of the heterosynaptic rules to the STDP rules prevented those phenomena and the synaptic weights were distributed approximately evenly after 150 seconds (see Figure 5.2(H,I)). Similar results were obtained by changing the rate of firing, the time scale or even the calcium threshold.

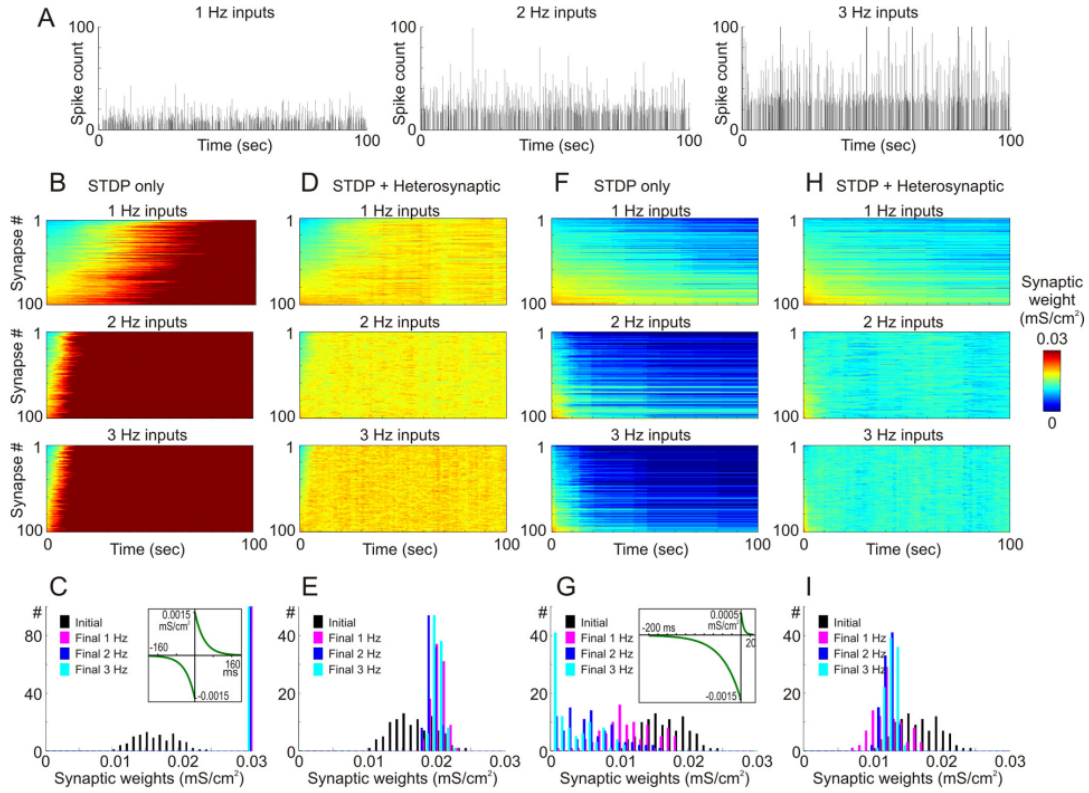


Figure 5.2 – *Heterosynaptic model established by Chen can effectively prevent the synaptic weights from the runaway dynamics* (A) Spike count as a function of time with different frequencies. (B)(C) STDP model with a symmetrical time window induces a potentiation runaway dynamic. (D)(E) Adding the heterosynaptic rules to the STDP model prevents the runaway dynamic and leads to a distribution of the weights. (F)(G) STDP model with an asymmetrical time window favoring depression leads to a depression runaway mechanism. (H)(I) Adding the heterosynaptic rules to the STDP model prevents the runaway mechanism and leads to a distribution of the weights. *From [Chen et al., 2013]*

5.2 Heterosynaptic excitatory-inhibitory balance

As explained in chapter 1, this thesis only focuses on excitatory-excitatory interactions. However, since very few heterosynaptic models are available, it is interesting to see the functioning of models focusing in heterosynaptic excitatory-inhibitory interactions. Two models have been found analyzing this excitatory-inhibitory balance with heterosynaptic plasticity rules.

5.2.1 Effect of pairing presynaptic and postsynaptic activity

Field and colleagues were interested in the balance that takes place between inhibitory and excitatory neurons [Field et al., 2020]. Indeed, when excitatory neurons undergo potentiation, the inhibitory neurons must also undergo potentiation in order to maintain an excitatory-inhibitory (E/I) balance. This balance has no fixed definition but the authors define it as *"the correlation between excitation and inhibition over a stimulus dimension"*. This balance is very important because several experimental and computational studies have reported that a bad balance between inhibition and excitation could cause epileptic or seizure type problems. It is therefore important that this balance is respected and that the mechanisms in place to regulate it are fast and efficient. The known mechanisms are homeostatic adjustments but it has not been proven that it can act in the short term as mentioned in

section 3.3. In this paper, the authors show that pairing presynaptic and postsynaptic activity induces LTP at the paired input and heterosynaptic plasticity at the strongest unpaired input. Thus a study of heterosynaptic plasticity is performed to see its impact on the inhibitory-excitatory balance.

Computational model

The biophysical model is based on 12 input channels, each consisting of 10 excitatory and 10 inhibitory neurons onto a single postsynaptic neuron. The postsynaptic neuron is modeled as a conductance-based leaky integrate-and-fire model where when the membrane potential reaches a certain threshold, a spike is fired and the membrane potential is put back to its reset value.

Homosynaptic plasticity model is based on a pair-based STDP plasticity rule. Those rules govern the weight change of excitatory and inhibitory synaptic inputs. The rules are a little different between excitatory and inhibitory neurons. For an excitatory neuron, if we have a pre-post spike pairing ($\Delta t = t_{post} - t_{pre} \geq 0$), excitatory LTP is observed. If we have a post-pre spike pairing ($\Delta t \leq 0$), excitatory LTD is observed.

$$W^E(\Delta t) = \begin{cases} A^E e^{-\Delta t/\tau^E}, & \text{for } \Delta t \geq 0 \\ -A^E e^{\Delta t/\tau^E}, & \text{for } \Delta t \leq 0 \end{cases} \quad (5.3)$$

On the other hand, for an inhibitory neuron, no matter if we are in pre-post or in post-pre spike pairing, inhibitory LTP is always observed.

$$W^I(\Delta t) = \begin{cases} A^I e^{-\Delta t/\tau^I}, & \text{for } \Delta t \geq 0 \\ A^I e^{\Delta t/\tau^I}, & \text{for } \Delta t \leq 0 \end{cases} \quad (5.4)$$

The synaptic weight evolves as

$$w_j^{E/I} \rightarrow w_j^{E/I} + \eta_w^{E/I} W^{E/I}(\Delta t) \quad (5.5)$$

where η_w^E and η_w^I are the learning rates for excitatory and inhibitory synaptic plasticity respectively.

About the **heterosynaptic plasticity**, the heterosynaptic decrease of the synaptic weights is modeled based on an internal trace. The trace of each synapse increases with an incoming spike: $T_j^{E/I} \rightarrow T_j^{E/I} + w_j^{E/I}$ and otherwise decreases: $\tau_T^{E/I} (dT_j^{E/I}/dt) = -T_j^{E/I}$. Based on the mean trace per input channel $T_c^{E/I}$ where the channel index c ranges from 1 to 12, the synaptic weights corresponding to the maximum trace per channel are decreased by: $w_{c,max}^{E/I} \rightarrow w_{c,max}^{E/I} - \eta_{het}^{E/I} [T_c^{E/I}]_{max}$.

Sometimes, if the synaptic weights for several channels are similar, heterosynaptic plasticity is induced by this mechanism at the channel which was not the best-tuned channel. This is a result of the fact that the internal trace is not a perfectly good measurement of the strength of the synaptic weight.

Owing to the distinction between excitatory and inhibitory plasticity in the STDP rules (i.e. an excitatory cell can be in LTP or LTD while an inhibitory cell can only be in LTP), heterosynaptic inhibitory plasticity is faster than homosynaptic inhibitory plasticity, $\eta_{het}^E < \eta_{het}^I$. To enable the induction of heterosynaptic plasticity only after homosynaptic plasticity, they introduce a learning dependent trace T_{eLTP} , which can switch the heterosynaptic plasticity "on" or "off" based on accumulated excitatory LTP. Following the induction of LTP, $T_{eLTP} \rightarrow T_{eLTP} + \Delta w_j^E$ and otherwise decays exponentially according to $\tau_{T_{eLTP}} (dT_{eLTP}/dt) = -T_{eLTP}$. Whenever T_{eLTP} reaches the threshold θ_{on} ,

heterosynaptic plasticity is switched "on" and implemented as described above. Following the drop of the learning-dependent trace T_{eLTP} below the threshold θ_{off} , heterosynaptic plasticity is switched "off" again.

Finally, the inputs are modeled as Poisson spike trains (75 Hz for each activated input in the paired-phase, 0.5 Hz for all the other channels during the unpaired-phase).

Results

Using an *in vivo* experimental protocol, a probabilistic model and their biophysical model, the authors were able to demonstrate several things including that spike pairing induces STDP and excitatory and inhibitory heterosynaptic plasticity and that heterosynaptic plasticity normalizes the excitatory-inhibitory correlation.

In their experimental model made of 8 channels, they pair a channel with postsynaptic spiking. The other unpaired channels are inactive. They then observe the inhibitory or excitatory synaptic strength of the paired channel, the best unpaired channel and finally another unpaired channel. This allows them to observe the activity of the unpaired channel, which highlights the heterosynaptic plasticity. They are able to observe several scenarios. For a pre-post pairing, LTP is induced at the paired input while LTD is induced at the inhibitory and excitatory unpaired inputs (see Figure 5.3(A)). For a post-pre pairing, excitatory LTD and inhibitory LTP are induced for the paired channel while LTP is induced for the inhibitory and excitatory unpaired channels (see Figure 5.3(B)).

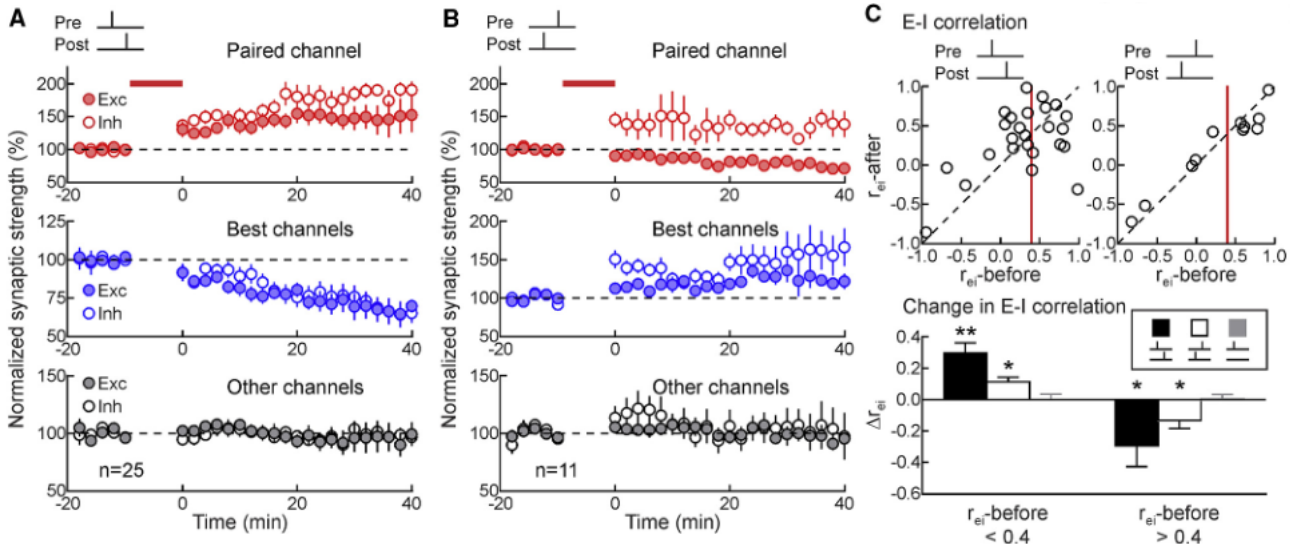


Figure 5.3 – Illustration of the results obtained with heterosynaptic plasticity model established by Field. (A) In a pre-post configuration, the inhibitory and excitatory paired channels experience potentiation. The strongest inhibitory and excitatory unpaired channels experience depression. Other channels don't undergo significant modification. (B) In a post-pre configuration, the inhibitory paired channel experiences potentiation while the excitatory paired channel experiences depression. The strongest inhibitory and excitatory unpaired channels both experience potentiation. The other channels don't undergo significant modifications. (C) A positive increase of the excitatory-inhibitory correlation r_{ei} between the inputs is observed when $r_{ei} < 0.4$ while a negative increase of the correlation between the inputs is observed when $r_{ei} > 0.4$. From [Field et al., 2020]

From a probabilistic side, they spotlight a rising in the inhibitory-excitatory correlation provoked by the spike-pairing. Initially, the EPSCs and the IPSCs were mostly independent from each other. Then, after the pairing, the correlation between the EPSCs and IPSCs amplitudes increases and thus the similarities between the synaptic strength of inhibitory and excitatory neuron increases. Moreover, they also observe that when the excitatory-inhibitory correlation r_{ei} was smaller than 0.4 before the pairing, $\Delta r_{ei} > 0$ is observed. On the other hand, when $r_{ei} > 0.4$, $\Delta r_{ei} < 0$ is observed (see Figure 5.3(C)). This observation was highlighted for only unpaired channels compared with only paired channels (not seen here).

5.2.2 Introduction of heterosynaptic rules in calcium-based homosynaptic models

It has been showed in experimental studies that the difference in spike times in neighboring synapses of a dendritic branch have a significant influence on the efficiency of synapses. This expresses a form of heterosynaptic spike-timing dependent plasticity (h-STDP) which could be important in the synaptic organisation on the dendritic tree. Hiratani and Fukai are interested in the inhibitory/excitatory balance specifically localized in dendritic branches where it is arguably preserved. Thus, to demonstrate the role of heterosynaptic plasticity in the robust achievement of the excitatory-inhibitory balance in dendritic branches, they developed a computational model of h-STDP. This model could reproduce some aspect of the h-STDP observed experimentally in roden. Moreover, it reveals that a temporally precise balance between excitatory and inhibitory inputs timings could be caused by h-STDP because of inhibitory inputs that shunt the LTD to nearby correlated excitatory synapses.

This model can be divided in two parts: the introduction of heterosynaptic rules in calcium-based model and, by extension of the model, a study of the h-STDP in the E/I balance. In the following, we will only describe the first part since the E/I balance is beyond the scope of this thesis and has already been presented in the previous model.

Computational model

The biophysical model reproduces a dendritic spine and, based on this model, a dendritic branch and a dendritic tree.

First, they consider the dynamics of a dendritic spine membrane. The membrane potential of a spine depends mainly on the activation of AMPA and NMDA receptors by presynaptic inputs, the backpropagation of postsynaptic spikes, the leakage currents, and current influx/outflux caused by inhibitory or excitatory synaptic inputs. This is expressed by the equation

$$\frac{du_i(t)}{dt} = -\frac{u_i(t)}{\tau_m} + \gamma_A x_i^A(t) + \gamma_N g_N(u_i) x_i^N(t) + \gamma_{BP} x_i^{BP}(t) - \gamma_I \sum_{j \in \Omega_i^I} x_j^I(t-d_I) + \gamma_E \sum_{j \in \Omega_i^E} x_j^E(t-d_E), \quad (5.6)$$

where u_i is the membrane potential of the spine, τ_m is the membrane time constant, x_i^A and x_i^N are the glutamate concentration at AMPAR and NMDAR respectively, and x_i^{BP} is the effect of backpropagation from the soma. $g_N(u_i) = \alpha_N u_i + \beta_N$ is the voltage dependence of current influx through NMDAR, with α_N and β_N being constant coefficients. This positive feedback is enhanced when additional current is provided through backpropagation. Thus the model reproduces a large depolarization caused by coincident spikes between presynaptic and postsynaptic neurons. AMPA receptor voltage dependence is neglected for more convenience. The last two terms represent heterosynaptic current which is given

as the sum of the inhibitory (resp. excitatory) currents x_j^I (resp. x_j^E) at nearby synapses Ω_i^I and Ω_i^E with delays d_I and d_E . $\gamma_A, \gamma_N, \gamma_{BP}, \gamma_I$ and γ_E are parameters. Γ_E was approximated as a constant. Each input x_i^Q with $Q = A, N, BP, I, E$, is given by

$$\frac{dx_i^Q(t)}{dt} = -\frac{x_i^Q(t)}{\tau_Q} + \sum_{s^k} \delta(t - s^k), \quad (5.7)$$

where s^k is the spike timing of the k th spike.

To model the spine plasticity, they considered the calcium influx to a spine through NMDAr and voltage-dependent calcium channels (VDCC). Following equation gives the calcium concentration at a spine i .

$$\frac{dc_i}{dt} = -\frac{c_i}{\tau_C} + g_N(u_i) x_i^N(t) + g_V(u_i), \quad (5.8)$$

where $g_V(u_i) = a_V u_i$ is the calcium influx through VDCC and $g_N(u_i) x_i^N(t)$ is the influx through NMDAr. In this configuration, Ca^{2+} influx in the spine is suppressed by the hyperpolarization of the membrane potential through inhibitory inputs. An illustration of the model can be seen on Figure 5.4(A).

Calcium concentration in the spine is a key indicator of synaptic plasticity. Several studies have shown that LTP is generally induced at spines with high Ca^{2+} concentration while LTD is generally induced at spines with low Ca^{2+} concentration (see chapter 4). Also, the sign of the plasticity is influenced by the speed of Ca^{2+} . Since existing homosynaptic calcium-based models can efficiently reproduce homosynaptic STDP experimental time windows observed *in vitro* [Graupner and Brunel, 2012, Shouval et al., 2002], they chose to use these models. Hiratani and Fukai's model is then an extension of Graupner and Brunel's model [Graupner and Brunel, 2012]. However, instead of considering a binary synaptic weight, they assumed that a synaptic weight is a continuous variable and they introduced an interim weight variable to ensure that the learning dynamics of synaptic weight is robust. This interim weight variable adds a threshold mechanism with the aim that minor synaptic modulation affecting the synaptic weight is prevented. It represents the approximate concentration of plasticity-related enzymes such as CaMKII or PP1. The interim weight y_i and the synaptic weight w_i are modeled as

$$\frac{dy_i(t)}{dt} = -\frac{y_i(t)}{\tau_y} + C_p[c_i - \theta_p]_+ - C_d[c_i - \theta_d]_+, \quad (5.9)$$

$$\frac{dw_i(t)}{dt} = B_p[y_i - y_{th}]_+ - B_d[-(y_i + y_{th})]_+, \quad (5.10)$$

$[X]_+$ being a sign function that returns 1 if $X \geq 0$ or 0 otherwise. Neural dynamics is defined such that the somatic potential caused by a presynaptic spike linearly depends on its synaptic weight w_i which reflects the amplitude of EPSP. The evolutions of those variables can be seen on Figure 5.4(B).

Results

In this model, presynaptic, postsynaptic and heterosynaptic activities control the calcium level in the spine because of the voltage-dependency of NMDA and VDCC. Moreover, because of the heterosynaptic inhibitory input, a negative regulation is applied to the calcium level through the hyperpolarization of the membrane potential. The model being an extension of the homosynaptic calcium-based model,

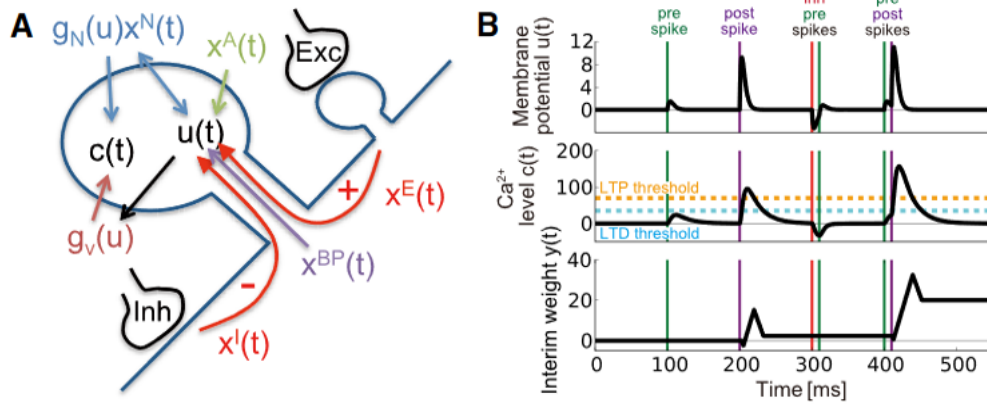


Figure 5.4 – Representation of the heterosynaptic calcium-based model implemented by Hiratani and Fukai. (A) Illustration of the dendritic spine model and the role of each parameters. (B) Dynamics of the membrane potential $u(t)$, amount of calcium $c(t)$ and interim weight variable $y(t)$. From [Hiratani and Fukai, 2017]

it could reproduce various homosynaptic STDP experimental results despite the introduction of the intermediary weight. For instance they could reproduce the dependency of the frequency of the pre-post stimulation on the time window.

Expressing the interactions between excitatory and inhibitory neurons, the model could reproduce several experimental observations:

- In the cortical excitatory neurons, the anti-Hebbian STDP normally observed during a pairwise stimulation protocol switches to a Hebbian type STDP when the GABA-A receptor is blocked.
- Excitatory synaptic plasticity is also disrupted by GABA effects in CA1 pyramidal neurons. Indeed, a post-pre configuration can only induce LTD if GABA uncaging is executed near the excitatory spine immediately before the postsynaptic spike reaches the spine. In contrast, in a pre-post configuration LTP can be induced without the intervention of GABA uncaging.
- An E-E effect can also be observed in CA1 pyramidal neurons. LTD can be observed in neighboring excitatory spines if GABA release is performed just before postsynaptic input. In the absence of GABA, however, this phenomenon is not observed.

A larger coefficient of the heterosynaptic inhibitory effect than the value required for fitting the data from CA1 was required in order to fit the experimental data from the striatum. Thus the CA1 model depends on weaker inhibition than striatum model. Authors also found that the reproduction of the CA1 experimental data is dependant from a high NMDA/AMPA ratio unlike the striatum model which is more robust against this ratio.

In summary, by introducing terms representing heterosynaptic interactions, the authors were able to show that a calcium-based model of plasticity can robustly reproduce several features of plasticity-related interactions between neighboring synapses that occur on a time scale of milliseconds.

5.3 Other models

The three models described above are not the only existing heterosynaptic models. Here we introduce two other heterosynaptic models whose goal is to maintain a stability by combining homosynaptic plasticity with other types of plasticity, including heterosynaptic plasticity.

Chen and Xie established a model a synaptic plasticity model using postsynaptic membrane potential and current density. This model is interesting since it can be used to study both homosynaptic and heterosynaptic plasticity. This is due to the fact that no information on the presynaptic spike is required. This model offers a new way to solve problem of weight out of control such as runaway dynamic in Hebbian learning [Chen and Xie, 2021].

Zenke et al. established a model showing that "the interaction of Hebbian homosynaptic plasticity with rapid non-Hebbian heterosynaptic plasticity is, when complemented with slower homeostatic changes and consolidation, sufficient for assembly formation and memory recall in a spiking recurrent network model of excitatory and inhibitory neurons" [Zenke et al., 2015]. Thus in their model, they consider that a combination between different type of synaptic plasticity was a good option in order to maintain stability. Here, the variation of the synaptic weight is thus dependent from several types of plasticity. Therefore, we have:

$$\frac{d}{dt}w_{ij}(t) = Az_j^+(t)z_i^{slow}(t - \epsilon)S_i(t) \quad \text{triplet LTP} \quad (5.11)$$

$$-B_i(t)z_i^-(t)S_j(t) \quad \text{doublet LTD} \quad (5.12)$$

$$-\beta(w_{ij} - \tilde{w}_{ij}(t))(z_i^-(t - \epsilon))^3S_i(t) \quad \text{heterosynaptic} \quad (5.13)$$

$$+\delta S_j(t). \quad \text{transmitter - induced} \quad (5.14)$$

5.4 Summary

In summary, we described five models illustrating heterosynaptic phenomena. The goal of the model established by [Chen et al., 2013] was to prevent the runaway mechanism and to enhance the synaptic competition. This model is a combination of a pair-based model and a calcium-based model. It uses a calcium threshold and the computation of a probability which is compared with a random variable to govern the weight modification experienced by the synapse. [Chen and Xie, 2021] also wanted to prevent the runaway mechanism. The particularity of this model is that it can model homosynaptic and heterosynaptic plasticity since it doesn't require any information on presynaptic spikes. The objective of [Zenke et al., 2015] by combining several types of plasticity was to maintain stability and thus, prevent the apparition of undesirable dynamics appearing with homosynaptic rules alone. Finally, [Field et al., 2020] and [Hiratani and Fukai, 2017] both established models illustrating the E/I balance which is a bit far from the scope of this thesis. However, the model established by Hiratani and Fukai was particularly interesting since it is an extension of the homosynaptic calcium-based model established by Graupner and Brunel [Graupner and Brunel, 2012].

Those models show different ways to model heterosynaptic plasticity. However, they are quite complex and sometimes difficult to understand properly. In this context, the addition of new heterosynaptic models is necessary to better understand the heterosynaptic phenomena.

Part II

Computational study

Chapter 6

Laying of the foundations

The objective of the computational study is to incorporate heterosynaptic plasticity rules into the two homosynaptic models described in chapter 4. Thus the goal is to obtain two new models in order to simulate heterosynaptic interactions between two synapses. Our new models will be extensions of the calcium-based model and the pair-based STDP model presented earlier. However, the adaptation of those models requires the establishment of some protocols and the creation of spike trains in order to simulate the new models in established conditions. This chapter explains the creation of the spike trains and the establishment of different protocols which will be used in our future experiments.

6.1 Choice of neurons

Homosynaptic plasticity models only need to simulate two neurons, one neuron postsynaptic and one neuron presynaptic, those neurons constituting one synapse. In order to model heterosynaptic plasticity phenomenon, we now are in need of more neurons. Indeed, as explained in section 3.4, heterosynaptic plasticity is expressed as the fact that the activity of two presynaptic neurons connected to the same postsynaptic neuron have an impact on each other. Thus, activity in one synapse will impact the activity of another synapse and eventually modify its strength. Therefore, we need more than one synapse to model heterosynaptic plasticity. In this thesis, we chose to model **two presynaptic neurons and one postsynaptic neuron**. The presynaptic neurons are both connected to the same postsynaptic neuron with which they form synapses as schematized in Figure 6.1.

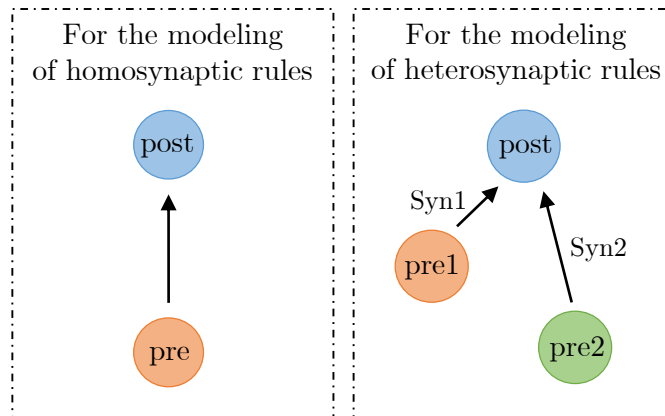


Figure 6.1 – *Neuron model*. Illustration of the synapse used in homosynaptic model and synapses which will be used in our heterosynaptic models.

6.2 Spike train with a Poisson process

Experimental observations reveal that neurons do not spike in a perfectly regular way. Thus, in order to reproduce reality as faithfully as possible, we have chosen to generate a spike train according to a Poisson process. Poisson process is a counting process which is widely used to simulate events which happen at a certain rate but randomly in a time interval [Pishro-Nik, 2014]. To do this, we generated a vector of random variables X taken according to an exponential law adjustable with a parameter λ . Thus we have

$$X \sim \text{Exp}(\lambda), \quad (6.1)$$

such as

$$f_X(x) = \lambda e^{-\lambda x}, \quad \text{for } x \in [0, \infty]. \quad (6.2)$$

Each of these random variables represents time of occurrence of a spike. Adding these variables one by one allowed us to obtain a vector representing the spike times during a given time interval. Hence, we have:

$$T_{\text{spike}_i} = T_{\text{spike}_{i-1}} + X, \quad (6.3)$$

where T_{spike_i} is the spike timing of the i th spike and X is random variable distributed on an exponential law. In order to have a spike-frequency of about 20 spikes per second, parameter λ was set to 50. Hence, in average, one spike every 50 ms is generated. This frequency has been chosen randomly but can easily be changed if needed.

Since we have two presynaptic neurons (pre_1 and pre_2) and one postsynaptic neuron ($post$), we need three trains of spikes. The Poisson train corresponds to the postsynaptic train. In order to have a correspondance between the pre and the postsynaptic neurons, we choose to generate the presynaptic trains according to a Gaussian distribution related to the postsynaptic train. This Gaussian distribution can be centered on the postsynaptic spike times themselves or with a delay. Centering this distribution in $(T_{\text{spike}}^{\text{post}} - 10)$ will favor a pre-post pattern, while centering the distribution in $(T_{\text{spike}}^{\text{post}} + 10)$ will favor a post-pre pattern. Centering this distribution in $T_{\text{spike}}^{\text{post}}$ would not favor any pattern and the results would be more difficult to interpret. Indeed, in precedent homosynaptic models, it has been proven that the time delay between the spike timing of pre and $post$ can favor the potentiation or the depression of the synapse. Making pre spike 10 ms before $post$ would favor potentiation of the synapse while making pre spike 10 ms after $post$ would favor depression. Centering the Gaussian distribution on the spike times of $post$ would not favor any pattern.

In this thesis, with the aim of favoring the pre-post scheme, the Gaussian distribution has been centered in $(T_{\text{spike}}^{\text{post}} - 10)$ for the two presynaptic neurons. A scheme of the three trains is visible in Figure 6.2.

Finally, in order to be able to compare our results from one simulation to another, we choose to generate five times those three trains and to keep those trains exactly the same from one simulation to another. Under those conditions, it will be feasible to compare results obtained after different simulations.

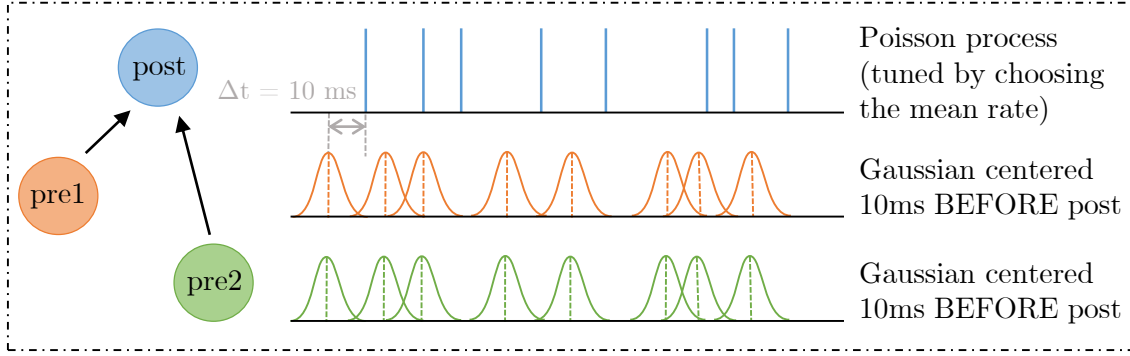


Figure 6.2 – *Spike trains of presynaptic and postsynaptic neurons*. Spike train of postsynaptic neuron is done via a Poisson process whose rate can be tuned thanks to a parameter λ defining the mean time between two spikes. Spike trains of presynaptic neurons are done via a Gaussian distribution centered 10 ms before the postsynaptic spikes.

6.3 Protocols

In order to simulate our models in different situations, we had to establish different protocols by choosing the frequency of the trains or the activity of each neuron. By having different protocols, we will be able to reproduce some results observed in the literature. Five protocols are established here.

6.3.1 First two protocols: Homosynaptic protocols

The two first protocols are homosynaptic protocols. In those protocols, we only have one presynaptic neuron and one postsynaptic neuron. In the first protocol only the postsynaptic neuron is active while the presynaptic neuron is kept silent. In the second protocol, the two neurons are active (see Figure 6.3). In this configuration, we use the five Poisson trains described earlier at a frequency of 20 Hz. This frequency has been chosen to begin with the simulations. Moreover, it has been shown in [Graupner et al., 2016] that synaptic weight undergoes potentiation at this frequency with a delay of 10 ms between the spike timing of *pre* and *post*. In those conditions, we know what we can expect from the results.

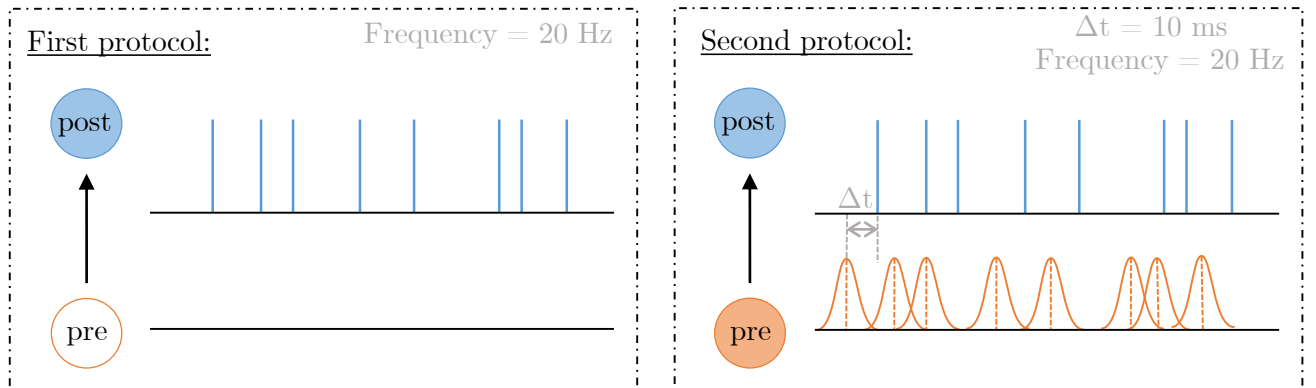


Figure 6.3 – *Homosynaptic protocols*. Homosynaptic protocols involve one presynaptic neuron and one postsynaptic neuron. First protocol keeps the presynaptic neuron silent. Both neurons are active in the second protocol. Spike trains used are the Poisson trains described earlier.

Simulating the homosynaptic models will allow us to compare our future heterosynaptic results with

homosynaptic results. This is important for the discussion and to see what are the changes brought in by our new models.

6.3.2 Third protocol

The third protocol is a protocol where only one presynaptic neuron is active. In this configuration, the post synaptic neuron and the second presynaptic neuron don't spike on their own. Moreover, the train is generated with a frequency of 100 Hz. This frequency is much higher than 20 Hz because in this case, making this new protocol will allow us to try to reproduce results showed in [Chistiakova et al., 2014]. Moreover, we are not in the case of [Graupner et al., 2016] anymore since we don't have pre-post or post-pre pattern and thus no delay between them.

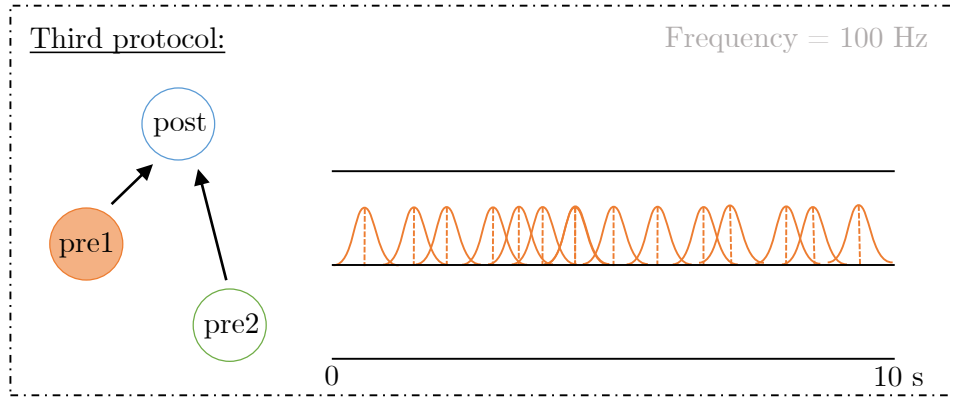


Figure 6.4 – *Third protocol*. Of the three neurons, only the first presynaptic neuron is active at a frequency of 100 Hz. Simulation lasts for 10 seconds.

6.3.3 Fourth protocol

Fourth protocol shows two presynaptic neurons and one postsynaptic neuron but only one of the presynaptic neuron is active, the other being maintained silent. The spike trains used here are the five Poisson trains described earlier with a frequency of 20 Hz. This protocol can be compared with the first homosynaptic protocol.

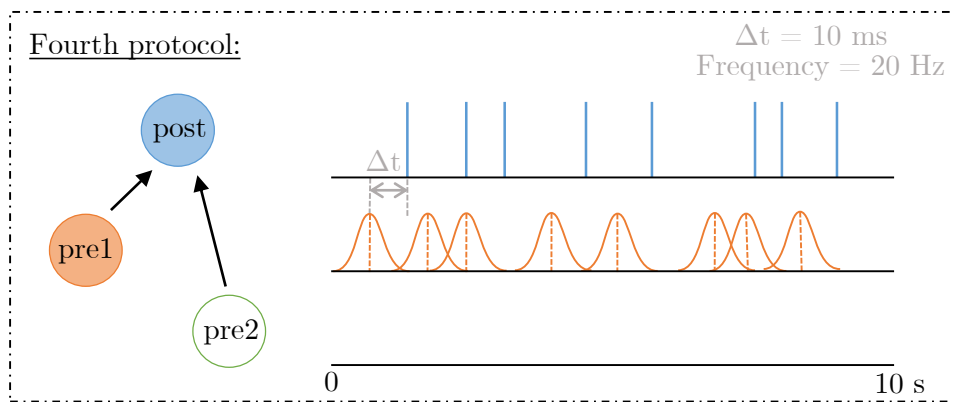


Figure 6.5 – *Fourth protocol*. Of the two presynaptic neurons, only one is active and the is kept silent. Post synaptic neuron is active. The spike trains have a frequency on 20 Hz and a delay of +10 ms. Simulation lasts for 10 seconds.

6.3.4 Fifth protocol

Fifth protocol shows two presynaptic neurons and one postsynaptic neuron, all active. Once again the spike trains used are the five Poisson trains described earlier with a frequency of 20 Hz. This protocol can be compared with the second homosynaptic protocol.

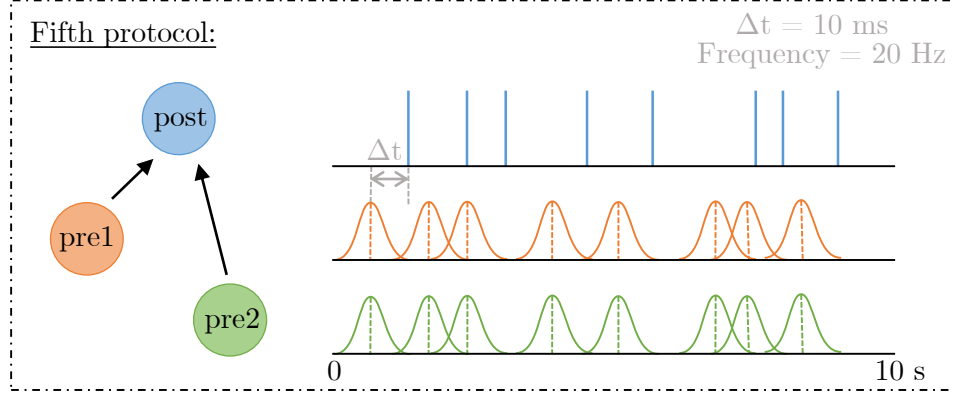


Figure 6.6 – *Fifth protocol*. The three neurons are active with Poisson spike trains with a frequency of 20 Hz and a delay of +10 ms. Simulation lasts for 10 seconds.

6.3.5 Sixth protocol

Finally, the sixth protocol is the simulation of the STDP experimental protocol. This model will present two presynaptic neurons and one postsynaptic neuron. Only one of the presynaptic neurons will be stimulated while the second will be kept silent. In this protocol, our neurons will be stimulated with a constant spike train of 1 Hz for 60 pulses. Several simulations will be performed for different delays going from -80 to 80 ms between the two spike trains. This will provide results in the form of kernels (i.e. time windows). This protocol being simulated with our model, it has not yet been performed experimentally. The goal of those type of kernels is to be confirmed by real experimental STDP protocol. Therefore, real experimental STDP protocols should be latter applied to validate these kernels.

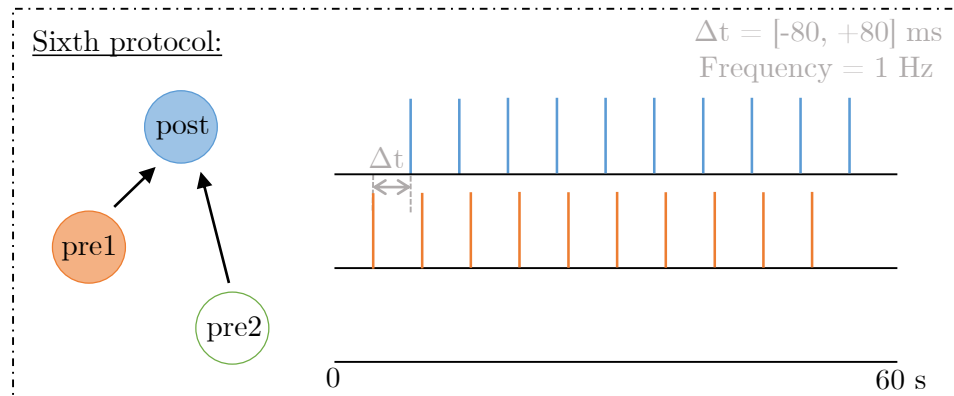


Figure 6.7 – *Sixth protocol*. Postsynaptic neuron and first presynaptic neuron are active. Second presynaptic neuron is maintained silent. The spike trains are composed of 60 pulses at 1 Hz for 60 seconds. The time delay between *pre1* and *post* varies from -80 ms to +80 ms.

Chapter 7

Integration of heterosynaptic rules in the different models

We have chosen to add heterosynaptic plasticity rules to the two homosynaptic models described in section 4.1. Thus, the models presented here are extensions of the calcium-based model developed by Graupner [Graupner et al., 2016] and implemented in [Jacquerie et al., 2022b] and the pair-based STDP model presented in [Morrison et al., 2008]. This chapter is dedicated to the implementation of the new heterosynaptic rules and the exploration of the results obtained when simulating the new models with the protocols established in chapter 6.

7.1 Modelisation of postsynaptic membrane

In both models, we chose to model a network of three neurons composed of two presynaptic neurons and one postsynaptic neuron. The evolution of the membrane potential of the postsynaptic neuron is governed by a Hodgkin and Huxley type conductance-based model in which the two presynaptic neurons are modeled as current pulses I_{syn1} and I_{syn2} :

$$C \frac{dV}{dt} = - \sum_n g_{ion} (V - V_{ion}) + I_{app} + I_{step} + (w_1/n_{cell})I_{syn1} + (w_2/n_{cell})I_{syn2} \quad (7.1)$$

where C is the capacitance of the membrane, dV is the change of the potential of the membrane, g_{ion} is the ion conductance, $V_m - V_{ion}$ is the difference between the potential of the membrane and the equilibrium potential of each ion, I_{app} is the applied current representing an external stimulus, I_{step} is the postsynaptic stimulus, I_{syn1} and I_{syn2} are the presynaptic current pulses and w_1 and w_2 are the weights of the two synapses and n_{cell} is the number of presynaptic cells. In our case, this number is equal to 2 since we have two presynaptic neuron as explained earlier.

When the postsynaptic neuron spikes, $I_{step} = 50$. When the first (resp. second) synaptic neuron spikes, $I_{syn1} = 9.8$ (resp. $I_{syn2} = 9.8$). 9.8 is the limit value to obtain an EPSP from the postsynaptic neuron and not a spike in response to the activity of the presynaptic neurons. Values of other parameters as well as a detailed description of the Hodgkin and Huxley model are shown in Appendix B.

7.2 Heterosynaptic plasticity with calcium rules

Previously, homosynaptic plasticity was only considered with one synaptic connection at a time. Regardless of the number of presynaptic neurons, only active neurons were involved and each pre-post relationship was independent of the others. Heterosynaptic plasticity does not see things the same

way. For heterosynaptic plasticity, if two presynaptic neurons communicate with the same postsynaptic neuron, these two relationships will have an impact on each other. If we look at the level of calcium exchanges, the relationship between *pre1* and *post* neurons causes an entry of calcium into the postsynaptic neuron and a change in the weight of this synapse. As the postsynaptic neuron is also in communication with *pre2*, the calcium concentration of *post* in contact with synapse 2 will be slightly modified because of the exchange between *pre1* and *post*. This change in calcium concentration will induce a change of the synaptic weight. My work here is therefore to understand how and to what extent this synaptic weight is modified. Here, we then have

$$\begin{aligned}\frac{dw_1}{dt} &= f([Ca_1], [Ca_2]) \\ \frac{dw_2}{dt} &= f([Ca_2], [Ca_1])\end{aligned}\tag{7.2}$$

7.2.1 Description of the model

We started with the homosynaptic calcium-based model of a synapse in which potentiation and depression are activated above calcium thresholds established by [Graupner et al., 2016] as implemented in [Jacquie et al., 2022b] described in section 4.1. The addition of heterosynaptic rules to this model will link the two presynaptic neurons (*pre1* and *pre2*). Thus, when *pre1* spikes, this spike will impact not only the calcium trace of *pre1* but also that of *pre2*. Then the evolution of calcium traces in the model becomes

$$\tau_{Ca} \frac{dC_i^{pre}}{dt} = -C_i^{pre} + C_{i,max}^{pre} \delta(t - t_i^{pre} - D) + \boxed{\alpha C_{j,max}^{pre} \delta(t - t_j^{pre} - D)}\tag{7.3}$$

$$\tau_{Ca} \frac{dC^{post}}{dt} = -C^{post} + C_{max}^{post} \delta(t - t^{post})\tag{7.4}$$

with the modification in box, where τ_{Ca} is the time constant governing the evolution of calcium concentration, C_i^{pre} , C_j^{pre} and C^{post} are the calcium concentration of presynaptic i , j and postsynaptic neuron respectively, $C_{i,max}^{pre}$, $C_{j,max}^{pre}$ and C_{max}^{post} are the maximum calcium concentration of presynaptic i , j and postsynaptic neuron respectively, D is a delay between the spike time of presynaptic neurons i and j (t_i^{pre} and t_j^{pre}) and the change in C_i^{pre} and C_j^{pre} . This expresses the fact that there is a delay between the onset of the presynaptic spike and the calcium entry resulting from this spike (see section 4.1). Finally, α is a new parameter governing heterosynaptic rules. This parameter will be analysed later.

The equations governing the change in synaptic weights as well as the thresholds determined in the homosynaptic model remain the same (see section 4.1).

The equations governing the evolution of the synaptic weights are not directly modified from the original homosynaptic model. However, they are modified in an indirect way. Indeed, the evolution of the synaptic weight depends on the calcium concentration of the synapse. Hence the modification of the rules governing the neuronal calcium concentration has an impact on the weight evolution. Thus, if the presynaptic neuron i spikes, the calcium concentration related to the synapse j will be increased and the chances of potentiation will be increased.

7.2.2 Methodology

Figure 7.1 illustrates an example of the simulation of our new model. In this configuration, we used the fourth protocol and put parameter α to 0.4. Poisson train 1 was used. We can see that, even if pre_2 is silenced, its calcium trace evolves thanks to the spikes generated by pre_1 . Thus, the weight of synapse 2 changes even if pre_2 is inactive. However, since $\alpha = 0.4$, the calcium in synapse 2 is lower than it would be if pre_2 was active in an homosynaptic configuration. Because of that, the calcium threshold θ_p is less often crossed and the weight of synapse 2 is then less increased than the weight of synapse 1. At the end of the simulation, synapse 1 has been more potentiated than synapse 2. But would it be the case for all values of α ? We have to analyze this parameter to understand what is its functionality in our new model.

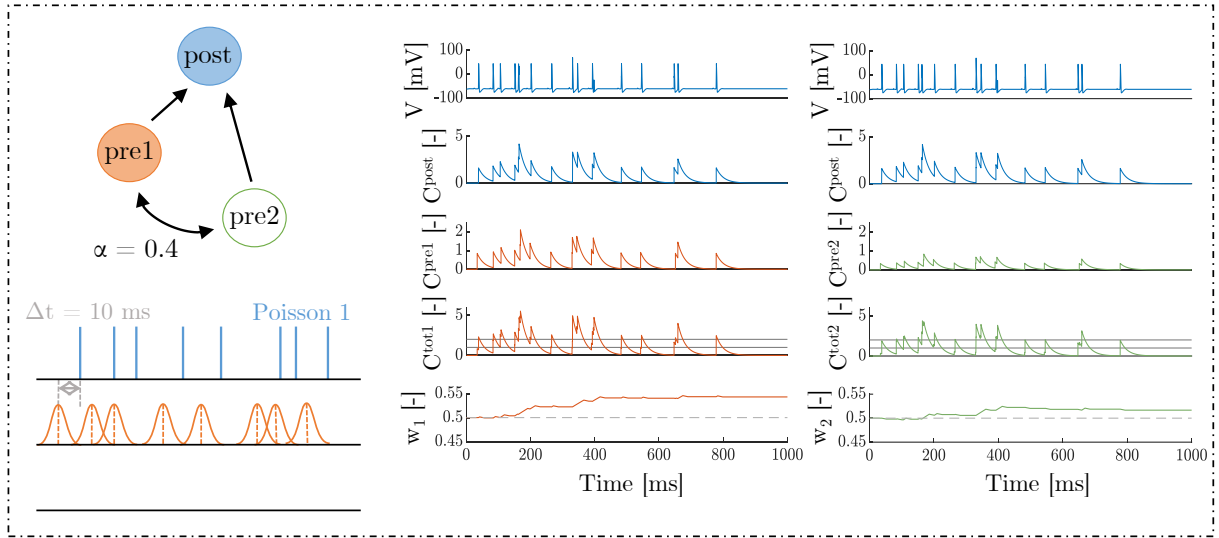


Figure 7.1 – *Example of calcium-based simulation with protocol 4 and $\alpha = 0.4$ for the first Poisson spike train.* In blue, membrane potential and calcium concentration of postsynaptic neuron. In orange, calcium concentration of pre_1 , sum of the calcium of synapse 1 and synaptic weight evolution of synapse 1. In green, calcium concentration of pre_2 , sum of calcium of synapse 2 and synaptic weight evolution of synapse 2. A potentiation of the synaptic weight is observed for both synapses. Synapse 1 is more potentiated than synapse 2. Because of the heterosynaptic dimension of the model, synapse 2 has been potentiated even if it was inactive.

Analysis of parameter α

α is a parameter added to the equation in order to define the heterosynaptic plasticity. This parameter governs the impact of pre_1 on pre_2 and vice-versa. To analyze the effect of α on the evolution of the synaptic weight, we simulated our new calcium-based heterosynaptic model for $\alpha = 0, 0.4, 0.8, 1.2, 1.6$ with each of the six protocols described in chapter 6. From these simulations, we extracted the final weight (after 10 s) of each synapse which allowed us to establish a link between the final synaptic weight w_f and α .

7.2.3 Results

This section presents results obtained after the simulations of our heterosynaptic model with the six protocols described in chapter 6.

Homosynaptic protocols

Figure 7.2 represents the data obtained when simulating the calcium-based homosynaptic model with the first two protocols. First protocol is equivalent to simulate our heterosynaptic model when keeping the two presynaptic neurons silent. Second protocol is equivalent to simulate our heterosynaptic model when keeping the presynaptic neuron 2 silent. In the two protocols, synaptic weight is independant from α since we are in homosynaptic plasticity. With the first protocol, the synaptic weight is close to the initial weight and a slight potentiation of the synapse can be observed. With the second protocol, synapse has been highly potentiated. The results obtained with those two protocols will be compared with the results of the fourth and the fifth protocols in the next sections.

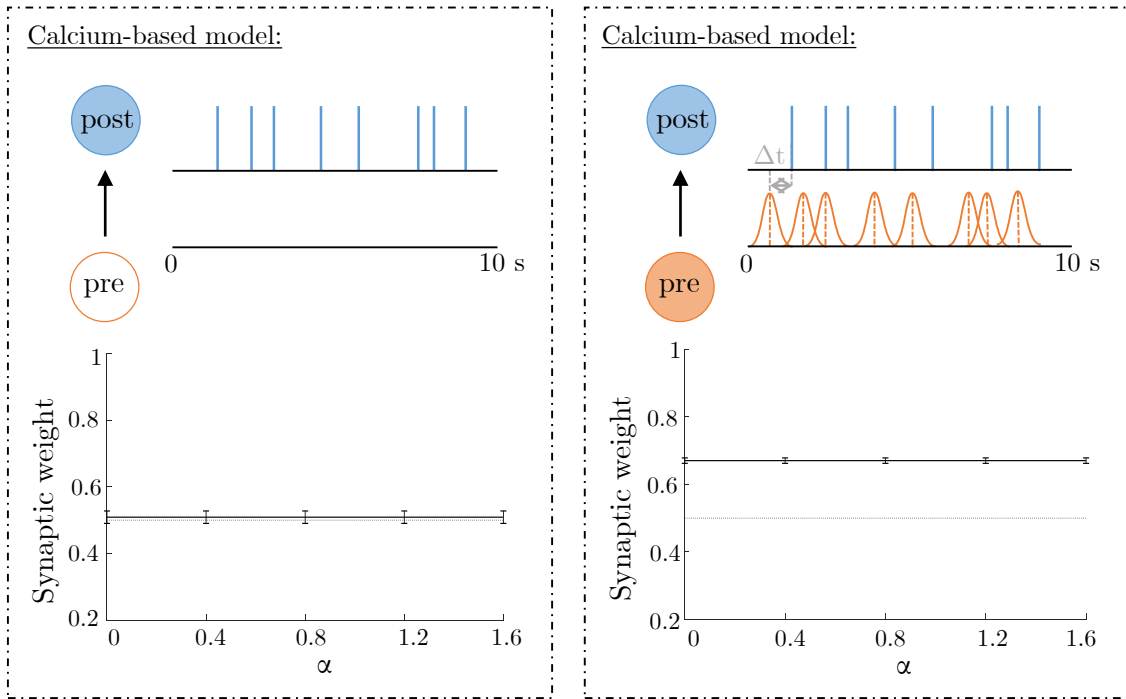


Figure 7.2 – *Calcium-based model simulation with homosynaptic protocols*. Representation of synaptic weight after 10 s of simulation. With the first protocol, a slight potentiation of the synaptic weight is observed. With the second protocol, a larger potentiation of the synapse is observed. With both protocols, synaptic weight doesn't depend of α .

Third protocol

Figure 7.3 represents the data obtained when the model is simulated with the third protocol. For this protocol, since the goal is to reproduce results shown in [Chistiakova et al., 2014], we chose to simulate our model with $\alpha = 0, 0.1, 0.2, 0.3, 0.4, 0.5, 0.6, 0.7, 0.8, 0.9, 1$. The two synaptic weights are represented as a function of α after 10 seconds of simulation. Synaptic weight 1 doesn't depend on α since it is the only active synapse. It represents the homosynaptic LTP induction at an activated synapse. Synaptic weight 2 strongly depends on α . For low α ($\alpha < 0.2$), no modification of the weight is observed. For middle values of α , depression is observed. The strongest depression being observed at $\alpha = 0.5$. Finally, for high values of α , synaptic potentiation can be observed. If we look at the global curve, this forms what is called a Mexican hat, also observed in [Chistiakova et al., 2014] with the same protocol.

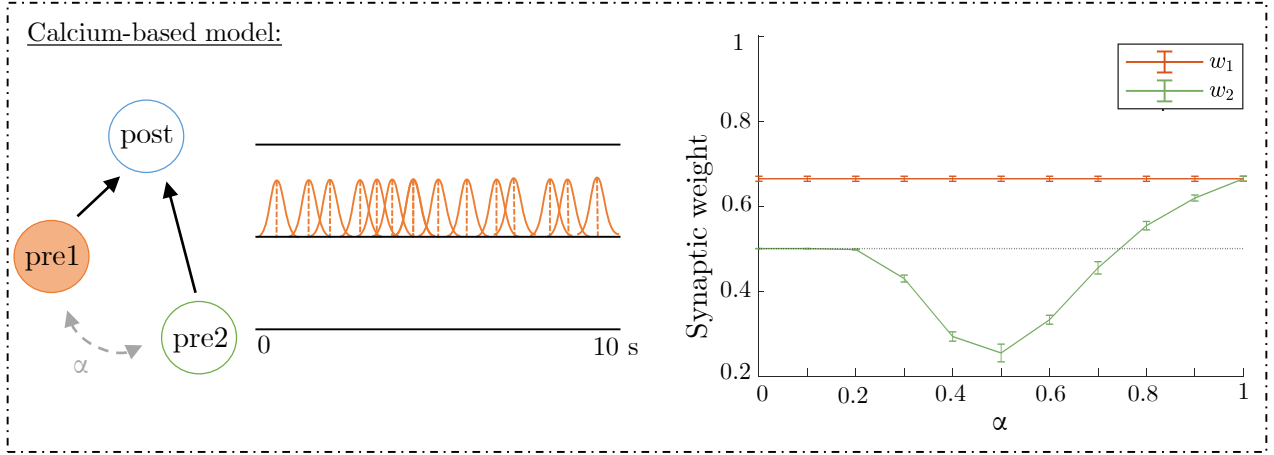


Figure 7.3 – *Calcium-based model simulation with the third protocol.* Representation of both final synaptic weights after 10 s of simulation as a function of α . The weight of synapse 1 remains constant no matter the value of α . The weight of synapse 2 follows a Mexican hat pattern. It shows no modification for low α , depression for middle α and potentiation for high α .

Fourth protocol

Figure 7.4 represents the data obtained when the model is simulated with the fourth protocol. We can see that the data for *pre1* and *pre2* are quite different. Orange (resp. green) curve represents the mean value of synaptic weight 1 (resp. 2) for each value of α . The corresponding errorbars represent the standard deviations of the mean values. Black lines represent the simulations obtained with the homosynaptic protocols. Dotted grey line represents the initial weight value of the synapses ($w_i = 0.5$). Both synapses have been potentiated. However, if w_2 increases with α , it is not the case for w_1 . Indeed, w_1 doesn't vary at all, no matter the α value. Moreover, evolution of w_1 is identical to the evolution of the synaptic weight obtained with the homosynaptic second protocol. Due to the increase of w_2 and the stagnation of w_1 , the two curves cross each other when $\alpha = 1$. Then, for $\alpha < 1$, *pre1* undergoes a greater potentiation than *pre2*. For $\alpha > 1$, *pre1* is less potentiated than *pre2* even if *pre2* is inactive.

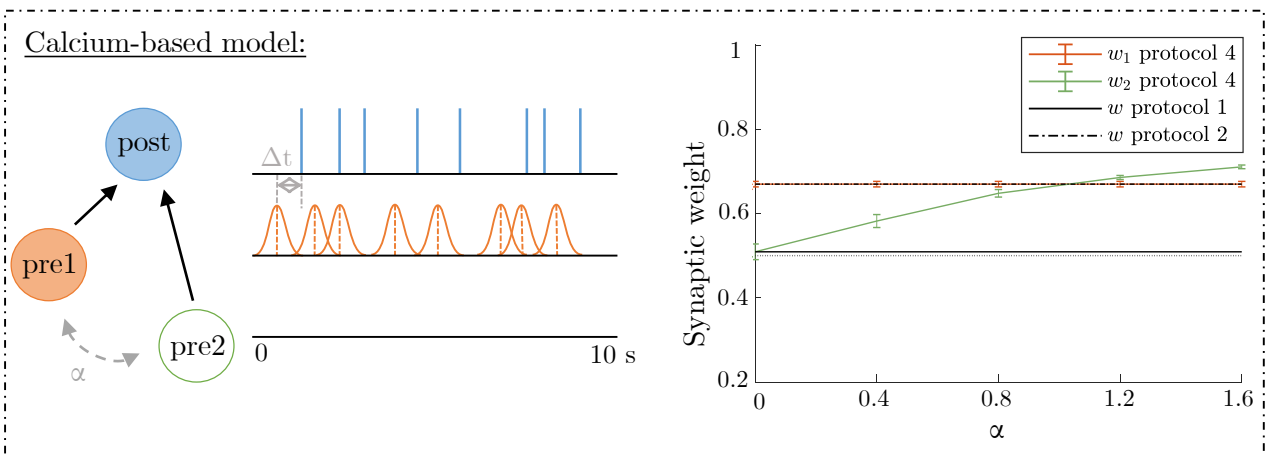


Figure 7.4 – *Calcium-based model simulation with fourth protocol (green and orange) compared with homosynaptic results (black).* Representation of both final synaptic weights after 10 seconds of simulation. The weight of synapse 1 remains constant and equal to the homosynaptic case. The weight of synapse 2 increases with α . When $\alpha < 1$, $w_1 > w_2$. When $\alpha > 1$, $w_1 < w_2$.

Fifth protocol

Figure 7.5 represents the final weight of the two synapses when the model is simulated with the fifth protocol. Orange (resp. green) curve represents the mean value of synaptic weight 1 (resp. 2) for each value of α . The corresponding errorbars represent the standard deviations of the mean values. Black dotted line represents the value of the synaptic weights in the case of homosynaptic plasticity (second protocol). Finally, the grey dotted line represent the initial weight value of the synapses ($w_i = 0.5$). Thus, if the weight values are above this line, synapses have undergone potentiation while if they are below this line, synapses have undergone depression. Now if we look at the data, we can see that the synaptic weights 1 and 2 are quite identical and have both undergone potentiation regardless of the α value. Moreover, we notice that as the value of α increases, the value of the final weights also increases. There is thus a positive correlation between both synaptic weights and the value of α .

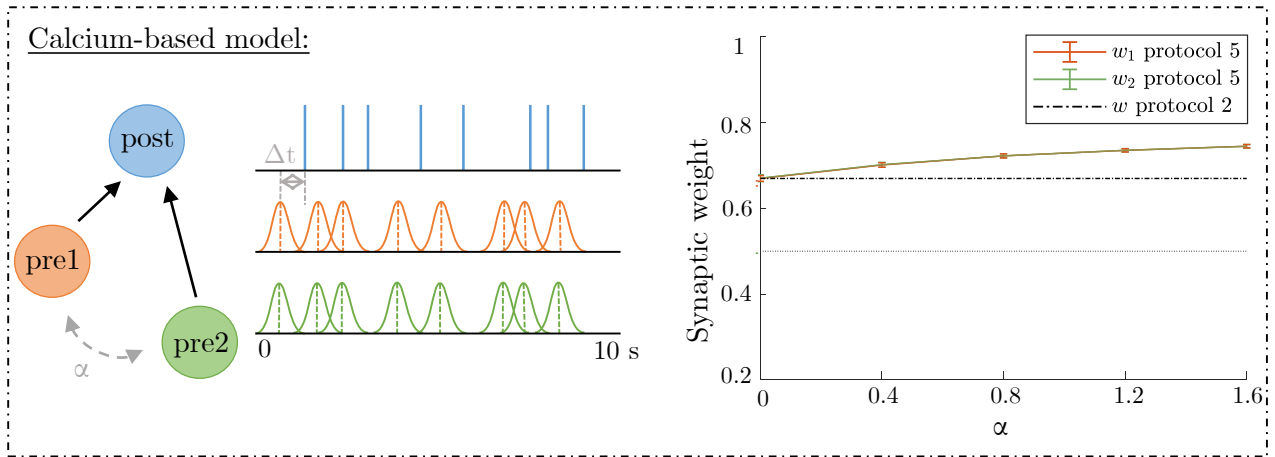


Figure 7.5 – *Calcium-based model simulation with the fifth protocol (green and orange) compared with homosynaptic results (second protocol in dotted black)*. Representation of both final synaptic weights after 10 seconds of simulation. Both synaptic weights are very similar and increase with α . Both synaptic weights show potentiation above the homosynaptic data no matter the value of α .

Sixth protocol

For this protocol, note that we used the parameters corresponding to the hippocampus area while simulations with the other protocols were performed with the parameters of the cortex.

Simulating our model with the sixth protocol, we obtained two kernels visible on Figure 7.6, one for each synapse. This represents the synaptic weight of each synapse as a function of the time delay imposed between the spikes of the presynaptic neuron 1 and the postsynaptic neuron. *Pre2* being silent, the kernel obtained for synapse 1 is the same as the homosynaptic kernel. The kernel obtained for *pre2* shows the plastic modification experienced by an inactive synapse depending on α and on the delay between the spikes of *pre1* and *post*. Looking at the homosynaptic kernel, it is clear that the delay between the two spikes of the two neurons has an impact on the final weight of a synapse. This is the trace we expected since this protocol aims to reproduce experimental results. Looking at the heterosynaptic kernel, it is also clear that α has an impact too. In particular, the impact of α is more pronounced for low delays. The lower is α , the flattened is the curve. Thus the greater is α , the greater is the potentiation experienced by the synapse 2 and moreover, the longer is the Δt zone of potentiation.

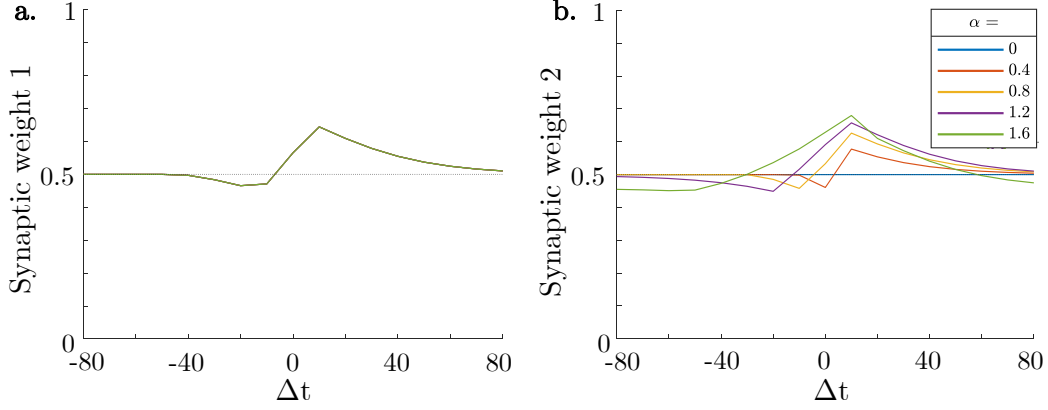


Figure 7.6 – *Kernels representing the impact of the time delay on the synaptic weight.* (a) Kernel obtained for synaptic weight 1 is the same as the homosynaptic kernel since pre_2 is inactive and has then no impact on synapse 1. Depression of the synapse is observed for $\Delta t < 0$ while synapse potentiation is observed for $\Delta t > 0$. (b) Kernel obtained for synaptic weight 2 shows an impact of α on the depression or the potentiation experienced by synapse 2. The greater the α , the greater the potentiation and the longer is the Δt zone of potentiation.

7.3 Heterosynaptic plasticity with STDP rules

7.3.1 Description of the model

We start with the pair-based STDP model described in section 4.1. As a reminder, STDP rules govern synaptic plasticity and thus synaptic weight based on the time interval between the presynaptic spike and the postsynaptic spike. The time interval between the spikes is provided by the internal traces of the neurons. The addition of heterosynaptic rules to this model will link the two presynaptic neuron traces' evolution which become

$$\tau_{+i} \frac{dx_i}{dt} = -x_i + \delta(t - t_i^{pre}) + \boxed{\alpha \delta(t - t_j^{pre})} \quad (7.5)$$

$$\tau_- \frac{dy}{dt} = -y + \delta(t - t^{post}) \quad (7.6)$$

where x_i and y are the internal traces of presynaptic neuron i and postsynaptic neuron respectively, τ_{+i} and τ_- are the time constants governing the evolution of x_i and y respectively, t_i^{pre} , t_j^{pre} and t^{post} are the spike timing of presynaptic neuron i and j and postsynaptic neuron respectively. With the new rules, a new parameter α makes its appearance. This parameter governs the impact of presynaptic neuron j (resp. i) on presynaptic neuron i (resp. j). An analysis of this parameter will be performed later.

With homosynaptic rules, the trace of a neuron is incremented by 1 when it spikes and decreases according to a constant τ otherwise. The introduction of heterosynaptic rules adds a modification of this trace when a neighboring presynaptic neuron spikes. Indeed, the trace of a neuron is now equal to 1 when the neuron itself spikes, α when a neighboring neuron spikes, and decreases exponentially according to τ otherwise. Thus, when the presynaptic neuron 1 spikes, this spike will impact not only the trace of pre_1 itself but also that of the presynaptic neuron 2.

Unlike calcium rules, weight change rules are not governed by thresholds but by the time delay between the presynaptic and the postsynaptic spikes (see section 4.2).

- When we are in a **pre_i-post** configuration the equation governing the new weight is indirectly modified by heterosynaptic rules. Indeed, since $w_{i,new}$ depends on the presynaptic trace x_i which has been modified previously by heterosynaptic term, the weight change will be impacted by the new heterosynaptic rules even if the equation is not modified.
- When we are in a **post-pre_i** configuration, with the homosynaptic rules, the synapse would undergo a depression and the new weight would follow the law depending on the postsynaptic trace:

$$w_{i,new} = -A_- w_i y_{prev} + w_i \quad (7.7)$$

where A_- is a parameter governing the depression and y_{prev} is the postsynaptic trace at the previous time. However, intuitively, this equation can't stay like that with heterosynaptic rules. Indeed, it only modifies the weight of the synapse whose presynaptic neuron has spiked. However, since this spike has also modified the trace of the other presynaptic neuron, logic would want that this weight would have to change too. The modification of this equation is not so easy and several cases need to be investigated.

Three cases can be considered to integrate heterosynaptic rules when we are in a **post-pre_i** configuration:

- First case would change the weight of the two presynaptic neurons in the same way. Then if a presynaptic neuron spikes (no matter which one), the two synaptic weights evolve following:

$$\begin{aligned} w_{i,new} &= -A_- w_i y_{prev} + w_i \\ w_{j,new} &= -A_- w_j y_{prev} + w_j \end{aligned} \quad (7.8)$$

In this case, the two presynaptic neurons evolve in the exact same way no matter if they spiked themselves or not. From a logical point of view, this does not seem right.

- Second case would only change the weight of the presynaptic neuron which spiked. It is the homosynaptic rule case. We would then have

$$\begin{aligned} w_{i,new} &= -A_- w_i y_{prev} + w_i \\ w_{j,new} &= -A_- w_j y_{prev} + w_j \end{aligned} \quad (7.9)$$

But as said earlier, from a logical point of view this does not seem right neither. Indeed, the second synapse undergoing changes, we expect to observe some changes at the weight level.

- Third case would be to change the two presynaptic neurons but to introduce a new parameter A_{het} to govern the weight change of the inactive synapse. We would have then

$$\begin{aligned} w_{i,new} &= -A_- w_i y_{prev} + w_i \\ w_{j,new} &= -A_{het} w_j y_{prev} + w_j \end{aligned} \quad (7.10)$$

From a logical point of view, this case seems to suit best our problematic. However, we need to investigate the effect of the three cases before making a decision.

Introduction of a parameter A_{het}

In order to integrate heterosynaptic plasticity in the post- pre_i configuration, we chose to introduce a new parameter A_{het} which would govern the weight change of the second synapse such as in Equation 7.10. We now need to assign a value to this parameter. First of all, in order to investigate each case mentioned above, A_{het} can be equal to 0.0053, which is the value of A_m , to illustrate the first case and to 0 to illustrate the second case. Since those values represents the extreme cases (nothing or all), they will be our limits. Then, to explore what could happen between those extreme values, we chose to simulate our model with $A_{het} = 0.001$ and $A_{het} = 0.003$. Finally, since α governs the potentiation of the synapses and A_{het} governs the depression of the synapse, we judged that it would be interesting to link those two parameters. Thus we linked the two parameters linearly such as $A_{het} = 0 \alpha$, $A_{het} = 0.001 \alpha$, $A_{het} = 0.003 \alpha$ and finally $A_{het} = 0.0053 \alpha$. This way of linking the two parameters is only one of the many ways which could be chosen. This model and those parameters being completely new, we had to begin investigating one way at a time.

7.3.2 Methodology

Figure 7.7 illustrates an example of simulation of our new pair-based STDP model. In this configuration, we used the fourth protocol, put parameter $\alpha = 0.4$ and $A_{het} = 0.0053 \alpha$. Poisson train 1 was used. We can see that, even if pre_2 is silenced, its trace evolves thanks to the spikes generated by pre_1 . Thus the weight of synapse 2 changes even if pre_2 is inactive. However, since $\alpha = 0.4$, the trace of synapse 2 is lower than that of synapse 1. Because of that, the weight of synapse 2 is less increased when we are in a pre-post configuration. On the other hand, the decrease in weight of pre_2 is less pronounced since $A_{het} = 0.0053 * \alpha = 0.00212$, which is smaller than $A_m = 0.0053$. At the end of the simulation, w_1 has been more potentiated than w_2 but, would it be the case for all the values of α and A_{het} ? An analysis is necessary to understand what are the roles of those parameters in our model.

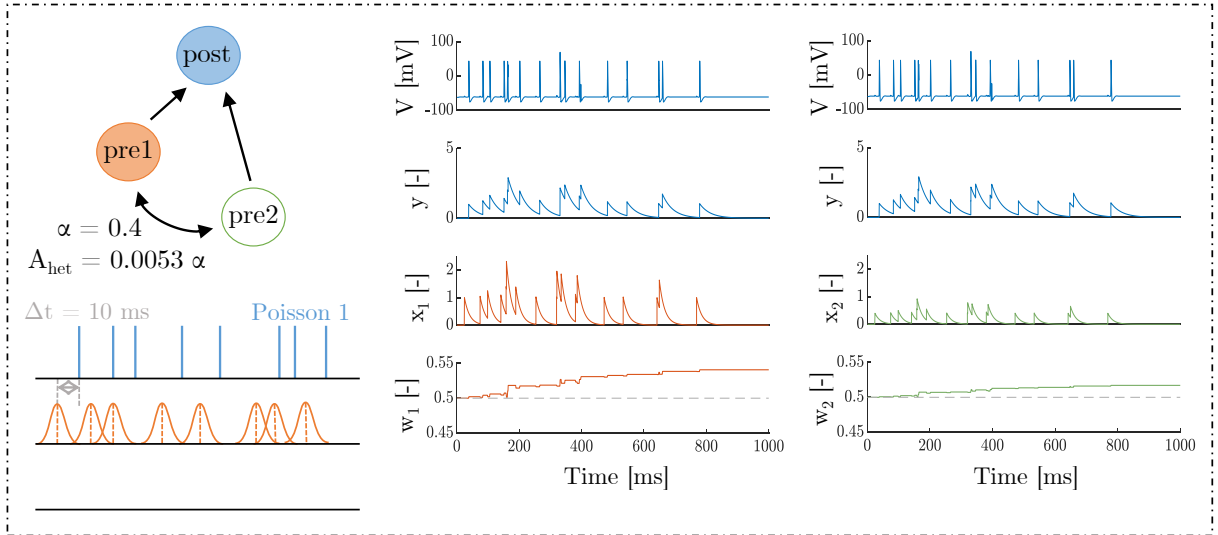


Figure 7.7 – Example of pair-based simulation with protocol 4, $\alpha = 0.4$ and $A_{het} = 0.0053 * \alpha$ with the first Poisson spike train. In blue, membrane potential and internal trace of postsynaptic neuron. In orange, internal trace of pre_1 and synaptic weight 1. In green, internal trace of pre_2 and synaptic weight 2. A potentiation of the synaptic weight is observed for both synapses. Synapse 1 is more potentiated than synapse 2. Because of the heterosynaptic dimension of the model, synapse 2 has been potentiated even if it was inactive.

Analysis of parameters

Heterosynaptic rules added two new parameters that we need to analyze. Those two parameters have both an impact on the evolution of the synaptic weight. Indeed, α has an impact on the synapse potentiation while A_{het} governs the depression of the inactive synapse. Those parameters are then quite linked and it is then difficult to analyse them separately. In the next two paragraphs, the results centered on each parameter separately despite the influence of the other will be presented.

Analysis of A_{het} To analyze A_{het} , we simulated our model with each of the six protocols described in chapter 6 for $A_{het} = 0, 0.001, 0.003, 0.0053$ and then for $A_{het} = 0, 0.001, 0.003, 0.0053$ for each value of α . From these simulations, we extracted the final weight (after 10 s) of each synapse which allowed us to establish a link between the synaptic weight, our α and A_{het} parameters.

Analysis of parameter α To analyze α , we simulated our model with each of the six protocols described in chapter 6 for $\alpha = 0, 0.4, 0.8, 1.2, 1.6$ for each value of A_{het} . From these simulations, we extracted the final weight (after 10 s) of each synapse which allowed us to establish a link between the synaptic weight and our α and A_{het} parameters.

7.3.3 Results

This section presents the results obtained after the simulation of our new pair-based model with the six protocols described in chapter 6.

Homosynaptic protocols

Figure 7.8 represents the data obtained for the simulation of the pair-based homosynaptic model with the two first protocols. First protocol is equivalent to simulate our heterosynaptic model when keeping the two presynaptic neurons silent. Second protocol is equivalent to simulate our heterosynaptic model when keeping the presynaptic neuron 2 silent. In the two protocols, synaptic weight is independent from α and from A_{het} since we are in homosynaptic plasticity. With the first protocol, the synaptic weight stays equal to w_{init} since there is no pre-post or post-pre configuration. With the second protocol, synapse has been potentiated. As with the calcium-based model, the results obtained with those two protocols will be compared with the results of the fourth and the fifth protocols in the next sections.

Third protocol

The third protocol was made in order to reproduce results described in [Chistiakova et al., 2014] with a calcium-based model. In this protocol, only pre_1 is active while pre_2 and $post$ are maintained silenced. Since we need to be in a $pre - post$ or $post - pre$ configuration to modify the weight of a synapse, this wouldn't make sense to simulate our pair-based STDP model with this protocol. Indeed, without any $post$ spike, the weight can only remain constant.

Fourth protocol

Figure 7.9(A) represents the final weight of synapse 1 and synapse 2 simulated with the fourth protocol when α and A_{het} are *independent* from each other. The x axis represents the α values while the y axis represents the final weight of the synapses. The different colored lines represent different A_{het} values. We have $A_{het} = 0$ in blue, $A_{het} = 0.001$ in orange, $A_{het} = 0.003$ in yellow and finally $A_{het} = 0.0053$

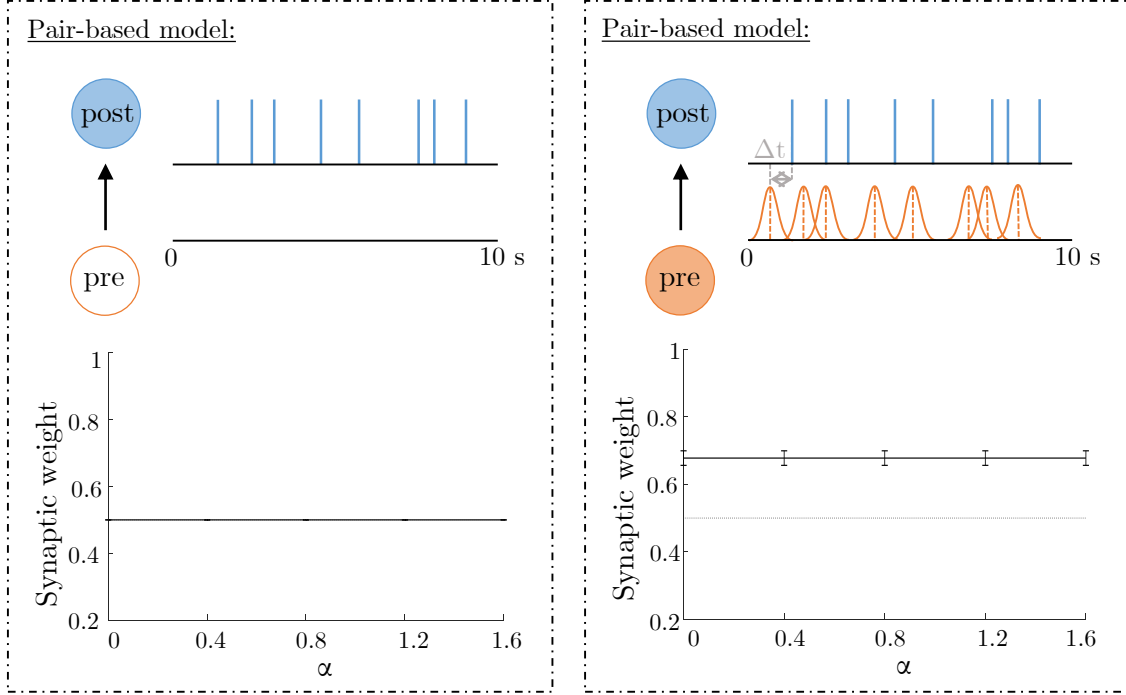


Figure 7.8 – *Pair-based model simulation with homosynaptic protocols*. Representation of synaptic weight after 10 s of simulation. With the first protocol, no modification of the synaptic weight is observed. With the second protocol, a potentiation of the synapse is observed. With both protocols, synaptic weight doesn't depend of α .

in purple. Black line represents homosynaptic results obtained with protocol 1 while dotted black line represents homosynaptic results obtained with protocol 2. Grey dotted line represents $w_{init} = 0.5$. The weight of pre_1 is constant no matter the values of α and A_{het} . This constant weight being above the grey dotted line, synapse 1 always undergoes potentiation in those conditions. Moreover, w_1 evolves as it was in homosynaptic conditions since it is identical to results of protocol 2. Concerning synapse 2, we can see that depending on α and A_{het} , the synapse undergoes potentiation or depression. Thus for all values of A_{het} and for $\alpha = 0$, the synapse undergoes depression or doesn't change. For $A_{het} = 0.0053$ and $\alpha = 0.4$, the synapse is depressed too. Otherwise, the synapse undergoes potentiation. All the colored lines seem to follow the same scheme being parallel with each other. Figure 7.9(A.iii) shows the superposition of the weight of the two synapses. Orange (resp. green) lines represent the synaptic weight of synapse 1 (resp. synapse 2). It is here obvious that the two synapses evolve very differently from each other. One can notice that synaptic weight 2 can be higher or lower than synaptic weight 1 depending on the α and A_{het} values. In particular, w_2 is higher than w_1 no matter the value of A_{het} when $\alpha > 1$. When $\alpha < 1$, this depends on the value of A_{het} .

Figure 7.9(B) represents the weight of synapse 1 and synapse 2 with the fourth protocol and when α and A_{het} are **dependent** from each other. A_{het} depends linearly of α with different factors comprised between 0 and 0.0053 included. The weight of synapse 1 is constant no matter the values of α and A_{het} . This synapse undergoes potentiation since its weight is above the grey dotted line representing the initial weight of the synapse. Once again, w_1 evolves as it was in homosynaptic conditions. The weight of synapse 2 always undergoes potentiation except when $\alpha = 0$ where the synapse stays at its initial weight ($w_i = 0.5$) no matter the value of A_{het} . The higher is α the higher is the final synaptic weight and the bigger is the gap between the lines representing each A_{het} . Thus the blue line for

$A_{het} = 0$ α goes from 0.5 for $\alpha = 0$ to almost 1 for $\alpha = 1.6$ while the purple line for $A_{het} = 0.0053 \alpha$ goes from 0.5 for $\alpha = 0$ to less than 0.7 for $\alpha = 1.6$. The higher is the linear coefficient between A_{het} and α , the lower is the slope of the curves. Finally, Figure 7.9(B.iii) shows the superposition between synapse 1 and synapse 2 and homosynaptic results. When $\alpha > 1$, the weight of synapse 2 is always higher than that of synapse 1 no matter the value of A_{het} . When $\alpha < 1$, it depends on the value of A_{het} .

Fifth protocol

Figure 7.10(A) represents the final weight of synapse 1 and synapse 2 simulated with the fifth protocol and when α and A_{het} are **independent** from each other. For the two synapses we can see that the synaptic weight increases with α . Thus the synaptic weight and α are positively correlated. On the other hand, the synaptic weight decreases with the increase of A_{het} . It means that the synaptic weight and A_{het} are negatively correlated. Synapse 1 and synapse 2 always undergo potentiation regardless of the value of α and A_{het} . Comparing the different lines, one can notice that they all look quite parallel. Both synapses cross the line representing results obtained with protocol 2. Figure 7.10(A.iii) shows the superposition of the two previous graphs. When the two synapses are active, their weights are very similar for each α and A_{het} . Compared with homosynaptic rules, when $A_{het} = 0$, heterosynaptic rules result in higher potentiation than homosynaptic rules. This gap of potentiation becomes lower and lower with the increase of A_{het} and the decrease of α . When $\alpha > 1$, synapses always experience a higher potentiation with heterosynaptic rules than with homosynaptic rules. When $\alpha < 1$, this depends on A_{het} .

Figure 7.10(B) represents the weight of synapse 1 and 2 simulated with the fifth protocol and when α and A_{het} are **dependent** from each other. As explained before, here, A_{het} depends linearly of α with different factor comprised between 0 and 0.0053 included. Looking at the weight of synapse 1 and synapse 2, it appears that they always undergo potentiation no matter the values of α and A_{het} . Once again, the weights are positively correlated with α . Thus the higher α , the higher the synaptic weight. On the other hand, the weight is also negatively correlated with A_{het} . Thus the higher A_{het} , the lower the synaptic weight. The lines representing different A_{het} are not parallel and cross each other at the same point when $\alpha = 0$. Figure 7.10(B.iii) shows the superposition of the two previous graphs. The two synaptic weights are very similar. Compared with homosynaptic rules, heterosynaptic rules always result in a greater potentiation no matter the values of α and A_{het} . The higher the linear coefficient linking A_{het} and α , the closer are the homosynaptic and heterosynaptic weights.

Sixth protocol

Sixth protocol was simulated for the case where α and A_{het} are independent from each other and for the case where A_{het} is linearly dependent from α such that $A_{het} = 0 \alpha, 0.001 \alpha, 0.003 \alpha, 0.0053 \alpha$. Thus, for each cases we obtained six kernels: one representing pre_1 and five representing pre_2 where each one represent a value of α . The kernel of pre_1 is the same as the kernel we would have obtained with homosynaptic rules since pre_2 is silent.

The kernels obtained when α and A_{het} are independent from each other are visible in Figure 7.11. In addition to the kernel representing the weight of synapse 1 and then the homosynaptic kernel, five kernels, one for each α value, are visible. Those kernels show that α and A_{het} have an impact on the shape of the graph. In particular, α has an impact when the delay between pre_1 and $post$ is going

from -80 to 10 ms while A_{het} has an impact when the delay between pre_1 and $post$ is going from 10 to 80 ms.

The kernels obtained when α and A_{het} are linearly dependent are visible in Figure 7.12. As previously mentioned, in addition to the kernel representing the weight of synapse 1 and then the homosynaptic kernel, five kernels, one for each α value, are visible. The kernels obtained are not very different from those obtained when α and A_{het} are independent. However, it seems now that the value of α has an impact for all the values of the delay between pre_1 and $post$. Thus the shape is "edgier". The most different kernel is the one for $\alpha = 0$ which is now completely flat.

Pair-based model:

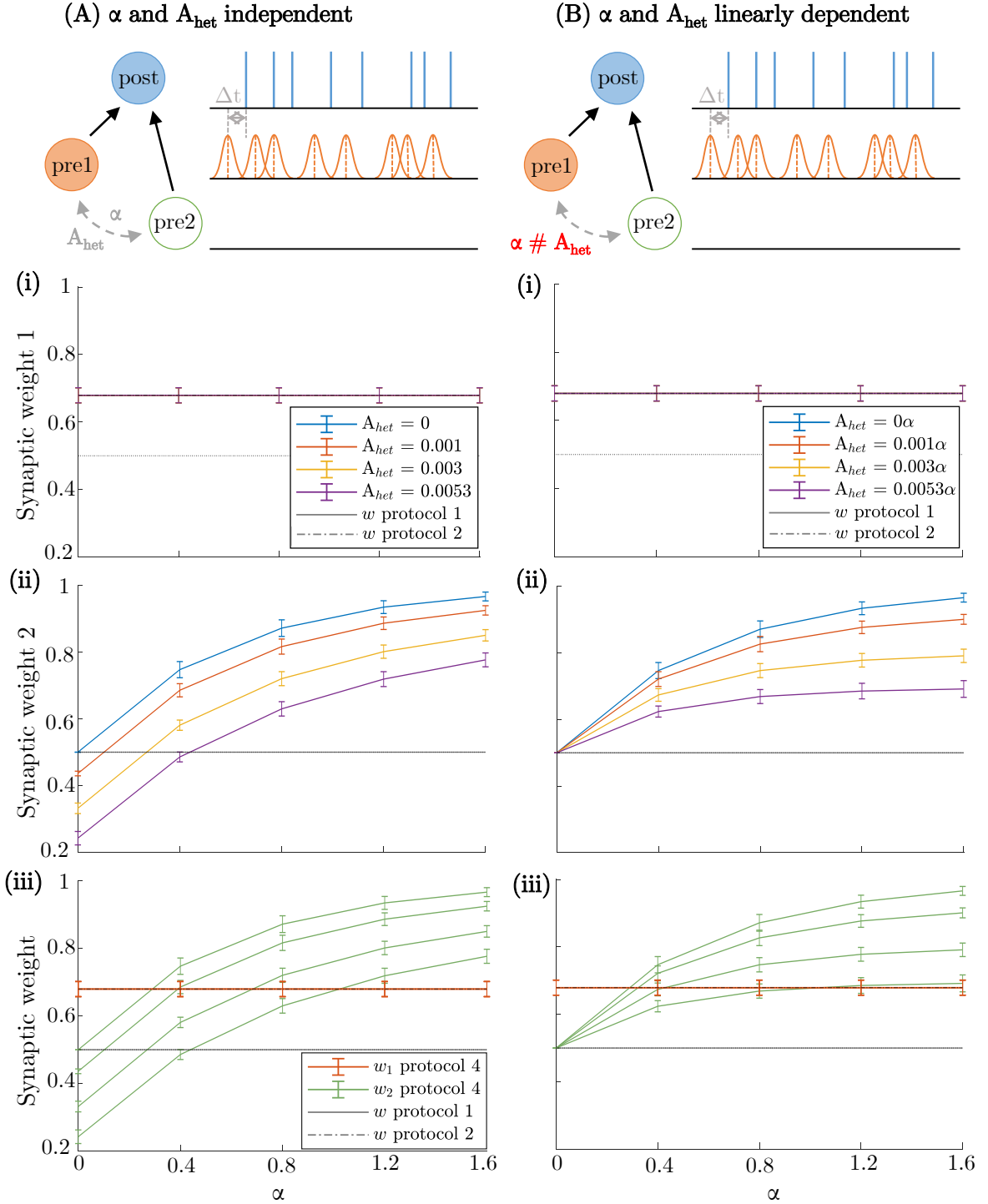


Figure 7.9 – *Pair-based model simulation with fourth protocol.* **(A)** α and A_{het} are independent. (i) Evolution of synaptic weight 1 after 10 s of simulation. It is similar to results obtained with protocol 2. (ii) Evolution of synaptic weight 2. It crosses the curve representing results obtained with protocol 1. (iii) Comparison between (i) (in orange), (ii) (in green) and the homosynaptic results (protocol 1 in black, protocol 2 in dotted black). **(B)** α and A_{het} linearly dependent. (i) Evolution of synaptic weight 1 after 10 s of simulation. (ii) Evolution of synaptic weight 2. (iii) Comparison between (i) (in orange), (ii) (in green) and the homosynaptic results (protocol 1 in black, protocol 2 in dotted black).

Pair-based model:

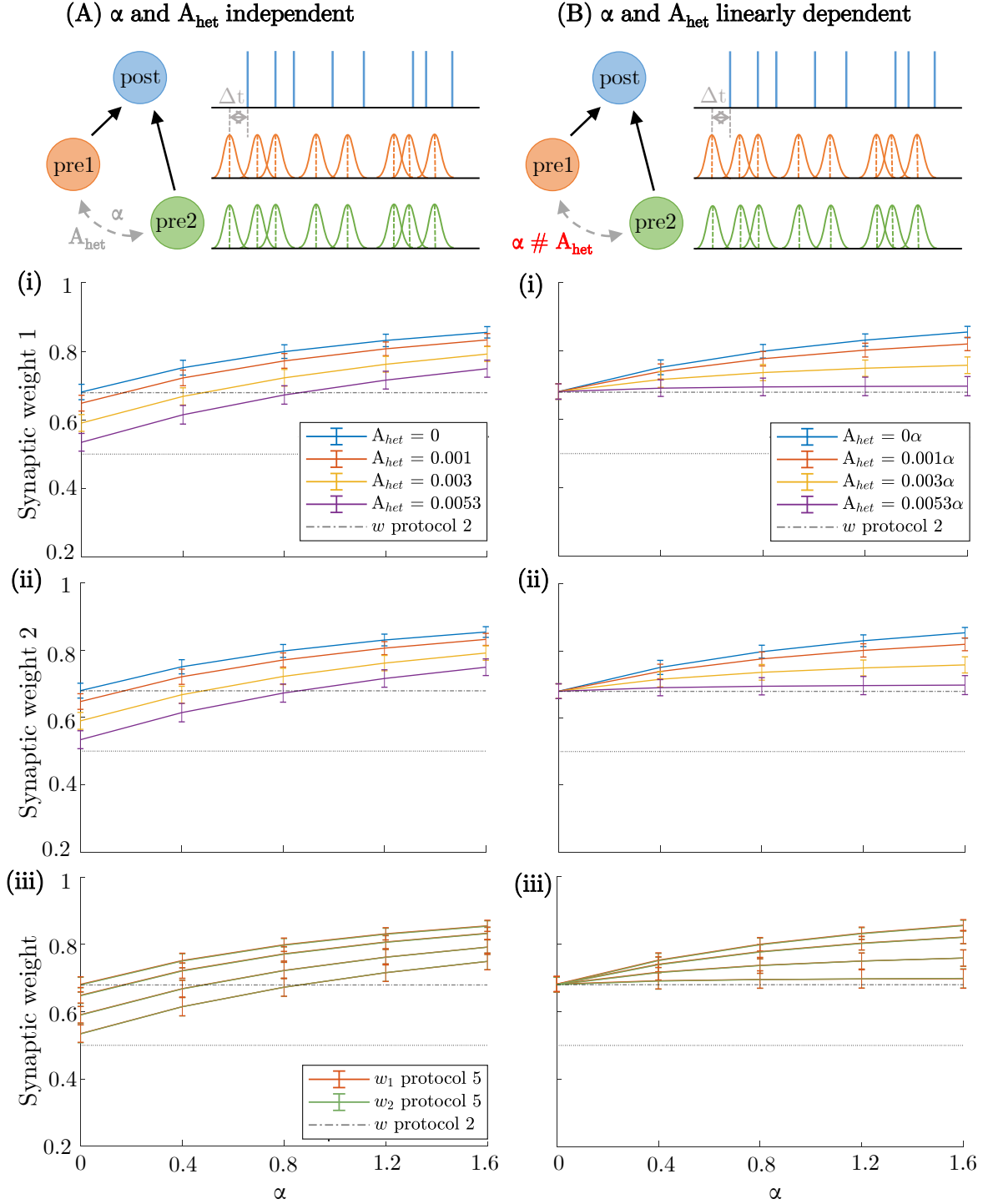


Figure 7.10 – *Pair-based model simulation with fifth protocol.* **(A)** α and A_{het} independent. (i) Evolution of synaptic weight 1 after 10 s of simulation. (ii) Evolution of synaptic weight 2. (iii) Comparison between (i) (in orange), (ii) (in green) and the homosynaptic results (protocol 1 in black, protocol 2 in dotted black). **(B)** α and A_{het} linearly dependent. (i) Evolution of synaptic weight 1 after 10 s of simulation. (ii) Evolution of synaptic weight 2. (iii) Comparison between (i) (in orange), (ii) (in green) and protocol 2 (in dotted black).

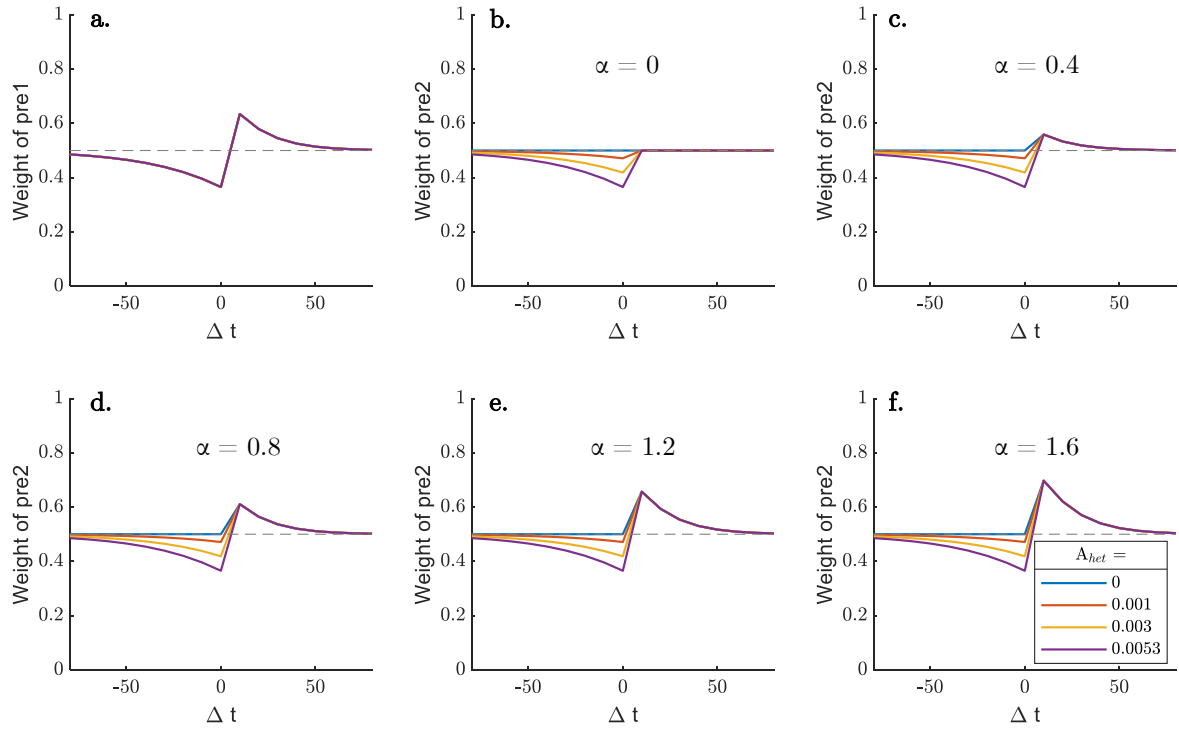


Figure 7.11 – Kernels representing the impact of the time delay on the synaptic weight for pair-based STDP model with α and A_{het} independent. (a) Kernel obtained for synaptic weight 1 is the same as the homosynaptic kernel since pre_2 is inactive and has then no impact on synapse 1. Depression is observed for $\Delta t < 0$. Potentiation is observed for $\Delta t > 0$. (b)(c)(d)(e)(f) Kernels representing synaptic weight 2 for different α and different A_{het} . α has an impact on the potentiation zone while A_{het} has an impact on depression zone.

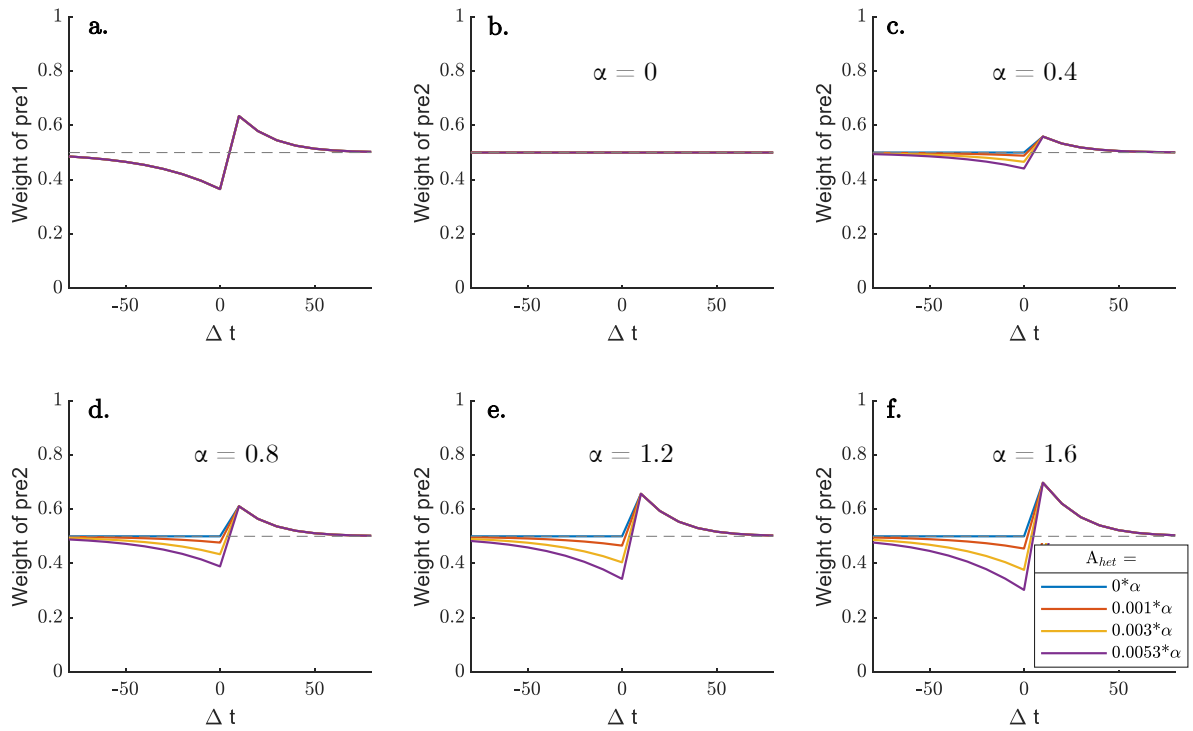


Figure 7.12 – *Kernels representing the impact of the time delay on the synaptic weight for pair-based STDP model with α and A_{het} dependent.* (a) Kernel obtained for synaptic weight 1 is the same as the homosynaptic kernel since *pre2* is inactive and has then no impact on synapse 1. Depression is observed for $\Delta t < 0$. Potentiation is observed for $\Delta t > 0$. (b)(c)(d)(e)(f) Kernels representing synaptic weight 2 for different α . Kernels are flattened with the decrease of α .

Chapter 8

Heterosynaptic models: Discussion and application

Looking at the results described previously (see chapter 7), some cases can be isolated and discussed further. This chapter is dedicated to the interpretation of the results obtained and to the analysis of the roles of the new parameters integrated in our new heterosynaptic model.

8.1 Calcium discussion

Results obtained need to be interpreted in order to find a biological signification of parameter α . In this section, calcium-based results obtained with the different protocols will be discussed and interpreted in order to find biological meaning to our observations.

8.1.1 Distance interpretation

As explained in section 3.4, a "mexican hat" pattern of the plasticity changes experienced by the synapses has been observed in heterosynaptic experiments [Chistiakova et al., 2014]. This pattern showed the influence of the **distance** between the synapses on which heterosynaptic rules was applied on the nature and the strength of the plasticity phenomenon undergone by those synapses. Based on these observations, α could be representative of the distance between the synapses. Thus, when α is low, the synapses are far from each other and the effect of the induction of LTP in synapse 1 on synapse 2 would be a weak LTP or even LTD (see Figure 8.1). In that case, α should be maintained under 1. Indeed, the mexican hat pattern only shows a diminution in intensity of plasticity phenomenon. Then, an inactive synapse couldn't be more potentiated than the active synapse from which it depends which is precisely the case when $\alpha > 1$. Results obtained with the third protocol illustrate that phenomenon and reproduce the results obtained in [Chistiakova et al., 2014].

8.1.2 Calcium release

Another biological interpretation of α would be the level of calcium in the synapse. Indeed, the heterosynaptic plasticity can be due to the intervention of calcium. When *pre*₁ communicates with *post*, this triggers calcium entrance in the postsynaptic neuron. In the case of heterosynaptic rules, this calcium could diffuse through the postsynaptic neuron toward the synapse 2 which would lead to a Mexican hat pattern just as explained in the previous section. Thus, α could represent the amount of calcium diffusing toward synapse 2. Moreover, it has been proven that calcium flux can come not only through the cell membrane but also from internal stocks such as the endoplasmic reticulum or

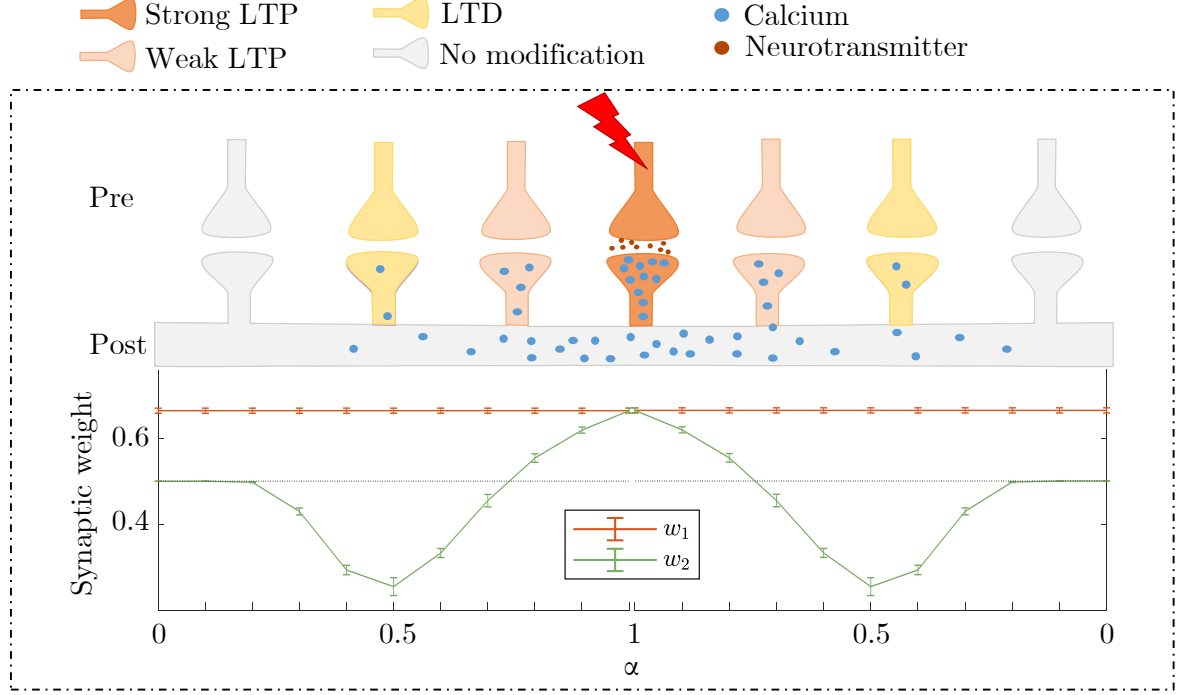


Figure 8.1 – *Illustration of the Mexican hat with results obtained with our new calcium-based heterosynaptic model.* (Above) Scheme of the Mexican hat pattern. (Below) Zoom on the results obtained when simulating the calcium-based heterosynaptic model with protocol 3. This expresses that α is a parameter representing the distance between two synapses.

the mitochondria [Kawamoto et al., 2012, Padamsey et al., 2019]. Moreover, studies have shown that heterosynaptic LTD could be triggered by strong stimulation associated with IP_3R -mediated Ca^{2+} waves. IP_3R , standing for Inositol trisphosphate receptor, is a protein acting as a calcium channel. It is a key factor in the release of calcium from intracellular store sites such as the endoplasmic reticulum [wik, 2022]. It has been observed that genetic deletion or pharmacological inhibition of IP_3R could lead to the abolishment of heterosynaptic LTD [Nagase et al., 2003, Nishiyama et al., 2000]. Thus, considering not only diffusion but also the release of calcium stock triggered by the diffused calcium, we could consider some cases where $\alpha > 1$. Considering diffusion of calcium, once again α could represent the distance between the synapses by considering that the larger the distance between synapses the smaller the amount of calcium reaching the inactive synapse. On the other hand, if we consider the release from intracellular calcium storage, the distance between the synapses could be of no importance. Then, a high α ($\alpha = 1.6$) would mean that some release of calcium from intracellular store sites could happen whether the two synapses are close from each other or not.

In our results this case can be observed in Figure 7.4 and Figure 7.5. Indeed, the higher is α , the higher is the synaptic weight. Thus α representing the amount of calcium in neurons could explain those observations. Indeed, in our equations, α intervenes in the evolution of the calcium trace of the presynaptic neurons. This totally makes sense. Moreover, when $\alpha > 1$, the phenomenon of calcium release can be observed too, in particular in Figure 7.4 when the model is simulated with the third protocol. In this figure, we can clearly see that the weight of the inactive synapse is able to exceed the weight of the active synapse. This can be due to a release of calcium from internal store sites, increasing the amount of calcium in inactive synapses.

8.1.3 Conditioning

Model tested with the third protocol and the fourth protocol shows a phenomenon of conditioning which can be observed in the case of central sensitization in the spinal cord (see subsection 2.3.1). Looking at Figure 7.4, the stimulation of a presynaptic neuron will have an impact on the weight of an inactive synapse connected to the same postsynaptic neuron. Thus, by doing nothing, an inactive synapse can see its weight increases. This increase in weight could have the effect of triggering some response from the postsynaptic neuron which can't respond when the synaptic weight is too low.

8.1.4 Questionable results

Simulating our model with the fifth protocol when the two presynaptic neurons are active shows a higher potentiation than what is obtained with the second homosynaptic protocol. This potentiation increases with the value of α which seems logical since α will always have the effect of increasing the calcium trace of the concerned neuron. However, the fact that both synapses undergo potentiation is not really a phenomenon we are glad to see. Indeed, this can lead to a runaway phenomenon which is what the heterosynaptic rules seek to avoid. However, this can also express the phenomenon of heterosynaptic **facilitation** evoked in section 3.4. Moreover, our models have been tested for a frequency of 20 Hz. Thus, further investigations need to be performed with different frequencies.

8.1.5 Discussion of protocol 6

Looking at the kernels in Figure 7.6, we can see that homosynaptic rules always result in synaptic depression for $\Delta t < 0$ and in synaptic potentiation for $\Delta t > 0$. The synaptic potentiation is more pronounced than the synaptic depression. The impact of α is a flattening of the shape of the kernel. In particular, this flattening is centered on the initial weight $w_{init} = 0.5$ when $\alpha = 0$. It seems logical that the weight of synapse 2 stays constant when pre_1 has no impact on it. In this case, the weight of pre_2 will only be influenced by the spikes of $post$ which has always the same frequency no matter the delay with pre_1 . The greater α , the greater the potentiation and the longer is the Δt zone of potentiation. Comparing the two kernels, one can observe four cases (visible in Figure 8.2):

1. Depression at the active synapse can induce depression at the inactive synapse.
2. Depression at the active synapse can provoke potentiation at the inactive synapse for large α and low negative delay.
3. Potentiation at the active synapse can induce depression at the inactive synapse for low α and low Δt .
4. Finally, induction of potentiation at the active synapse can provoke a higher (for $\alpha > 1$) or a lower (for $\alpha < 1$) potentiation at the inactive synapse.

This is very interesting since those results have been already observed in experimental protocols gathered in [Chater and Goda, 2021]. Thus it shows that our new model is able to reproduce experimental heterosynaptic plasticity results.

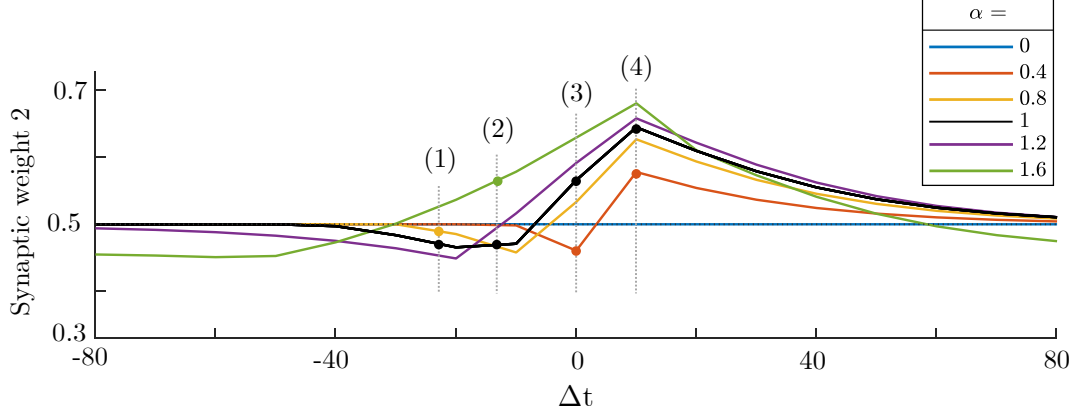


Figure 8.2 – Zoom on the different cases observable with calcium-based model simulated with the sixth protocol. Black line represents the homosynaptic kernel ($\alpha = 1$). (1) Depression at the active synapse leads to depression at the inactive synapse. (2) Depression at the active synapse leads to potentiation at the inactive synapse. (3) Potentiation at the active synapse leads to depression at the inactive synapse. (4) Potentiation at the active synapse leads to potentiation at the inactive synapse.

8.2 Pair-based STDP discussion

Results obtained need to be interpreted in order to show the impact of parameters α and A_{het} . In this section, pair-based STDP results obtained with the different protocols will be discussed and interpreted in order to find an explanation to our observations. Since we are in a phenomenological model, the biological interpretation of the new parameters is more complicated and not really necessary. Indeed, the internal traces x and y described in the pair-based homosynaptic STDP model do not have a real biological signification.

8.2.1 Dependency between α and A_{het}

This work experiencing a very new heterosynaptic model, the parameters α and A_{het} are completely new and they need to be investigated and their impact evaluated. For those reasons, we chose to consider those parameters independently from each other and linearly dependent from each other. The results obtained show that when α and A_{het} are independent from each other, synapses can be potentiated or depressed depending on parameters. Moreover, the obtained curves aren't really similar with curves obtained with homosynaptic rules. In particular, when pre_2 is silent. Indeed, the slope of the curves is very important in those conditions. On the other hand, when α and A_{het} are dependent from each other, heterosynaptic rules always results in potentiation. Moreover, the obtained curves are quite similar with curve obtained with homosynaptic rules. In particular, when both synapses are active with $A_{het} = 0.0053 \alpha$.

When α and A_{het} are independent from each other, a case in particular is very interesting. When $\alpha = 0$ and $A_{het} \neq 0$, is it right that A_{het} has an impact on the inactive synapse? If so, it would mean that when two presynaptic neurons are connected to a same postsynaptic neuron, when pre_1 spikes, even if it doesn't change the internal trace of pre_2 , pre_2 will be depressed. In this configuration, an inactive synapse will always be depressed when an active neuron connected to the same postsynaptic neuron spikes. This could be interpreted at the level of the memory. When a synapse is silent for a long time, its weight falls to 0. This is the phenomenon of pruning. However, if $\alpha = 0$, does pre_1 should have an impact on pre_2 ?

8.2.2 Conditioning

As with the calcium-based model, a phenomenon of conditioning can be observed when our pair-based STDP model is simulated with the fourth protocol. Indeed, as it can be seen in Figure 7.9 inactive synapse sees its weight modified because of the activity of a synapse connected to the same postsynaptic neuron. Thus in Figure 7.9(B), synapse 2 goes from $w_{init} = 0.5$ to potentiation values just because of the activity of synapse 1. Here, the conditioning is influenced by α but also by A_{het} .

8.2.3 Pruning

Looking at Figure 7.9(A), we can see that when $\alpha = 0$, the inactive synapse is depressed. This is because A_{het} and α are independent from each other. Thus, when $\alpha = 0$, A_{het} can be equal to 0, 0.001, 0.003 or 0.0053. In those conditions, the internal trace of the inactive synapse stays at 0. The potentiation experienced by the synapse depending on its own trace, no potentiation is possible in those conditions. However, the depression of the inactive synapse depends on A_{het} and the trace of the postsynaptic neuron. Thus, every time pre_1 spikes, the synaptic weight 2 is decreased as a function of A_{het} and y , the internal trace of the postsynaptic neuron. In this case, the inactive synapse can't experience any potentiation because of $\alpha = 0$ but experienced depression because of $A_{het} \neq 0$. This phenomenon can be seen as "weird" but in fact, it can be associated with a phenomenon of **pruning**. Pruning is the mechanism by which some neuronal connections are eliminated after some time. This phenomenon has the advantage of increasing the efficiency of neuronal transmissions [Santos and Noggle, 2011]. Some papers talk about this phenomenon as being caused by heterosynaptic plasticity [Chater and Goda, 2021] but it is still unclear if those two phenomena are linked [Jenks et al., 2021]. However, in our simulation (see Figure 7.9(A)), we can see that an inactive synapse will be depressed because of the activity of another synapse. This will only happen when $\alpha = 0$ and if A_{het} and α are independent from each other. The intensity of the pruning is thus governed by the value of A_{het} .

8.2.4 Prevention of saturation

In Figure 7.10(A), when $\alpha \approx 0$, the synaptic weights are below the homosynaptic curve. Once again this is due to the fact that, here, heterosynaptic plasticity only brings depression via A_{het} because $\alpha = 0$. This case could express the fact that heterosynaptic plasticity, with those parameters, can avoid saturation. Indeed, when both synapses are active, both synapses undergo potentiation which, when A_{het} and α are dependent from each other, is higher than the homosynaptic values. A phenomenon of runaway which we want to avoid could then be observed. By keeping A_{het} and α independent from each other, it's a phenomenon we could avoid.

8.2.5 Questionable results

As said in previous section, simulating the model with fifth protocol when A_{het} and α are dependent from each other (Figure 7.10(B)), both synapses are more potentiated than they would be with homosynaptic rules. This phenomenon happens for each value of α except for $\alpha = 0$ where the weight remains equal to 0.5. As observed with the calcium-based model, this phenomenon could be associated to a runaway mechanism which is what we would like to avoid. On the other hand, this also can be seen as facilitation. This phenomenon also appears when A_{het} and α are independent from each other with the highest values of α and the lowest value of A_{het} . Otherwise, as explained previously, this phenomenon can be avoided with low values of α and high values of A_{het} . This seems logical since α governs the heterosynaptic potentiation and A_{het} governs the heterosynaptic depression. Thus, increasing A_{het} when decreasing α can prevent the synapse from overpotentiating.

8.2.6 Discussion of the protocol 6

The shape of the pair-based kernels are all similar. The homosynaptic kernel shows a symmetrical repartition of potentiation and depression around $\Delta t = 0$. Thus, when $\Delta t > 0$, the synapse experiences potentiation while when $\Delta t < 0$, the synapse undergoes depression. This is the principle of the pair-based model explained in section 4.2. Indeed, when $\Delta t > 0$, we are in a pre-post configuration and the synapse will be potentiated. On the other hand, when $\Delta t < 0$, we are in a post-pre configuration and the synapse will be depressed. This is for those reasons that A_{het} only has an impact when $\Delta t < 0$ since it governs the depression experienced by the synapse while α only has an impact when $\Delta t > 0$ since it governs the potentiation experienced by the synapse.

As for the calcium-based model, if we zoom on the different time windows, we can see the four different cases described in [Chater and Goda, 2021] (listed in subsection 8.1.5). However, the case (3) where homosynaptic potentiation induces heterosynaptic depression can't be observed when α and A_{het} are dependent from each other. This case expresses the pruning described earlier and can only be observed for $\alpha = 0$ and $A_{het} \neq 0$ when α and A_{het} are independent. Moreover, one can notice that the cases (3) and (4) have only been observed when $0 < \Delta t < 10$ which is between two tested time delays. Thus those cases have not been observed with the tested values but the graphs make us guess that they could happen in between Figure 8.3.

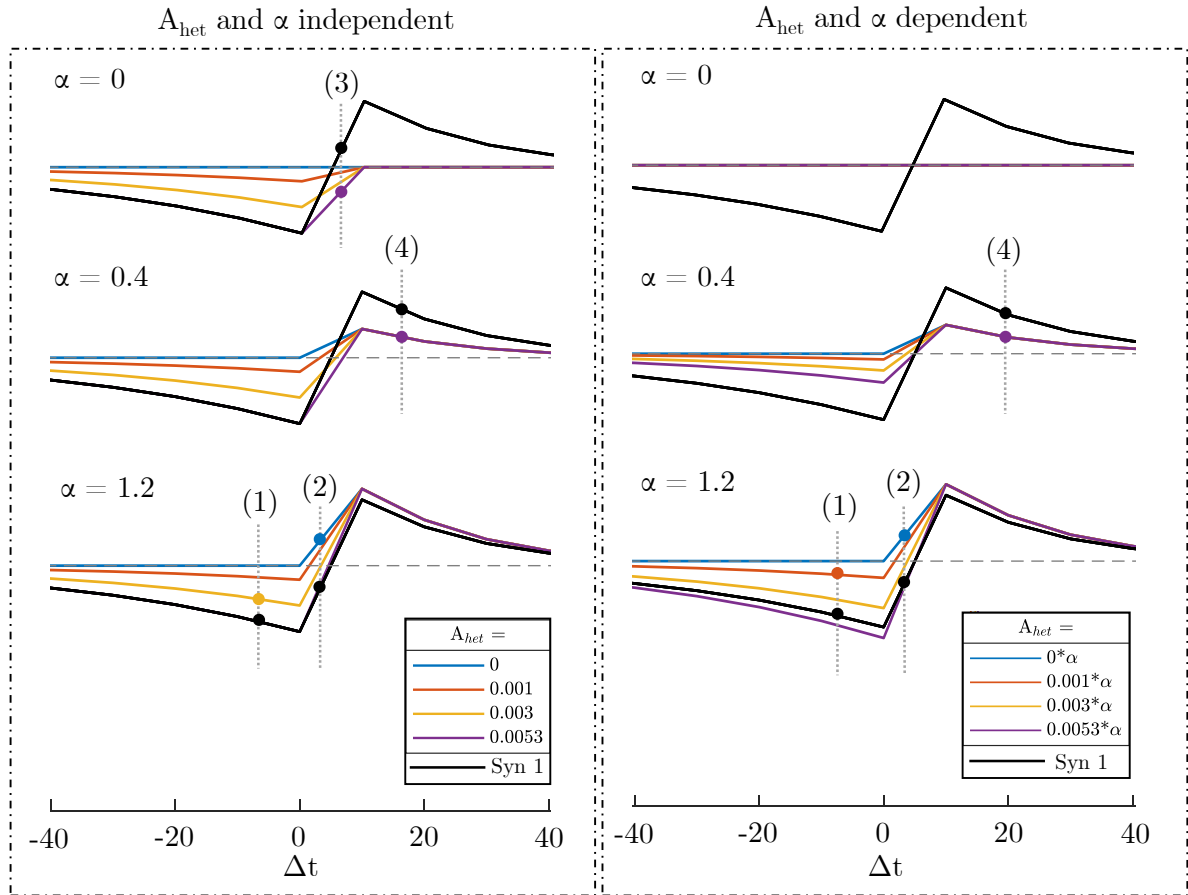
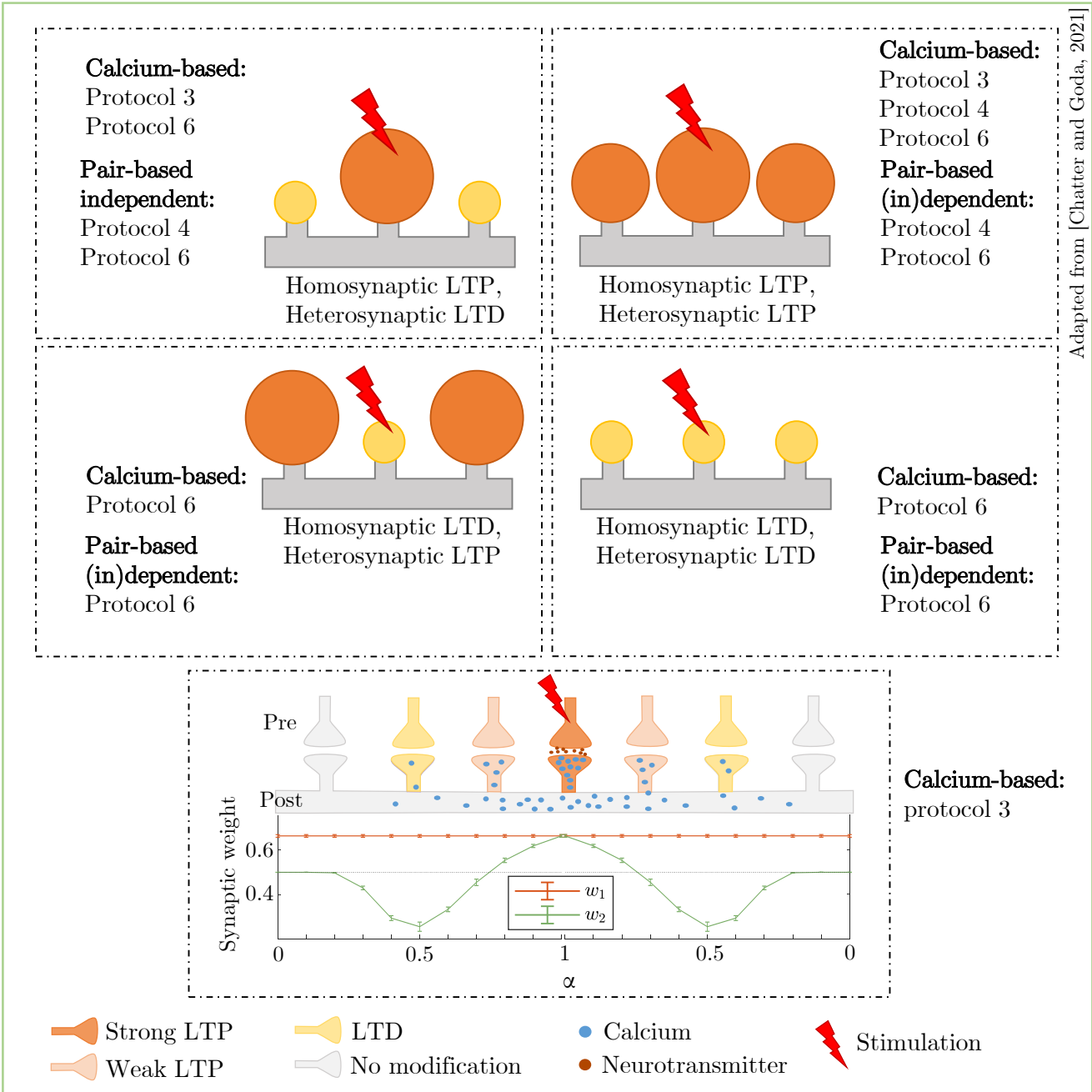


Figure 8.3 – Zoom on the different cases observable with pair-based model simulated with the sixth protocol. (1) Depression at the active synapse leads to depression at the inactive synapse. (2) Depression at the active synapse leads to potentiation at the inactive synapse. (3) Potentiation at the active synapse leads to depression at the inactive synapse. (4) Potentiation at the active synapse leads to potentiation at the inactive synapse

8.3 Summary

SUMMARY: RESULTS AND DISCUSSION



Chapter 9

Toy model: implementation of heterosynaptic rules in the context of allodynia

Now that we have two heterosynaptic models, it is time to apply them to a practical case. In the case of pain, the phenomenon of central sensitization has an important heterosynaptic plasticity dimension. In the case of allodynia, a heterosynaptic phenomenon could appear between the C fibers and the $A\beta$ fibers through a conditioning input and a test input (see section 2.3). Although several mechanisms could be involved in this phenomenon, we chose here to try to model allodynia with our heterosynaptic model, making it a purely heterosynaptic phenomenon.

The principle of allodynia is that non-nociceptive fibers provoke a sensation of pain after the induction of pain by nociceptive fibers. At first, if $A\beta$ spikes alone, nothing happens and the projection neuron does not react. This is just a sensation of touch which doesn't produce any pain. Then, the activation of C fibers will have the impact of activating the projection neuron. In response to C fibers, this neuron spikes which will induce the sensation of pain by sending the signal via the spinothalamic pathway. We are now in pain. The phenomenon of allodynia can take place. Now, if $A\beta$ fiber spikes again, this will cause a reaction from the projection neuron which, once activated will induce the sensation of pain. After some time without any spike, the reactivation of $A\beta$ won't produce any reaction from the projection neuron anymore. This is the scenario that we want to reproduce with our heterosynaptic models.

9.1 Adaptation of the models

Before adapting the model, it is important to note that our heterosynaptic models are not adapted to the neurons of the spinal cord. Indeed, our calcium model is simulated with the parameters of the cortex while the pair-based model is simulated with the parameters of the hippocampus. However, we are still trying to adapt those to spinal cord since we didn't find any heterosynaptic model adapted to the spinal cord. It is then important to keep in mind that lots of alterations can be needed to best adapt our models to the phenomenon of allodynia.

9.1.1 Choice of the neurons

To link our models to the phenomenon of allodynia, we first had to chose the neurons to model. As explained before, the fibers concerned by the central sensitization in allodynia are the nociceptive C fibers and the non nociceptive $A\beta$ fibers. Those fibers are linked to a projection neuron which, once activated, produces pain through the pain pathway. Thus, our postsynaptic neuron will be the projection neuron and the two presynaptic neurons will be a C fiber and an $A\beta$ fiber.

9.1.2 New Poisson train

To simulate allodynia, we needed a new spike train. We chose to keep a Poisson train but we needed a longer duration and to "clip" the train during the simulation. At first, in order to test the model, we simulated a train with a frequency of either 20 Hz for 60 000 ms. Since each fiber spikes in turn we simulated four Poisson trains. A first train was simulated from 0 to 1000 ms for $A\beta$, then another train from 1000 to 45 000 ms for C , a third train from 45 000 ms to 46 000 ms and finally, the last train from 59 000 to 60 000 ms was attributed to $A\beta$. Note that all Poisson trains are newly created at each stimulation.

In a second time, since central sensitization is a phenomenon which can be induced by a stimulation at a frequency ~ 10 Hz for 10 to 20 seconds [Ji et al., 2003, Woolf, 2011], we generated a new train with those parameters. Thus, a first train was simulated from 0 to 1000 ms for $A\beta$, then another train from 1000 to 15 000 ms for C , a third train from 15 000 ms to 16 000 ms and finally, the last train from 59 000 to 60 000 ms was attributed to $A\beta$. This allowed us to simulate a stimulation of 14 sec. Moreover, the period when nobody spikes is longer to express the fact that central sensitization can last in time. Ideally, this period should be longer than 43 sec. Figure 9.1 shows a general pattern of the different spike trains. $A\beta$ and C have both Poisson train each in turn. The projection neuron doesn't spike by itself as in previous models. It will be triggered by the activity of $A\beta$ and C .

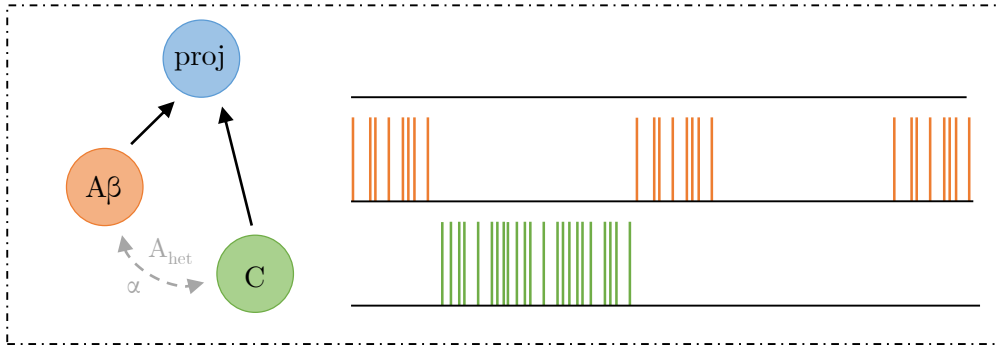


Figure 9.1 – *Adapted Poisson train in order to simulate an allodynia toy model.* In this configuration, postsynaptic neuron doesn't spike on its own. $A\beta$ spikes alone in a first time. Then C spikes alone for some time. $A\beta$ spikes alone again. Then neither $A\beta$ nor C spikes for a while. Finally, $A\beta$ spikes on its own again.

9.1.3 Tuning of parameters α , A_{het} and C_{pre2}

We then had to adapt our parameter α for the calcium model and α and A_{het} for the pair-based model.

Parameter α having the same function in the two models, we can tune it only once. To explain the fact that $A\beta$ is capable of inducing a sensation of pain after C fibers have been activated for a

while, we have to tune our parameter α so that the activation of the C fiber potentiates the $A\beta$ fiber. However, we need to do a distinction between the impact of C on $A\beta$ and the impact of $A\beta$ on C . Indeed, if we want $A\beta$ to be potentiated thanks to the activity of C , we don't want the activity of $A\beta$ to have an impact on the weight of C . Thus we now have two parameters: α_1 which governs the impact of C on $A\beta$ and α_2 which governs the impact of $A\beta$ on C . As previous α , α_1 can take several values from 0.4 to 1.6 modeling the distance between the two fibers or the calcium release. However, since we don't want any impact of $A\beta$ on C , $\alpha_2 = 0$ for all the simulation. For more convenience, we will consider the value of α_1 when talking about α in the following.

Parameter A_{het} also needs to be duplicated for the same reason. Thus A_{het1} governs the depression of $A\beta$ linked to the spikes produced by C while A_{het2} governs the depression of C linked to the spikes produced by $A\beta$. A_{het1} can keep all the values previously tested while $A_{het2} = 0$. Indeed, touching a zone doesn't have the impact of increasing the pain threshold for a future pain. For more convenience, we will consider the value of A_{het1} when talking about A_{het} in the following.

About the parameter C_{pre2} , when simulating the calcium-based model with a frequency of 10 Hz, we had to set C_{pre2} from 0.84410 to 1.5 in order to obtain a high enough potentiation. In these conditions and with $\alpha = 1.6$, we could obtain the expected results. When simulating the model with a frequency of 20 Hz, this tuning was not necessary.

9.1.4 Tuning of current intensity

The simulation of that model is different from the previous models since we don't chose the time of spike of the post synaptic neuron anymore. Here, it's the intensity of the current generated by the presynaptic neuron multiplied by the weight of the synapse which will determine if the post synaptic neuron will spike or not. This is governed by the Hodgkin-Huxley conductance model such that

$$C \frac{dV}{dt} = - \sum_n g_{ion}(V - V_{ion}) + I_{app} + I_{step} + w_1 I_{syn1} + w_2 I_{syn2} \quad (9.1)$$

Previously, we had $I_{app} = 0$, $I_{step} = 50$ when *post* spiked and $I_{syn1} = I_{syn2} = 9.8$ which was the limit to induce an EPSP and not an action potential when *pre1* or *pre2* spiked. Now the goal is that the projection neuron spikes with $C = pre2$. To do so, we set $I_{syn2} = 50$ when C spikes. On the other hand, the projection neuron can't react to $A\beta$'s activity in a first time but then, it has to react for some time before not reacting again. To do so, we have to find the limit value of I_{syn1} which, when w_1 is low enough produces an EPSP but when w_1 is potentiated, produces an action potential. In order to have more margin to tune I_{syn1} , we decided to remove the term dividing $w_1 I_{syn1}$ and $w_2 I_{syn2}$ by the number of cells (see section 7.1).

9.1.5 Tuning of the weight evolution

In order to cancel the effect of central sensitization after some time, we had to add an equation governing the weight in order that the weight of an inactive synapse decreases slightly over time. Thus, if no spike occurs for some time, the weight of the synapse will decrease slowly toward 0.5.

For the calcium model, this was done by making the weight converge toward 0.5 with a very high time constant each time the calcium trace was below the depression threshold θ^d . Thus we have: If $[Ca]_{i,tot}$ ranges below θ^d , synaptic weight is decreased such that

$$\tau_w^{slow} \frac{dw_i}{dt} = w_{init} - w_i, \quad (9.2)$$

where $\tau_w^{slow} = 30000$. Thus it means that w_i will reach w_{init} after 30 000 ms.

The same method was used for the STDP model. Indeed we made the weight converge to $w_{init} = 0.5$ with a very high time constant each time there was no spike. Thus we have:

If no one spikes, synaptic weight is decreased such that

$$\tau_w^{slow} \frac{dw_i}{dt} = w_{init} - w_i \quad (9.3)$$

with $\tau_w^{slow} = 20000$. Thus, it means that w_i will reach w_{init} after approximately 20 000 ms. As anyone can notice, the time variable of the pair-based model is lower than the one of the calcium-based model. Indeed, we noticed during the simulations that when $\tau_w^{slow} = 30000$, the weight had not enough time to correctly decrease toward w_{init} . Thus, we took the decision to set $\tau_w^{slow} = 20000$.

We can note that the time constant τ_w^{slow} in those two models is not very important and can be tunable as we want since its role is to represent the elapsed time. Here, as we wanted to show that the effect of central sensitization can last longer than the time of stimulation, we chose those values. But if the model is simulated on longer periods, the two variables will need to be increased.

9.2 Methodology

The two models have been simulated with several values of α . Results shown here were simulated for $\alpha = 1.6$ and $\alpha = 1.2$. For the pair-based model, we chose $A_{het} = 0.003$. The choice of those values is not very important here since the goal is to see the impact of pre_2 on pre_1 to show a phenomenon comparable to allodynia. However, by choosing those values, we are sure that the effect will be big enough so that pre_2 (C fiber) will have an impact on pre_1 (A β fiber). As observed in previous chapters, the bigger α and the smaller A_{het} , the bigger effect of pre_1 on pre_2 will be observed.

When simulating the models, we realized that they were very fragile. Indeed, the results weren't the same with different Poisson trains. The tuning of I_{syn} was very complicated since its value could trigger a reaction from the projection neuron or not depending on the Poisson train followed.

Concerning the frequency, central sensitization is a phenomenon where the conditioning input has a low frequency (10 Hz in [Ji et al., 2003]). Since our model has been tested at 20 Hz in previous chapters (those results are shown in Appendix C), we kept this frequency in a first time and then simulated the model at a frequency of 10 Hz as explained previously.

9.2.1 Calcium-based model

Model was simulated for several Poisson trains to check whether the obtained results were reliable. Unfortunately, we realized that our model was very fragile and very sensible to the used Poisson train. We first tested the model with a frequency of 20 Hz then with a frequency of 10 Hz. We used the value $\alpha = 1.6$.

9.2.2 Pair-based model

For the pair-based model, we tested several values of I_{syn1} until obtaining satisfying results. Eventually, we chose $I_{syn1} = 14$ with which we could obtain results presented in Figure 9.3. As said earlier, the

model was very fragile and it was really difficult to evaluate the right I_{syn1} since the model was very dependent on the Poisson train used.

9.3 Results

This section presents the results obtained with the calcium-based model and with the pair-based model.

9.3.1 Calcium-based model

Results obtained with calcium-based model are shown in Figure 9.2. This shows exactly what we expected from the simulation. Indeed, at the beginning, $A\beta$ fiber spikes alone activated by a light touch (represented by the feather) but this doesn't trigger any action potential from the projection neuron. Then, C fiber spikes during 14 seconds alone activated by a noxious stimulus (represented by a punch). This has the effect of activating the projection neuron and increasing the synaptic weight $w_{A\beta}$ of $A\beta$. After that, $A\beta$ fiber spikes again alone for 1 second activated by a light touch stimulus. This time, this has the effect of triggering the projection neuron which emits action potentials in response to $A\beta$. The three neurons are then left inactivated for 43 seconds which has the effect of decreasing $w_{A\beta}$. Finally, the activation of $A\beta$ fiber doesn't trigger the projection neuron anymore.

Those are the results for one set of parameter but we could also observe some good results for $\alpha = 0.8$ and a frequency of 20 Hz despite an observed fragility of the model triggering unwanted action potential depending on the generated Poisson train, and for $\alpha = 1.6$ and a frequency of 20 Hz (visible in Appendix C).

9.3.2 Pair-based model

Results obtained with pair-based model are shown in Figure 9.3. In Figure 9.3, we can see "perfect" results. Indeed, the simulation shows us exactly what we expected. At the beginning, $A\beta$ fiber spikes alone activated by a light touch stimulus but this doesn't trigger any action potential from the projection neuron. Then, C fiber spikes during 14 seconds alone, activated by a noxious stimulus. This has the effect of activating the projection neuron and of increasing the synaptic weight $w_{A\beta}$ of $A\beta$. After that, $A\beta$ fiber spikes again alone for 1 second activated by a light touch stimulus. This time, this has the effect of triggering the projection neuron which emits action potentials in response to $A\beta$. The three neurons are then inactivated for 43 seconds which has the effect of decreasing $w_{A\beta}$. Finally, the activation of $A\beta$ fiber doesn't trigger the projection neuron anymore.

9.3.3 Fragility of the model

Even if the results showed here present exactly what we expected, the fragility of the models need to be kept in mind. Indeed, some simulations, even when done with exactly the same parameters as in Figure 9.2 or Figure 9.3 show some undesirable spikes at the beginning. Besides those, the simulations showed the same behavior as observed in previous figures. Same observations could be done for different set of parameters. Indeed, while some simulations could show good results, other simulations with the same set of parameters showed unexpected action potentials at the end of the simulation or not enough action potentials between the 15th and the 16th seconds. This have been observed for different combination of α , A_{het} and I_{syn1} .

Calcium-based model:

$$\alpha = 1.6, C_{pre2} = 1.5, I_{syn1} = 15, \text{frequency} = 10 \text{ Hz}$$

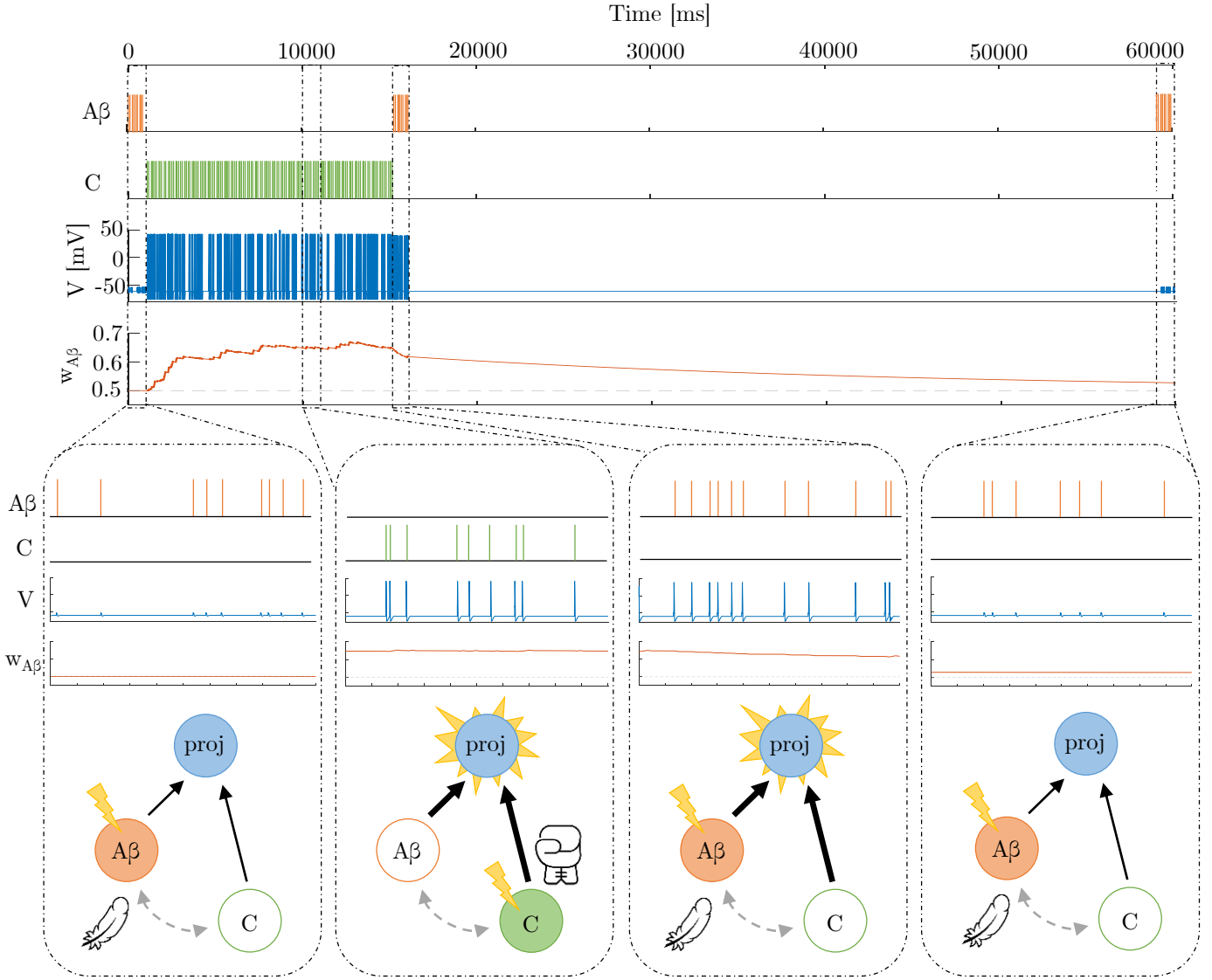


Figure 9.2 – Results obtained when simulating calcium-based allodynia toy model for $\alpha = 1.6$, $C_{pre2} = 1.5$ and $I_{syn} = 15$ with a frequency of 10 Hz. 1st row = spike train of $A\beta$, 2nd row = spike train of C , 3rd row = membrane potential of projection neuron and 4th row = synaptic weight between $A\beta$ and the projection neuron. Light touch stimulus (feather) activates $A\beta$ fiber which can't trigger the projection neuron. Noxious stimulus (punch) activate C fiber which triggers the projection neuron emitting action potential as a response. This has the effect of increasing the $w_{A\beta}$. Light touch stimulus activates $A\beta$ again which has now the power of triggering the projection neuron. After some time without any stimulus, light touch stimulus activates $A\beta$ fiber but this can't trigger the projection neuron anymore.

9.4 Discussion

The results obtained show that our model is capable of reproducing a heterosynaptic mechanism of central sensitization which could be responsible for the induction of allodynia. However, some limitations have been encountered during the simulations. For both models, satisfying results could be obtained for different values of α and A_{het} and for frequency of 10 Hz and 20 Hz. However, the model was very sensitive to the generated Poisson train. Thus, for the same parameters, undesirable action

Pair-based model:

$$\alpha = 1.2, A_{het} = 0.003, I_{syn1} = 14, \text{frequency} = 10 \text{ Hz}$$

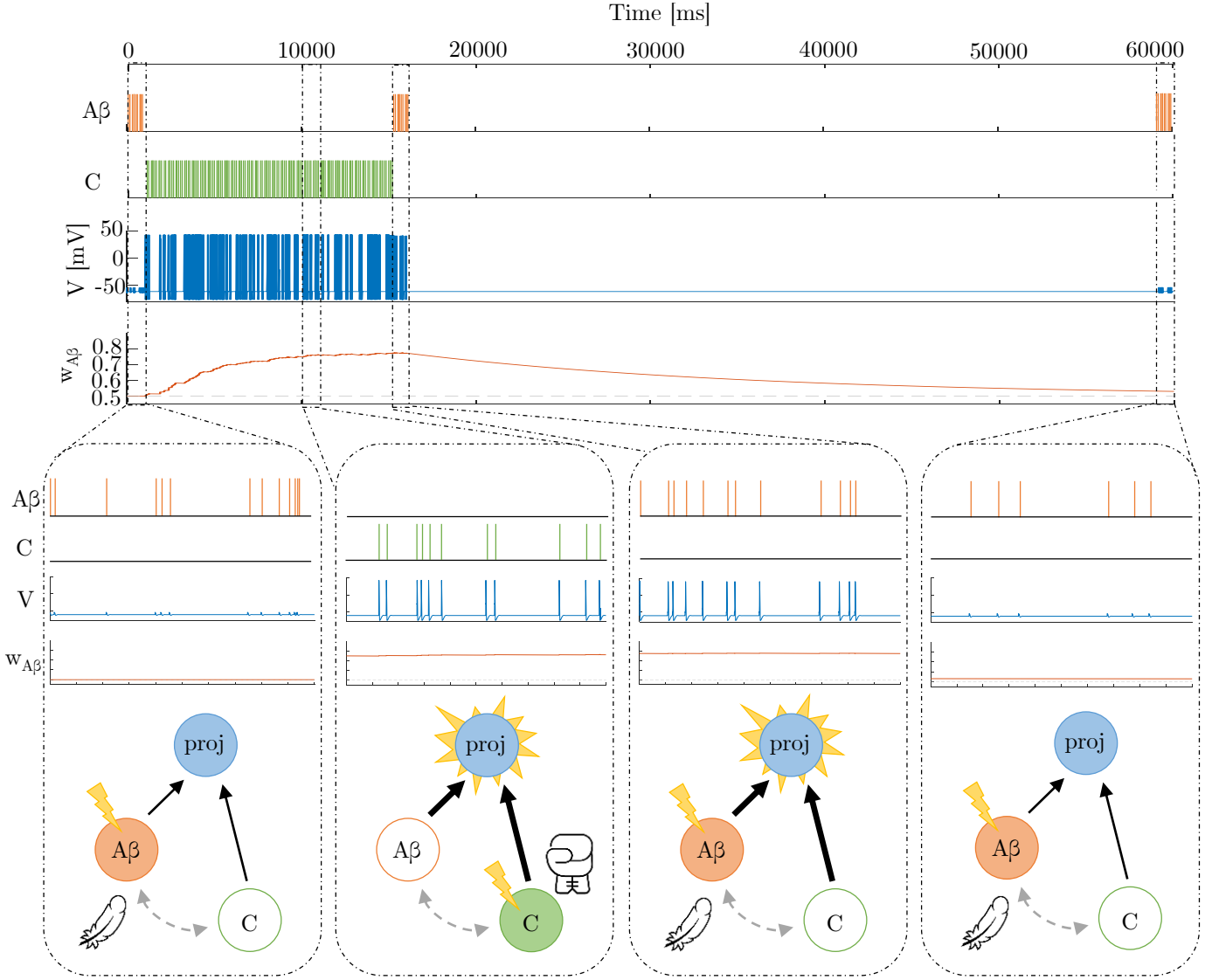


Figure 9.3 – Results obtained when simulating the pair-based allodynia toy model for $\alpha = 1.2$, $A_{het} = 0.003$, $I_{syn} = 14$ with a frequency of 10 Hz. 1st row = spike train of Aβ, 2nd row = spike train of C, 3rd row = membrane potential of projection neuron and 4th row = synaptic weight between Aβ and the projection neuron. Light touch stimulus activate Aβ fiber which can't trigger the projection neuron. Noxious stimulus activate C fiber which triggers the projection neuron emitting action potential as a response. This has the effect of increasing the $w_{A\beta}$. Light touch stimulus activates Aβ again which has now the power of triggering the projection neuron. After some time without any stimulus, light touch stimulus activates Aβ fiber but this can't trigger the projection neuron anymore.

potentials could be observed. Moreover, in the calcium-based model, with a frequency of 10 Hz, we had to increase the variable C_{pre2} in order to obtain satisfying results while for the pair-based model a wise combination of α and A_{het} could be found to obtain the expected results with this particular frequency. The fragility could be due to several things.

- Membrane potential of the projection neuron is modeled with the Hodgkin and Huxley conductance-based model which is a very simple model. Those undesirable spikes could be due to the limita-

tions imposed by this model.

- The value of I_{syn1} could be inadapted to the simulations despite multiple test in order to find the best frequency. This would be due to the change of Poisson train at each simulation. Since a Poisson train doesn't show a constant time interval between each spike, it could happen that multiple spikes happen in a short time period which could have the impact of triggering the projection neuron.
- Finally, our heterosynaptic models are based on homosynaptic models configured in the cortex for the calcium-based model and in the hippocampus for the pair-based model. Central sensitization being a phenomenon happening in the dorsal horn of the spinal cord, it is clear that a lot of parameters need to be tuned and tested before obtaining the perfect simulation model of central sensitization.

9.5 Summary

In this section we were able to reproduce a phenomenon assimilable to central sensitization inducing allodynia thanks to our new heterosynaptic models. To do so, we had to tune a bunch of parameters. The models have been simulated with a frequency of 10 Hz and 20 Hz. In the calcium-based model, in order to make it work for a frequency of 10 Hz, C_{pre2} , the parameter governing the value of the calcium trace of the C fiber had to be increased. In those conditions we could obtain satisfying results with $\alpha = 1.6$. For a frequency of 20 Hz, this tuning was not necessary. In the pair-based model, for the two tested frequencies, a right combination of α and A_{het} could be found in order to obtain the expected results. Both models showed a certain fragility which can be linked to the modeling of the postsynaptic membrane for example.

Part III

Conclusion and perspectives

Chapter 10

Conclusion and perspectives

10.1 Thesis summary

The goal of this thesis was first to model the heterosynaptic plasticity in neurons through a new model and second to apply this model to a case study to show its efficacy. To achieve this, the following questions have been answered:

- *What is pain? In particular what is central sensitization?* (CHAPTER 2)

The most important relay in the pain neural circuit is the dorsal horn of the spinal cord. It is there that the nociceptive and non nociceptive fibers can cross each other and interact with dorsal horn projection neurons. A type of plasticity taking place in the dorsal horn is the central sensitization. Central sensitization is characterized by an enhancement of the excitability in somatosensory neurons in the dorsal horn following the induction of a noxious stimulus. This plasticity mechanism is responsible for the phenomenon of allodynia in which, after an injury, a non-noxious stimuli applied on the wound induces pain.

- *What is synaptic plasticity?* (CHAPTER 3)

Homosynaptic plasticity can be a short-term or a long-term phenomenon. The introduction of homeostatic and heterosynaptic plasticity is sometimes necessary to prevent some undesirable phenomena from happening with homosynaptic plasticity alone. Heterosynaptic plasticity considers all the synaptic connections in a set and thus, an inactive synapse can experience strength modifications influenced by active neighbor synapses.

- *How synaptic plasticity can be modeled?* (CHAPTER 4 AND 5)

Homosynaptic plasticity can be modeled with biological or phenomenological models. In this thesis, we focused on the calcium-based homosynaptic model described in [Graupner et al., 2016] and the pair-based homosynaptic model described in [Morrison et al., 2008]. They form the basis on which we could graft heterosynaptic rules.

Heterosynaptic plasticity has not been widely modeled. Chen et al. established a model to prevent the runaway mechanism and to enhance the synaptic competition [Chen et al., 2013]. Field et al. established a model in order to set the E/I balance experimentally observed [Field et al., 2020]. Finally, Hiratani and Fukai established a model of the E/I balance in the cortical dendritic branches. This model started from homosynaptic calcium-based model to implement heterosynaptic rules [Hiratani and Fukai, 2017]. Others models such as the ones established by Chen and Xie or Zenke et al. were established in order to maintain stability [Chen and Xie, 2021, Zenke et al., 2015].

- *How to adapt existing homosynaptic models into heterosynaptic models?* (CHAPTER 6, 7, 8)

Starting from homosynaptic models described above, we could establish two new heterosynaptic models which are extensions of the calcium-based model and of the pair-based model. Those models could reproduce heterosynaptic phenomena such as the potentiation or the depression of an inactive synapse. We could reproduce experimental results reported in literature [Chistiakova et al., 2015, Chater and Goda, 2021] such as the Mexican hat pattern.

- *How to model allodynia?* (CHAPTER 9)

The two heterosynaptic plasticity models could be adapted in order to model the crosstalk between nociceptive and non nociceptive fibers involved in the phenomenon of allodynia. Results obtained were satisfying despite some limitations encountered.

10.2 Perspectives

Heterosynaptic models established in this thesis being totally new, many perspectives are to be considered for the future in order to improve those models. A few ideas are listed here:

- All the simulations have been performed with four heterosynaptic protocols: one protocol was at 100 Hz, two at 20 Hz and the last one at 1 Hz. However, new information could be obtained by simulating our models at other frequencies.
- The use of the conductance-based model of Hodgkin-Huxley to model the membrane potential of the postsynaptic neuron has some limitations. Indeed, this model is a very simple one which was suitable for the beginning of this work. However, in the future, maybe a more complex model would improve the performance of our heterosynaptic models. In particular to model allodynia where we met some difficulties to tune the conductance-based model in order to have the right action potentials.
- The models as they are at the moment are not the most physiological. This could be improved by adding a more detailed modeling of the calcium dynamic. For instance, parameters α and A_{het} could be redesigned in a more physiological way.
- Heterosynaptic experimental data are quite few at the moment. The realization of new experimental protocols could help to validate computational results. For example, time windows obtained with the protocol 6 could be reproduced experimentally in order to validate our results.
- Those experimental protocols could also be helpful to improve the toy model established in CHAPTER 9. Indeed, our heterosynaptic models are set in the hippocampus and in the cortex while central sensitization, responsible for allodynia, happens in the dorsal horn of the spinal cord.
- Allodynia model is very simple and need to be complexified in order to better mimic real-life allodynia. Moreover, the simulations were done on very short timescale compared to the timescale of allodynia phenomenon. Thus, new simulations should be performed on longer time intervals.

To conclude, even if good results could be obtained with our new heterosynaptic models, more precision and complexity should be added in the future in order for these models to become more faithful to the physiological phenomena.

Bibliography

- [Chr, 2017] (2017). Chronic pain and its treatment. <https://basicmedicalkey.com/chronic-pain-and-its-treatment/>.
- [wik, 2022] (2022). Inositol trisphosphate receptor. https://en.wikipedia.org/wiki/Inositol_trisphosphate_receptor. Accessed on 06.06.2022.
- [Abbott and Nelson, 2000] Abbott, L. F. and Nelson, S. B. (2000). Synaptic plasticity: Taming the beast. *Nature Neuroscience*, 3(11):1178–1183.
- [Bannon et al., 2015] Bannon, N. M., Chistiakova, M., and Volgushev, M. (2015). Homeostatic Role of Heterosynaptic Plasticity. In Boison, D. and Masino, S. A., editors, *Homeostatic Control of Brain Function*, pages 124–142. Oxford University Press.
- [Bear et al., 2007] Bear, M. F., Connors, B. W., and Paradiso, M. A. (2007). *Neuroscience: Exploring the Brain*. Lippincott Williams and Wilkins, 3rd edition.
- [Bi and Poo, 1998] Bi, G.-q. and Poo, M.-m. (1998). Synaptic Modifications in Cultured Hippocampal Neurons: Dependence on Spike Timing, Synaptic Strength, and Postsynaptic Cell Type. *The Journal of Neuroscience*, 18(24):10464–10472.
- [Bi and Poo, 2001] Bi, G.-q. and Poo, M.-m. (2001). Synaptic Modification by Correlated Activity: Hebb’s Postulate Revisited. *Annual Review of Neuroscience*, 24(1):139–166.
- [Bliss and Lomo, 1973] Bliss, T. V. and Lomo, T. (1973). Long-lasting potentiation of synaptic transmission in the dentate area of the anaesthetized rabbit following stimulation of the perforant path. *The Journal of Physiology*, 232(2):331–356.
- [Carew and Kandel, 1973] Carew, T. J. and Kandel, E. R. (1973). Acquisition and Retention of Long-Term Habituation in *Aplysia* : Correlation of Behavioral and Cellular Processes. *Science*, 182(4117):1158–1160.
- [Chater and Goda, 2021] Chater, T. E. and Goda, Y. (2021). My Neighbour Hetero — deconstructing the mechanisms underlying heterosynaptic plasticity. *Current Opinion in Neurobiology*, 67:106–114.
- [Chen and Xie, 2021] Chen, H. and Xie, L. (2021). Modeling on Heterosynaptic Plasticity Based on Postsynaptic Membrane Potential and Current Density. *Journal of Physics: Conference Series*, 1746(1):012004.
- [Chen et al., 2013] Chen, J.-Y., Lonjers, P., Lee, C., Chistiakova, M., Volgushev, M., and Bazhenov, M. (2013). Heterosynaptic Plasticity Prevents Runaway Synaptic Dynamics. *Journal of Neuroscience*, 33(40):15915–15929.

- [Chistiakova et al., 2014] Chistiakova, M., Bannon, N. M., Bazhenov, M., and Volgushev, M. (2014). Heterosynaptic Plasticity: Multiple Mechanisms and Multiple Roles. *The Neuroscientist*, 20(5):483–498.
- [Chistiakova et al., 2015] Chistiakova, M., Bannon, N. M., Chen, J.-Y., Bazhenov, M., and Volgushev, M. (2015). Homeostatic role of heterosynaptic plasticity: models and experiments. *Frontiers in Computational Neuroscience*, 9.
- [De Worm, 2021] De Worm, A. (2021). Integrate-and-fire modeling of dorsal horn neurons and their functional states in pain pathways. Master’s thesis, ULiège.
- [Field et al., 2020] Field, R. E., D’amour, J. A., Tremblay, R., Miehl, C., Rudy, B., Gjorgjieva, J., and Froemke, R. C. (2020). Heterosynaptic Plasticity Determines the Set Point for Cortical Excitatory-Inhibitory Balance. *Neuron*, 106(5):842–854.e4.
- [Fröhlich, 2016] Fröhlich, F. (2016). Synaptic Plasticity. In *Network Neuroscience*, pages 47–58. Elsevier.
- [Graupner and Brunel, 2012] Graupner, M. and Brunel, N. (2012). Calcium-based plasticity model explains sensitivity of synaptic changes to spike pattern, rate, and dendritic location. *Proceedings of the National Academy of Sciences*, 109(10):3991–3996.
- [Graupner et al., 2016] Graupner, M., Wallisch, P., and Ostojic, S. (2016). Natural Firing Patterns Imply Low Sensitivity of Synaptic Plasticity to Spike Timing Compared with Firing Rate. *The Journal of Neuroscience*, 36(44):11238–11258.
- [Groves and Thompson, 1970] Groves, P. M. and Thompson, R. F. (1970). Habituation: a dual-process theory. *Psychological Review*, 77(5):419–450.
- [Hebb, 1949] Hebb, D. O. (1949). *The organization of behavior : a neuropsychological theory*. A Wiley book in clinical psychology. John Wiley, New York, NY.
- [Heidelberger et al., 2014] Heidelberger, R., Shouval, H., Zucker, R. S., and Byrne, J. H. (2014). Synaptic Plasticity. In *From Molecules to Networks*, pages 533–561. Elsevier.
- [Hiratani and Fukai, 2017] Hiratani, N. and Fukai, T. (2017). Detailed Dendritic Excitatory/Inhibitory Balance through Heterosynaptic Spike-Timing-Dependent Plasticity. *The Journal of Neuroscience*, 37(50):12106–12122.
- [Hodgkin and Huxley, 1952] Hodgkin, A. L. and Huxley, A. F. (1952). A quantitative description of membrane current and its application to conduction and excitation in nerve. *The Journal of Physiology*, 117(4):500–544.
- [IASP, 2020] IASP (2020). Iasp announces revised definition of pain. <https://www.iasp-pain.org/publications/iasp-news/iasp-announces-revised-definition-of-pain/>.
- [Jacquerie et al., 2022a] Jacquerie, K., Minne, C., and Drion, G. (2022a). Neuromodulation of excitability and synaptic plasticity: an underestimated challenge for computational models. BSN 2022.
- [Jacquerie et al., 2022b] Jacquerie, K., Minne, C., and Drion, G. (2022b). Synaptic plasticity, neuronal excitability and neuromodulation: are they compatible from a computational approach? page Unpublished Manuscript.

- [Jenks et al., 2021] Jenks, K. R., Tsimring, K., Ip, J. P. K., Zepeda, J. C., and Sur, M. (2021). Heterosynaptic Plasticity and the Experience-Dependent Refinement of Developing Neuronal Circuits. *Frontiers in Neural Circuits*, 15:803401.
- [Ji et al., 2003] Ji, R.-R., Kohno, T., Moore, K. A., and Woolf, C. J. (2003). Central sensitization and LTP: do pain and memory share similar mechanisms? *Trends in Neurosciences*, 26(12):696–705.
- [Kandel, 2013] Kandel, E. R., editor (2013). *Principles of neural science*. McGraw-Hill, New York, 5th ed edition.
- [Kawamoto et al., 2012] Kawamoto, E. M., Vivar, C., and Camandola, S. (2012). Physiology and Pathology of Calcium Signaling in the Brain. *Frontiers in Pharmacology*, 3.
- [Klein et al., 2008] Klein, T., Stahn, S., Magerl, W., and Treede, R.-D. (2008). The role of heterosynaptic facilitation in long-term potentiation (LTP) of human pain sensation. *Pain*, 139(3):507–519.
- [Latremoliere and Woolf, 2009] Latremoliere, A. and Woolf, C. J. (2009). Central Sensitization: A Generator of Pain Hypersensitivity by Central Neural Plasticity. *The Journal of Pain*, 10(9):895–926.
- [Leprince, 2019] Leprince, P. (2019). Plasticité synaptique. Technical report, ULiège.
- [Li et al., 1999] Li, J., Simone, D. A., and Larson, A. A. (1999). Windup leads to characteristics of central sensitization. *Pain*, 79(1):75–82.
- [Lynch et al., 1977] Lynch, G. S., Dunwiddie, T., and Gribkoff, V. (1977). Heterosynaptic depression: a postsynaptic correlate of long-term potentiation.
- [Mendell, 2022] Mendell, L. M. (2022). The Path to Discovery of Windup and Central Sensitization. *Frontiers in Pain Research*, 3.
- [Meriney and Fanselow, 2019] Meriney, S. D. and Fanselow, E. E. (2019). *Synaptic plasticity*. Pages: 329 Publication Title: Synaptic Transmission.
- [Minne, 2021] Minne, C. (2021). Interactions between synaptic plasticity and switches in brain states for memory consolidation: a modeling study. Master’s thesis, ULiège.
- [Morrison et al., 2008] Morrison, A., Diesmann, M., and Gerstner, W. (2008). Phenomenological models of synaptic plasticity based on spike timing. *Biological Cybernetics*, 98(6):459–478.
- [Nagase et al., 2003] Nagase, T., Ito, K.-I., Kato, K., Kaneko, K., Kohda, K., Matsumoto, M., Hoshino, A., Inoue, T., Fujii, S., Kato, H., and Mikoshiba, K. (2003). Long-term potentiation and long-term depression in hippocampal CA1 neurons of mice lacking the IP3 type 1 receptor. *Neuroscience*, 117(4):821–830.
- [Nicoll, 2017] Nicoll, R. A. (2017). A Brief History of Long-Term Potentiation. *Neuron*, 93(2):281–290.
- [Nishiyama et al., 2000] Nishiyama, M., Hong, K., Mikoshiba, K., Poo, M.-m., and Kato, K. (2000). Calcium stores regulate the polarity and input specificity of synaptic modification. 408:5.
- [Padamsey et al., 2019] Padamsey, Z., Foster, W. J., and Emptage, N. J. (2019). Intracellular Ca^{2+} Release and Synaptic Plasticity: A Tale of Many Stores. *The Neuroscientist*, 25(3):208–226.

- [Pishro-Nik, 2014] Pishro-Nik, H. (2014). *Introduction to probability, statistics, and random processes*. Kappa Research LLC.
- [Purves, 2004] Purves, D., editor (2004). *Neuroscience*. Sinauer Associates, Publishers, Sunderland, Mass, 3rd ed edition.
- [Sandkühler, 2009] Sandkühler, J. (2009). Models and Mechanisms of Hyperalgesia and Allodynia. *Physiological Reviews*, 89(2):707–758.
- [Santos and Noggle, 2011] Santos, E. and Noggle, C. A. (2011). *Synaptic Pruning*, pages 1464–1465. Springer US, Boston, MA.
- [Shouval et al., 2002] Shouval, H. Z., Bear, M. F., and Cooper, L. N. (2002). A unified model of NMDA receptor-dependent bidirectional synaptic plasticity. *Proceedings of the National Academy of Sciences of the United States of America*, 99(16):10831–10836.
- [Sjöström and Gerstner, 2010] Sjöström, J. and Gerstner, W. (2010). Spike-timing dependent plasticity. *Scholarpedia*, 5(2):1362.
- [Thompson et al., 1993] Thompson, S. W., Woolf, C. J., and Sivilotti, L. G. (1993). Small-caliber afferent inputs produce a heterosynaptic facilitation of the synaptic responses evoked by primary afferent A-fibers in the neonatal rat spinal cord in vitro. *Journal of Neurophysiology*, 69(6):2116–2128.
- [Tsagareli, 2013] Tsagareli, M. G. (2013). Pain and memory: Do they share similar mechanisms? *World Journal of Neuroscience*, 03(01):39–48.
- [Turrigiano et al., 1998] Turrigiano, G. G., Leslie, K. R., Desai, N. S., Rutherford, L. C., and Nelson, S. B. (1998). Activity-dependent scaling of quantal amplitude in neocortical neurons. *Nature*, 391(6670):892–896.
- [van Rossum et al., 2000] van Rossum, M. C. W., Bi, G. Q., and Turrigiano, G. G. (2000). Stable Hebbian Learning from Spike Timing-Dependent Plasticity. *The Journal of Neuroscience*, 20(23):8812–8821.
- [Watt, 2010] Watt, A. J. (2010). Homeostatic plasticity and STDP: keeping a neuron’s cool in a fluctuating world. *Frontiers in Synaptic Neuroscience*, 2.
- [Woolf, 1996] Woolf, C. J. (1996). Windup and central sensitization are not equivalent:. *Pain*, 66(2):105–108.
- [Woolf, 2010] Woolf, C. J. (2010). What is this thing called pain? *Journal of Clinical Investigation*, 120(11):3742–3744.
- [Woolf, 2011] Woolf, C. J. (2011). Central sensitization: Implications for the diagnosis and treatment of pain. *Pain*, 152(3):S2–S15.
- [Zenke et al., 2015] Zenke, F., Agnes, E. J., and Gerstner, W. (2015). Diverse synaptic plasticity mechanisms orchestrated to form and retrieve memories in spiking neural networks. *NATURE COMMUNICATIONS*, page 13.

Part IV

Appendix

Appendix A

Computational details

A.1 Pyramidal neuron model [Chen et al., 2013]

Full model of the pyramidal neuron can be written:

$$C_m(dV_S/dt) = -g(V_S - V_D) - I_S^{int}, \quad (\text{A.1})$$

$$C_m(dV_D/dt) = -g_{leak}(V_D - E_{leak}) - g(V_D - V_S) - I_D^{int} - I_{syn}. \quad (\text{A.2})$$

where C_m is the membrane capacitance, V_S and V_D are the membrane potentials in the axosomatic and dendritic compartments, g is conductance coupling between the compartments, I_S^{int} and I_D^{int} are the sums of all active currents in the axosomatic and dendritic compartments, respectively, and I_{syn} is the sum of synaptic currents. Equation A.1 can be replaced by

$$g(V_S - V_D) = -I_S^{int}, \quad (\text{A.3})$$

since Na^+ and K^+ conductances in the axosomatic compartment were much stronger than in the dendrite. This new reduced model match closely spiking patterns of different classes of cells.

$$I_{syn} = W_{syn}[O](V - E^{syn}), \quad (\text{A.4})$$

$$d[O]/dt = \alpha(1 - [O])[T] - \beta[O], \quad (\text{A.5})$$

$$[T] = AH(t_0 + t_{max} - t)H(t - t_0), \quad (\text{A.6})$$

where W_{syn} is the strength (weight) of a synapse, $[O]$ is the fraction of open channels, E_{syn} is the reversal potential ($E_{syn} = 0\text{mV}$ for excitatory synapses), $H(x)$ is the step function, t_0 is the time instant of receptor activation, $A = 0.5$, and $t_{max} = 0.3$ ms. $\alpha = 1.1 \text{ ms}^{-1}$ and $\beta = 0.19 \text{ ms}^{-1}$ are the rate constants. The synaptic weight was defined in the range between 0 mS/cm^2 and maximum of 0.03 mS/cm^2 . The initial weights were randomly assigned to the 100 synapses from a Gaussian distribution with the mean 0.015 mS/cm^2 and SD 0.003 mS/cm^2 . Short-term dynamics of synaptic transmission at each synapse were simulated using a simple phenomenological model. This model specifies the postsynaptic current as a product of a maximal synaptic conductance W_{syn} and the depression variable D which obeys to the law

$$D = 1 - [1 - D_i(1 - U)]\exp[-(t - t_i)/\tau],$$

where $U = 0.07$ is the fraction of resources used per action potential, $\tau = 700$ ms is the time constant of recovery of the synaptic resources, D_i is the value of D immediately before the i th event, and $(t - t_i)$ is the time after the i th event.

STDP rules are described such as if the presynaptic spike occurs before the postsynaptic spike within the proper time window, the weight of the synapse is increased. If the presynaptic spike occurs after the postsynaptic spike within the proper time window, the weight of the synapse is depressed. This is resumed by the equations

$$dW_{syn}^+ = a^+(\exp[-(t^{post} - t^{pre})/\tau^+]), \quad (\text{A.7})$$

$$dW_{syn}^- = -a^-(\exp[(t^{post} - t^{pre})/\tau^-]), \quad (\text{A.8})$$

where dW_{syn} is the change of synaptic strength, a^+ and a^- are the maximal amplitude of potentiation and depression that could be induced by a single postsynaptic spike, t^{post} and t^{pre} are the timing of postsynaptic and presynaptic spikes, and τ^+ and τ^- are the time constants of potentiation and depression windows.

Appendix B

Hodgkin and Huxley model

In order to implement the homosynaptic plasticity models, we chose to start from the conductance model established by Hodgkin and Huxley in 1952 [Hodgkin and Huxley, 1952]. As a reminder, a conductance model allows us to draw a parallel between a neuron and an electrical circuit, our neuron being only an excitable cell in which a current flows through the membrane. This circuit is illustrated in Figure B.1.

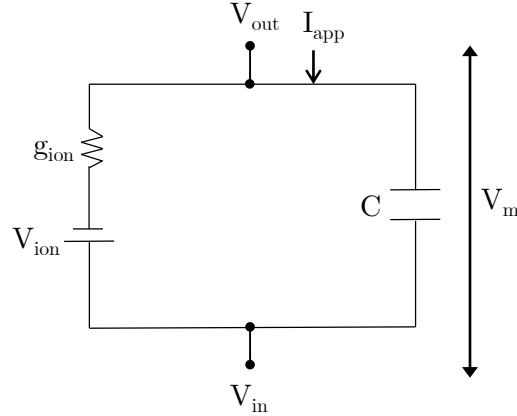


Figure B.1 – *Electrical circuit representing a neuron with the conductance-based model of Hodgkin and Huxley.*

From this figure, we can write

$$C_m \frac{dV_m}{dt} = -I_{Na} - I_K - I_{leak} + I_{app}, \quad (B.1)$$

where C_m is the capacitance of the membrane, dV_m is the variation of the potential of the membrane, I_{app} is the applied current representing an external stimulus, and

$$I_{Na} + I_K + I_{leak} = I_{ion} = g_{ion}(V_m - V_{ion}), \quad (B.2)$$

where $(V_m - V_{ion})$ is the driving force i.e. a measure of how far the membrane potential is from the equilibrium potential of each ion species. g_{ion} is the ion conductance.

In order to introduce the notion of closure and opening of the different ion channels of the plasma membrane, we can introduce the variables m_{Na} , h_{Na} and m_K with m_{Na} and h_{Na} the variables of

activation and inactivation of sodium and m_K the variable of activation of potassium as well as \bar{g}_{ion} , the maximum conductance reachable by each ion when all channels are open. We have

$$\begin{aligned} g_{Na}(V_m, t) &= \bar{g}_{Na} m_{Na}(V_m, t)^3 h_{Na}(V_m, t), \\ g_K(V_m, t) &= \bar{g}_K m_K(V_m, t). \end{aligned} \quad (\text{B.3})$$

Finally,

$$\begin{aligned} C_m \frac{dV_m}{dt} &= -\bar{g}_{Na} * m_{Na}^3 * h_{Na} * (V - V_{Na}) - \bar{g}_K * m_K^4 * (V - V_K) - \bar{g}_{leak} * (V - V_{leak}) + I_{app}, \\ \tau_{m_{Na}}(V_m) \dot{m}_{Na}(V_m, t) &= m_{Na, \infty}(V_m) - m_{Na}(V_m, t), \\ \tau_{h_{Na}}(V_m) \dot{h}_{Na}(V_m, t) &= h_{Na, \infty}(V_m) - h_{Na}(V_m, t), \\ \tau_{m_K}(V_m) \dot{m}_K(V_m, t) &= m_{K, \infty}(V_m) - m_K(V_m, t), \end{aligned} \quad (\text{B.4})$$

where $\tau(V_m)$ is an activation time constant, $m_{Na, \infty}$ is the fraction of channels open at equilibrium for a particular voltage, $h_{Na, \infty}$ is the fraction of channels open at equilibrium for a particular voltage, and $m_{K, \infty}$ is the fraction of channels open at equilibrium for a particular voltage.

Appendix C

Additional results from the Toy model

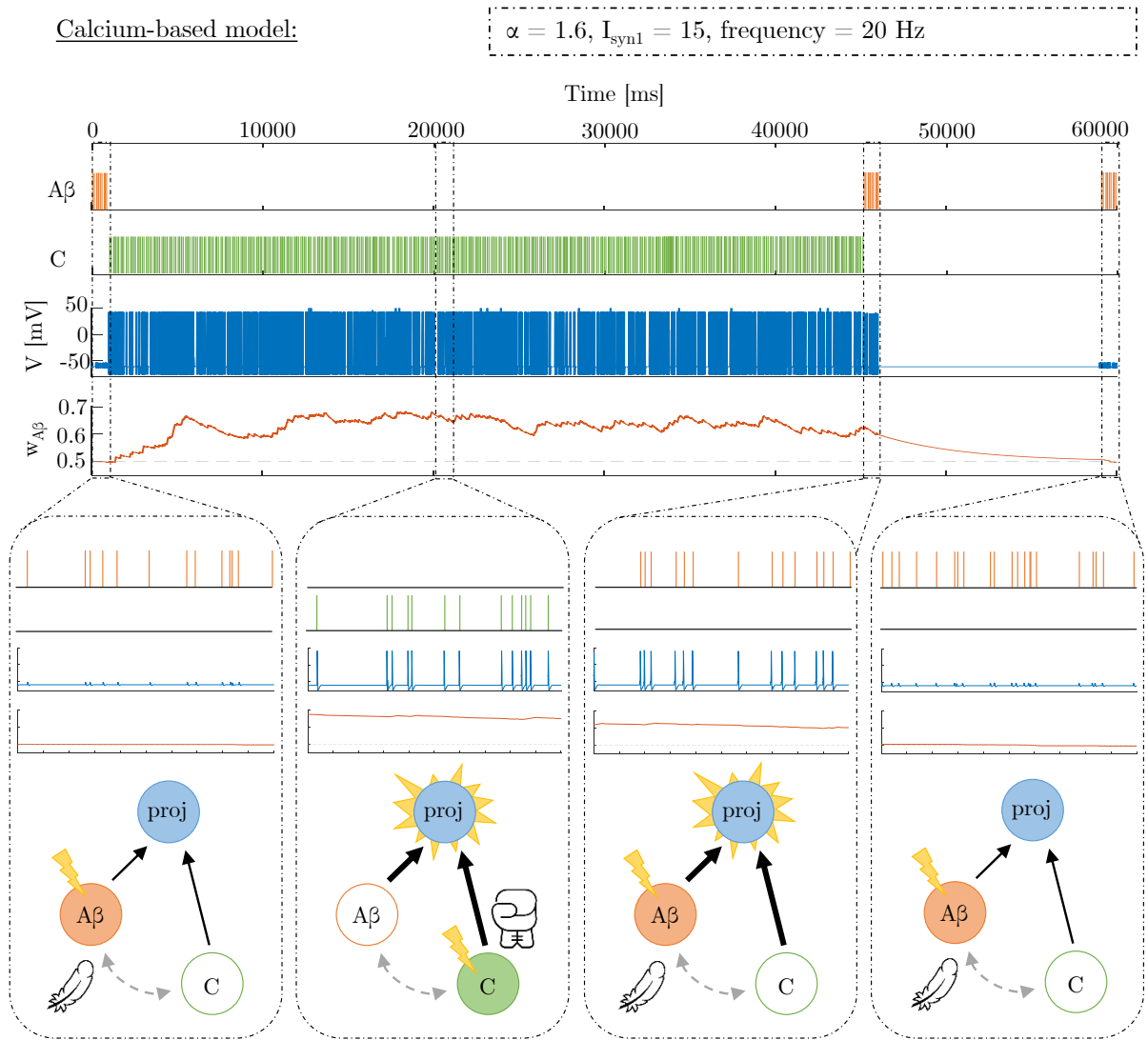


Figure C.1 – Results obtained when simulating calcium-based allodynia toy model for $\alpha = 1.6$ and $I_{syn} = 15$ with a frequency of 20 Hz. Light touch stimulus activate Aβ fiber which can't trigger the projection neuron. Noxious stimulus activate C fiber which triggers the projection neuron emitting action potential as a response. This has the effect of increasing the $w_{A\beta}$. Light touch stimulus activates Aβ again which has now the power of triggering the projection neuron. After some time without any stimulus, light touch stimulus activates Aβ fiber but this can't trigger the projection neuron anymore.

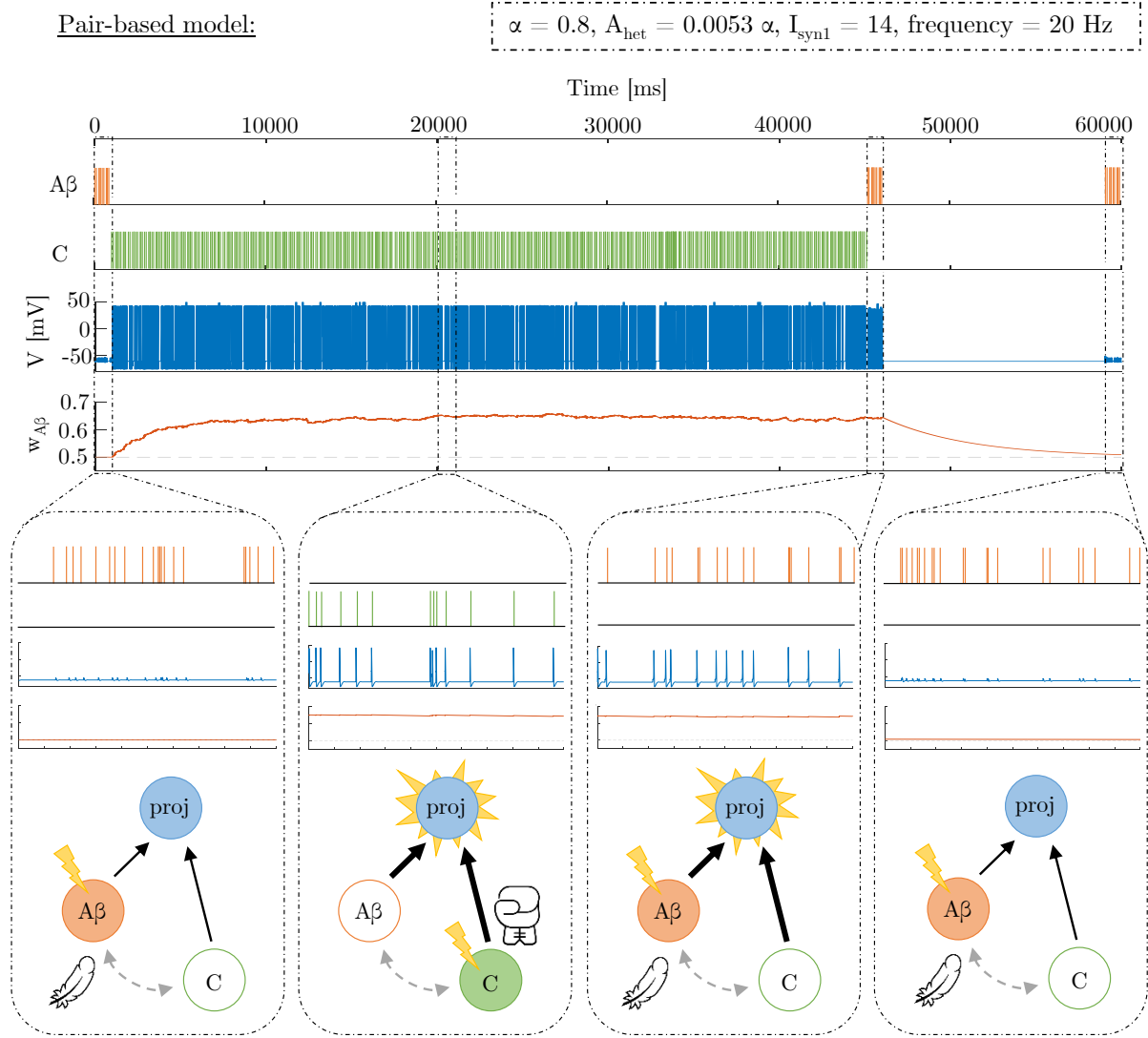


Figure C.2 – Results obtained when simulating the pair-based allodynia toy model for $\alpha = 0.8$, $A_{het} = 0.0053 \alpha$, $I_{syn} = 13$ with a frequency of 20 Hz. Light touch stimulus activate A β fiber which can't trigger the projection neuron. Noxious stimulus activate C fiber which triggers the projection neuron emitting action potential as a response. This has the effect of increasing the $w_{A\beta}$. Light touch stimulus activates A β again which has now the power of triggering the projection neuron. After some time without any stimulus, light touch stimulus activates A β fiber but this can't trigger the projection neuron anymore.